A GENERAL METHOD FOR GENERATING EFFECTIVE RESONANCE CROSS SECTIONS FOR HETEROGENEOUS MEDIA

A THESIS

Presented to

The Faculty of the Division of Graduate

Studies and Research

By

Kenneth David Kirby

In Partial Fulfillment

of the Requirements for the Degree

Doctor of Philosophy

in the School of Nuclear Engineering

Georgia Institute of Technology

September, 1974

A GENERAL METHOD FOR GENERATING EFFECTIVE RESONANCE CROSS SECTIONS FOR HETEROGENEOUS MEDIA

Approved:

R. A. Karam, Chairman

G. G. Eichholz

J. D. Clement

J. M. Kallfelz

W. Carlson

Date approved by Chairman: 9/20/74

ACKNOWLEDGMENTS

Throughout the course of this work I have been especially grateful to Dr. R. A. Karam, my thesis advisor, for his assistance and encouragement. His insight and familiarity with this area have given valuable input which I could not have obtained elsewhere. My thesis committee members, Dr. G. G. Eichholz, Dr. J. D. Clement, Dr. J. M. Kallfelz, and Dr. R. W. Carlson, have also helped me in this research and provided invaluable professional support throughout my studies at Georgia Tech. I would also like to thank Dr. W. J. Kammerer for his willingness to serve late in the work.

I would like to acknowledge Dr. P. H. Kier and Dr. W. L. Woodruff of Argonne National Laboratory for their suggestions and assistance in obtaining several computer codes used in this work. I would also like to thank Dr. L. Penn and Mr. D. Matthews of the University of Georgia for their excellent assistance in implementing these computer codes on the IBM 360 system at the University.

Several fellow students have also assisted me during my work. I am especially grateful to Claude Mildrum, Tony Matthews, David Rehbein, and Young Nam Chang for their help.

I would like to thank the secretaries of the School of Nuclear Engineering for their assistance during my work. Mrs. Lydia Geeslin has been invaluable in the preparation of this manuscript, and Mrs. Phyllis Frost has been a constant source of encouragement.

To my parents, I am deeply grateful for their guidance. Finally, to my wife Sharon, I would like to express my deep appreciation for her love, understanding, and help throughout this work. Her companionship has made the trying times more bearable and the rewarding moments more valuable.

TABLE OF CONTENTS

LIST OF TABLES

LIST OF ILLUSTRATIONS

LIST OF ILLUSTRATIONS (Concluded)

SUMMARY

For nuclear reactors in which there is a heterogeneous arrangement of materials with resonance structure in the neutron cross sections, the neutron flux will have strong variations in space and energy. In order to obtain effective cross sections which account for these variations, validated methods for including the spatial component of resonance self-shielding are required. Current techniques generally include the effect of spatial self-shielding by applying an equivalence theory between homogeneous and heterogeneous cases or by integral transport theory methods which retain one of the assumptions of equivalence theory, namely, that the spatial neutron flux be flat. This work develops a general method of cross section averaging which does not resort to the flat-flux assumption, but uses a generalized reciprocity relation and defines an energy-dependent escape cross section which can account for spatial nonuniformity. The general method retains much of the simplicity of form as contained in equivalence theory and under necessary assumptions reduces to the more approximate methods.

Integral transport theory calculations are performed which determine the effects of nonuniformity in the resolved resonance region of ^{238}U for a typical fast reactor critical and are used to characterize the nonuniformity parameters of the general method. Cross section averages are determined by the general method with comparisons to equivalence theory and other current techniques. The resulting effects of nonuni-

formity on average cross sections is found to be small, generally less than 1%. Independent calculations are used to verify this result. The parameters of the general method show the small effect to be due to compensations which occur in the treatment of nonuniform sources, and these compensations are discussed. The results of this work tend to point out that current differences in calculated and experimental results are not due to the spatial treatment of the slowing-down source.

CHAPTER I

INTRODUCTION

The development of accurate methods for the design and analysis of nuclear reactors is a fundamental part of an orderly and disciplined reactor technology program. One of the more important areas for such development is the determination of the space-dependent neutron energy spectrum in the reactor. For reactors in which there are materials present in a heterogeneous arrangement of plates or pins there will be variations in the spatial neutron flux within and near the plates or pins. If these materials contain cross section resonances the neutron flux will also have strong variations in space and in energy near the resonances. Accounting for these variations in the spectrum has been a central problem in reactor physics. To determine these detailed variations within a large reactor, even with current numerical techniques, would require literally thousands of energy and spatial mesh points. This is impossible with present computers and would probably be impractical even if larger and faster computers were available. Consequently, other procedures are required to solve this problem, and the predominant method of solution has been the determination of effective cross sections.[1-9]

The effective cross section is defined by the requirement that, when it is multiplied by a flux integral for an appropriate space-energy range, it must yield the same reaction rate as the integral of the product of the true rapidly varying cross section and flux over the same space-

energy range. This definition can be expressed as

$$\langle \sigma_x \rangle = \frac{\int_V \int_{\Delta E} \sigma_x(E) \phi(\vec{r},E)\, dE dV}{\int_V \int_{\Delta E} \phi(\vec{r},E)\, dE dV}, \qquad (1\text{-}1)$$

where $\sigma_x(E)$ is the energy-dependent differential cross section for reaction type x which is to be averaged over an appropriate energy and volume range. $\phi(\vec{r},E)$ is the neutron flux and $\langle \sigma_x \rangle$ denotes the effective cross section of type x. In order to determine effective cross sections one must have not only accurate differential cross sections over the entire energy range for each isotope, but also accurate procedures for obtaining the flux approximation. For the resonance range, the procedures used must include validated methods for treating resonance self-shielding in both energy and space.

Historically, the problem of treating resonance effects in heterogeneous lattices has been present since the origins of reactor technology. The earliest study of resonance effects in reactor fuel elements was that of Wigner developed during the days of the Manhattan Project which was not reported until 1955.[10] His experiments were confined to the radiative capture in the resonance lines of ^{238}U and its oxides, since this was the primary problem in the first attempts to decide the feasibility of sustaining a chain reaction with natural uranium fuel. The experiments of Wigner and Creutz[10-13] confirmed the observation that concentrating the uranium in lumps would decrease the parasitic absorption in the ^{238}U resonances. Within the framework of these experiments and the available information on ^{238}U resonance parameters, Wigner formed a theory for treating

heterogeneous effects which has largely been the basis of later developments. The thrust of his early work was to determine the size and shape of uranium lumps which would most likely lead to a self-sustaining chain reaction. It is Wigner's rational approximation for the escape probability from a fuel lump which serves as a key element in the theory to express heterogeneous cases in terms of equivalent homogeneous cases.[1,4,9,14]

Among the theoretical works subsequent to Wigner's was the work of Dancoff and Ginsburg. The most noted of their works was the consideration of the effect of resonance absorption in a lump due to the presence of adjacent lumps.[15] Their work also gave a more accurate description of absorption due to low resonance levels in ^{238}U which are rather important in the metal, but play a lesser role in the oxide. In the years prior to the 1955 Geneva Conference resonance parameters for most of the low-lying levels in ^{238}U and other isotopes were measured fairly accurately and better theoretical analysis was performed. However, at that conference an independent Russian treatment[16] was presented which appeared quite different from the Wigner theory. This apparent discrepancy prompted critical reexamination of both theories. Wigner pointed out that the Russian work ignored the effect of scattering collisions in the fuel lump and for cases where this was valid there was good agreement between the two theories.[17]

After 1955, added confidence in the theoretical models, more resonance data, and the availability of electronic computers stimulated an advance in the theoretical area of determining effective resonance absorption. The first reasonably successful attempt to calculate resonance absorption from resonance data was made in 1956 by Dresner for homogeneous

assemblies.[18] In 1958, independent calculations of resonance integrals for heterogeneous assemblies were made which included the same physical concepts and which yielded very similar results. These computations were performed by Adler, Hinman, and Nordheim,[19] Dresner,[20] and by Chernick and Vernon.[14] Included in these calculations were wide resonances using the infinite mass, or IM, approximation, as well as the narrow resonance, NR, approximation; also, provision was made for the unresolved resonances and Doppler broadening. The most serious compromise in these computations was the necessity of using either the NR or IM approximation, and although the errors produced by this selection tend to cancel, Spinney[21] pointed out that errors for individual resonances could be quite large.

Improved theoretical studies continued in the late 1950's and early 1960's. Second order corrections to the NR approximation were set forth by Corngold,[22] Dresner,[2] and Goldstein and Cohen.[23] These improvements, as well as the earlier work, were aimed at correctly accounting for energy self-shielding, whereas spatial effects were still based on Wigner's theory and an equivalence relation between lumps and homogeneous mixtures. There is extensive literature on the use of an equivalence principle between heterogeneous and homogeneous resonance integrals,[1,2,10,14,24,25] including extension to dense fuel lattices.[5,26,27] The primary basis of this equivalence is that the collision probability for a flat source of neutrons can be used inside and outside the fuel lump. Extensive compilations of escape probabilities for a flat source in various geometries such as that by Case, de Hoffman, and Placzek[28] are available, but the equivalence relation is also based on a rational approximation suggested by Wigner.[11]

Improvements in the treatment of resonance heterogeneous effects were sought for some time. Monte Carlo calculations by Richtmyer[29] and Sampson[30] gave rough agreement with earlier work but initiated more detailed examination of heterogeneous effects. Precise Monte Carlo calculations by Levine[31] showed that the Wigner rational approximation underestimated escape probabilities generally, and no simple correction could make the Wigner form valid over large energy ranges. The nature of the Monte Carlo method made it impractical for production use. Nordheim[8,9] and Chernick and Vernon[14] suggested a direct numerical integration of the integral transport equation. Although the rational approximation for escape probabilities is not involved in this approach, most of the current integral transport methods still assume a uniform neutron source. Nordheim[9] noted that with this approach the spatial distribution of absorption is not explicitly brought out and that a closer study of spatial effects would seem to be very desirable.

The desirability of the study suggested by Nordheim has been strengthened by the presence of discrepancies in comparisons between current experimental results and calculations. A possible source of the current discrepancy between measured and calculated reactor parameters may be due to using inappropriate methods for treating heterogeneity effects in the resonance range. The current methods which are normally used to analyze almost all the integral data from critical facilities are based on equivalence theory and the flat source approximation. An improved treatment of spatial nonuniformity and its effect on effective cross sections is then a fundamental area in which additional investigation is warranted.

The objective of this work is to pursue a more general approach to determining effective resonance cross sections for heterogeneous media. A general method of determining effective resonance cross sections is given which does not resort to the use of the flat source approximation, and which is capable of accurately accounting for detailed spatial and spectral effects while retaining a simple formulation.

A complete background of the current methods used to generate effective cross sections is given in Chapter II. The theoretical basis of the new method is set forth in Chapter III. In addition to eliminating the restrictions of most current methods, the generality and simple form of this method offers advantages over the few methods which include spatial effects. Using this theory the computational approach used to investigate the effect of spatial nonuniformity in the slowing-down source on effective cross sections is given in Chapter IV. Chapter V then gives results within a reactor lattice with pertinent conclusions noted in Chapter VI.

CHAPTER II

CURRENT METHODS

Current methods of generating effective resonance cross sections for heterogeneous media vary in many respects. The application of some methods is specialized while others are general; some have very sophisticated computational models and require a great deal of computational time and others are more approximate and quite fast. The purpose of obtaining the effective cross section is to account for the spatial flux dips or peaks within the heterogeneous configuration of a unit cell. The spatial flux dips or peaks will occur whenever the magnitude of the cross section in one region of the cell is large compared to that at another, and can result from two different cases. The first case occurs as the result of resonance structure in the heavy element cross sections, and the second is associated with large, slowly varying cross sections. The effects associated with these two cases are fundamentally the same, but they are analyzed separately because entirely different methods are applied to treat them. To analyze the resonance effect detailed resolution in energy as well as space is required, whereas, for slowly varying cross sections a broader, energy group approach may be adequate. The treatment of heterogeneity effects in the resonance range must then include validated methods for spatial self-shielding as well as the usual energy self-shielding associated with the homogeneous case. The emphasis of this work is in the area of the heterogeneous effects on resonance self-shielding.

For complete analysis of the neutronics of a large, multiregion reactor the computational approach consists of a sequence of calculations. Normally as a first step, resonance self-shielding is treated by analyzing a unit cell of a single region of the reactor without coupling to other regions. By generating effective cross sections for the unit cell and using them for the whole region, one effectively reduces the requirement for thousands of energy groups. Subsequent to these calculations more complete reactor configurations can be analyzed using effective cross sections which characterize each of the regions within the reactor.

Before examining the details of current methods for obtaining effective resonance cross sections for heterogeneous media, it would be well to note more completely how this area rests within the general framework of reactor analysis. Prior to examining resonance effects, accurate differential cross section data are required. The origin of cross section information is the differential data which have been obtained from experiment, complemented with theoretical models, and tested for validity. An excellent example of this type data is the Evaluated Nuclear Data Files (ENDF)[32] which have served the nuclear community for several years. Such a fundamental data base must undergo continuous scrutiny, and many studies[33-36] are aimed at verification and assessment of these data. Inaccuracies, of course, may exist and may amplify or partially cancel some computational problems; however, such data are obviously the primary input for cross section averaging methods.

The determination of effective cross sections accurately reflecting energy and spatial self-shielding in the resonance range must be complemented with parallel or subsequent calculations treating the heterogeneity

of the unit cell for other energy ranges. Such methods for cell calculations have progressed from the early determination of advantage and disadvantage factors[11,14,37] to the current use of several computational methods. The work of Honeck[38,39] in the thermal neutron area led to the THERMOS code[40,41] which is frequently used to determine effective cross sections accounting for heterogeneous effects in the thermal range. High energy heterogeneous effects are more often treated with transport theory methods such as the DTF[42] or ANISN[43] codes which can account for anisotropic effects. Cell calculations for fast reactor critical experiments have presented several problem areas due to the heterogeneous arrangement of thin plates. Meneghetti[44] used modified discrete ordinate quadratures for thin slab cells which relieved some of the problems in analysis by transport theory. Nicholson[45,46] has given general theoretical approaches using real and adjoint fluxes from one-dimensional transport theory calculations to generate effective cross sections for use in one- or two-dimensional calculations. Storrer[47] developed a method based on the use of collision probabilities in the integral transport equations, real and adjoint, which handled heterogeneous effects as perturbations on the homogeneous case. This approach has been used in several versions of the CALHET code[48] which is often used to examine multigroup heterogeneous effects in critical experiments.

Once the cell heterogeneity effects for the complete energy range of interest have been determined, subsequent analysis of a more complete reactor description can be performed. There are some additional effects that could be categorized as heterogeneous at this point in the analysis; they are due to region boundaries and the finite extent of the system.

of the unit cell for other energy ranges. Such methods for cell calculations have progressed from the early determination of advantage and disadvantage factors[11,14,37] to the current use of several computational methods. The work of Honeck[38,39] in the thermal neutron area led to the THERMOS code[40,41] which is frequently used to determine effective cross sections accounting for heterogeneous effects in the thermal range. High energy heterogeneous effects are more often treated with transport theory methods such as the DTF[42] or ANISN[43] codes which can account for anisotropic effects. Cell calculations for fast reactor critical experiments have presented several problem areas due to the heterogeneous arrangement of thin plates. Meneghetti[44] used modified discrete ordinate quadratures for thin slab cells which relieved some of the problems in analysis by transport theory. Nicholson[45,46] has given general theoretical approaches using real and adjoint fluxes from one-dimensional transport theory calculations to generate effective cross sections for use in one- or two-dimensional calculations. Storrer[47] developed a method based on the use of collision probabilities in the integral transport equations, real and adjoint, which handled heterogeneous effects as perturbations on the homogeneous case. This approach has been used in several versions of the CALHET code[48] which is often used to examine multigroup heterogeneous effects in critical experiments.

Once the cell heterogeneity effects for the complete energy range of interest have been determined, subsequent analysis of a more complete reactor description can be performed. There are some additional effects that could be categorized as heterogeneous at this point in the analysis; they are due to region boundaries and the finite extent of the system.

Transport theory methods noted earlier can be used here; and diffusion theory, which was inadequate in the cell calculation, may be applicable here. To perform complete design and performance analysis most reactor configurations will require multi-dimensional analysis. Time-dependent studies may also be required, and with the multitude of studies that must be performed using a rather complete reactor model, practical analysis requires the use of only a few energy groups. So a sequence of analyses that began with essentially continuous differential cross sections or thousands of groups culminates in an analysis using perhaps less than ten groups. The common link throughout the analysis, however, is the use of effective cross sections; and in the final assessment it will be the effective few-group cross sections which will determine reactor performance. Hence, the continuous development and refinement of methods to determine effective cross sections is requisite for quality reactor design.

Equivalence Theory

The current methods used to obtain effective cross sections which contain the heterogeneous effects of resonance self-shielding generally belong to one of two primary types--equivalence theory or integral transport theory. Equivalence theory is the most often used approach due to the tremendous simplifications it allows in the calculation of resonance cross sections. Integral transport theory methods are becoming more widely used for their more realistic models, but the computation time is usually much greater than required for equivalence theory.

The simplifying assumptions which are required to obtain equivalence theory are noted as follows[1,5,7-9]:

1. The narrow resonance (NR) or infinite mass (IM) approximation for the fuel region, which contains the resonance material,

2. The NR approximation for the moderator region,

3. The flat-source approximation in each region,

4. Escape probabilities have the form of Wigner's rational approximation.

The use of these assumptions in obtaining equivalence theory can be easily seen by considering the expression for the collision rate in the fuel region of a two-region cell:

$$\Sigma_{tF}(E)\bar{\phi}_F(E)V_F = (1-P_{F\to M}(E))\bar{\chi}_F(E)V_F + P_{M\to F}(E)\bar{\chi}_M(E)V_M \ . \qquad (2\text{-}1)$$

The symbols have their usual meaning--Σ_t is the total macroscopic cross section, ϕ is the neutron flux, V is volume, P is escape probability, and χ is the neutron source. The subscripts F and M denote the fuel and moderator regions, respectively; bars denote volume averages, and energy dependence is implied by E. Using the NR approximation for the fuel, the first approximation can be expressed by

$$\bar{\chi}_F(E) = \Sigma_{sF}\bar{\phi}_o/E \ , \qquad (2\text{-}2)$$

where Σ_s is the scattering cross section and $\bar{\phi}_o$ is a normalizing constant. The second approximation is then very similar,

$$\bar{\chi}_M(E) = \Sigma_{sM}\bar{\phi}_o/E \ . \qquad (2\text{-}3)$$

The energy dependence of the scattering cross section and 1/E dependence of the source are basic requirements for the NR approximation.[1] The third approximation concerns the spatial dependence of the source slowing down into the resonance. If the source is assumed to be flat in each region then it is well known that the reciprocity properties of the transport equation[1,5,7-9] yield a simple relation between escape probabilities,

$$P_{F\to M}(E)\Sigma_{tF}(E)V_F = P_{M\to F}(E)\Sigma_{tM}(E)V_M \ . \qquad (2\text{-}4)$$

The fourth approximation then gives a simple way to express the escape probability,[1]

$$P_{F\to M}(E) = \frac{\Sigma_e}{\Sigma_{tF}(E) + \Sigma_e} \ , \qquad (2\text{-}5)$$

where Σ_e is a constant with units of cross section. The simplest prescription for Σ_e, which makes Eq. 2-5 approach the correct value in either very small or very large regions, is given by

$$\Sigma_e = S/4V \ , \qquad (2\text{-}6)$$

where S is the surface area of the region.

The four approximations described in Eqs. 2-2 through 2-5 can be substituted into Eq. 2-1 to obtain an expression for the fuel region average flux and hence the basis for equivalence theory,

$$\bar{\phi}_F(E) = \frac{\Sigma_{sF} + \Sigma_e}{\Sigma_{tF}(E) + \Sigma_e} \frac{\phi_o}{E} \ . \qquad (2\text{-}7)$$

Note that $\Sigma_{tM} = \Sigma_{sM}$ has been used in accordance with the NR approximation in the moderator. The equivalence principle between homogeneous and heterogeneous cases can be easily deduced from Eq. 2-7 because the only parameter that implies any heterogeneity is the artificial escape cross section, Σ_e, and it always appears as an addition to the constant scattering cross section. (Σ_{sF} is, of course, one part of $\Sigma_{tF}(E)$.) Hence, if there is a homogeneous case in which the scattering cross section Σ'_{sF} is equal to the heterogeneous $\Sigma_{sF} + \Sigma_e$, then the resonance integrals and effective resonance cross sections will be the same. One can also note that, if two different heterogeneous systems have the same sum of Σ_{sF} and Σ_e, the resonance integrals are also equal. Equation 2-7 also reduces to the homogeneous case when $\Sigma_e = 0$.

With this approach refinements in models and computational methods are only reflected in the purely homogeneous, energy self-shielding. Many improvements have been made to the homogeneous theory to account for such things as temperature effects, interference from other resonances, inclusion of higher spin states, anisotropic scattering, and other areas. Methods of including these effects and the cases where they are important have been noted by Hwang,[49] Stacey,[50] and others.[9,14,21] For typical fast reactor systems many of these improvements may be necessary, but spatial effects are still handled by the simpler approach.

Of course the simplicity of equivalence theory is very advantageous and the improvements that have been suggested for better spatial treatment have gone to great lengths to avoid destroying the equivalence property. Since the presence of Σ_e as a constant yields equivalence theory and since this is the only parameter through which heterogeneity is considered, most

methods for improving the theory are aimed at adjusting Σ_e. Levine[31] performed Monte Carlo calculations and noted that the Wigner approximation generally underpredicted escape probabilities. He then suggested some geometry-dependent correction factors for Σ_e. Kelber[51,52] also noted this underprediction and offered a method determining correction factors for each resonance while preserving the equivalence relationship for each resonance. Corrections have also been made to the escape cross section to include Dancoff-type effects for adjacent plates. Bell[26] suggested a correction factor based on a rational approximation in the moderator similar to Wigner's approximation in the fuel. Hummel[27] gave an improvement to the Bell approximation for cylindrical lattices, and Travelli[53] extended the improvement to slab cells. Equivalence principles were also extended[54] to include more than two different types of regions, but such extensions could not easily be included in the currently available computational tools.

Two examples of current computational methods of equivalence theory are the MC^2 code[55] and the ERIC-2 code.[56] There are other codes available, but these are good examples of codes used in fast reactor analysis. MC^2 uses the NR approximation to determine resonance cross sections; heterogeneous treatment includes the Levine corrections for the escape probability and the Hummel improvements for Dancoff interactions. There are other capabilities of the MC^2 code which have made it attractive for fast reactor analysis; these include treatment of anisotropy and a fundamental mode spectrum calculation which can be used for group collapse. The code uses "ultra-fine" energy groups typically 1/120 lethargy units. MC^2 is currently incorporated in the modular Argonne Reactor Computation (ARC) System[57] and some improvements for heterogeneity treatment have been planned. These

improvements include more accurate treatment of Dancoff interaction[58] and an integral transport theory calculation option.[59] One capability which the ERIC-2 code has that is not present in MC^2 is the use of an intermediate approximation as opposed to the NR or IM approximation. This treatment basically determines a weighting factor between 0 and 1 which is applied to the resonance material scattering cross sections; a value of 1 yields the NR approximation and a value of 0 yields the IM approximation. This approach should yield a better treatment of resonances where the NR approximation is poor. The ERIC-2 code only determines effective resonance cross sections and does not have the other capabilities of the MC^2 code; however, the speed of computation is much faster, thus making it attractive for parametric studies.[60]

Integral Transport Theory

The use of integral transport theory to determine effective resonance cross sections was suggested by Nordheim[8,9] and Chernick and Vernon.[14] They noted that this approach would circumvent the necessity of picking the NR or IM approximation and could possibly include the effects of resonance overlap and moderator absorption. In integral transport theory one seeks the solution to the integral form of the neutron transport equation given as[1,61]

$$\Sigma_t(\vec{r},E)\phi(\vec{r},E,\hat{\Omega}) = \int_{V'} T(\vec{r}'\rightarrow\vec{r};E,\Omega)\chi(\vec{r}',E,\hat{\Omega})dV' \quad . \qquad (2\text{-}8)$$

Space, energy, and angle dependence are implied here, and T is the transport kernel, or probability of a neutron beginning at $\vec{r}'$, with energy E

and direction $\hat{\Omega}$, arriving at $\vec{r}$ and colliding there. For the case of an elastic scattering source only, one may write

$$\chi(\vec{r},E,\hat{\Omega}) = \int_{E'}\int_{\hat{\Omega}'} \Sigma_s(\vec{r};\hat{E}',\hat{\Omega}'\rightarrow E,\hat{\Omega})\phi(\vec{r},E',\hat{\Omega}')d\hat{\Omega}'dE' \quad . \qquad (2\text{-}9)$$

The problem of integral transport theory methods is, then, to solve the coupled set of equations, Eqs. 2-8 and 2-9. In order to perform this task, two simplifying assumptions are generally applied immediately; they are:

1. Isotropic scattering in the laboratory system,
2. Flat flux within each region.

The first approximation is contained in all currently available integral transport theory methods which are used to determine effective resonance cross sections. Although this approximation could be poor for light isotopes, particularly at high energies, the effect is probably small in the resolved resonance region for resonance isotopes. Anisotropy effects have been studied by an integral transport theory method[62] in the MeV range where the first assumption is poor. The assumption of flat-flux is actually the same as the flat-source approximation noted in equivalence theory, with the implication that only the region average flux due to a flat slowing-down source is computed. The use of these two approximations is generally necessary to allow adequate energy resolution and simple evaluation of the transport kernels or escape probabilities. Under these assumptions the differential scattering cross section of Eq. 2-9 is simplified and the flat-flux reciprocity relation of Eq. 2-4 can be applied to reduce the number of escape probabilities to be determined. The integral equation of Eq. 2-8 can be expressed exactly as given by Eq. 2-1 by properly

defining the escape probabilities, so one can easily note the fundamental differences in the integral transport theory approach and equivalence theory. The integral approach does not make the NR or IM approximation in either region and generally allows all cross sections to be energy dependent. Although escape probabilities are used in the integral approach, the Wigner form is not assumed. The common point between equivalence theory and most integral transport theory methods is the flat-flux assumption and the simple reciprocity relation of Eq. 2-4. Escape probabilities in the integral approach are then calculated exactly for the flat-flux case.

Two examples of integral transport theory methods that are currently used and contain the assumptions noted above are the GAROL code[63] and the RABBLE code.[64] GAROL solves the coupled integral equations for a two-region problem in general geometry and includes resonance overlap. Exact escape probabilities for standard geometries are built into the code or escape probabilities reflecting other geometry can be input. A mesh of energy points is used instead of a group structure and for the slowing-down source the scattering rate per isotope is assumed to be a linear function of energy. The RABBLE code handles either infinite slab or cylindrical geometry with up to 30 regions in the latest version.[65] The energy variable is treated by using broad groups which can be subdivided into arbitrarily small fine groups. Cross sections for resonance materials are fine-group dependent whereas other cross sections are broad-group dependent. Numerical difficulties have occurred with the RABBLE code for cases when the resonance escape probability is small, causing negative sources and fluxes to be calculated.[66] This problem has been attributed to the accumulation of small errors through thousands of fine groups due

to the approximation of no within-group scattering and a recursive source calculation. Various methods of correcting these errors have been devised,[66,67] and although the number of instances in which problems arise has been reduced, they have not been entirely eliminated. Even with the noted problem, the RABBLE code has been used in a variety of fast reactor analyses. With the rather complex description of fast reactor critical assemblies, the computation time required for analysis by integral transport theory is rather large. This is one of two disadvantages with integral transport theory. The second disadvantage is quite subjective and could perhaps be stated as the lack of ability to gain physical insight. Since the computational models and methods are quite complex, the integral transport approach is quite often used as a black-box flux calculator and hence some insight into the physical phenomenon is lost. Thus, one has the equivalence theory approach with its attendant approximations and simplistic form or the less approximate but more complicated integral transport theory approach.

Since the use of integral transport theory methods such as those noted above appears to have the best potential for determining heterogeneous effects, a few methods have been developed which do not contain the flat-flux assumption. Lewis[68,69] developed a method using Lagrangian interpolation polynomials to account for spatial shape and nonrecovery of the flux between resonances in a two-region cell. The major limitation in this work was the assumption of flux recovery at the cell boundary which would be poor for small cells. Within this method a reduction of 2 to 6% in the resonance integral for various ^{238}U-graphite lattices was found. Kier removed this boundary deficiency in his RIFF RAFF code[70] in

which he used a three-term polynomial to describe the slowing-down sources in a two-region cylindrical cell. The RIFF RAFF code requires that non-resonance materials have small 1/v absorption, and allows only two regions, and it exhibits numerical difficulties similar to those noted above for the RABBLE code. The RABID code was developed by Olson[71] to handle infinite slab cells of many regions with a linear shape assumed for the spatial dependence of the slowing-down source. Although this code appears to have the capability to examine heterogeneous effects in detail, the analysis of fast reactor critical assemblies with complex cell configurations probably does not allow enough spatial resolution to achieve its potential. Computational time also becomes a practical limitation. The RABID code is closely modeled after the RABBLE code and has had the same numerical problems[66] and required improvements.[72] For simple configurations RABID could possibly handle heterogeneity adequately.

Recalling the two current methods used to obtain effective resonance cross sections--equivalence theory and integral transport theory--the choice appears to be between approximate-but-simple and more accurate-but-complex. One can also note that, for detailed assessment of heterogeneous effects, the majority of the techniques, of both types, contain the flat-flux approximation. Hence, neither may be adequate if nonuniformity in the slowing-down sources is important. For those methods which do appear to have the capability to handle detailed heterogeneity, there are serious practical limitations in computational time and insight gained which can be applied to similar problems. Therefore, it would seem that there is a desire for a method to handle heterogeneous effects which could capitalize on the potentials of the integral transport theory approach but

still retain some of the simplicity of formulation exhibited by equivalence theory. The development, application, and assessment of such a method has constituted the major portion of this study; the need for an improved method is supported by the following evaluation of experimental evidence which implies deficiencies in current methods.

Experimental Implications

In order to develop the technology required to support the Liquid Metal Fast Breeder Reactor (LMFBR) program, critical facilities have been used to examine fast reactor characteristics and to evaluate methods and nuclear constants used for calculations. In past years the interest in fast reactors was limited to small systems with very hard neutron spectra. Consequently, the tools devised to analyze fast reactors included only a few groups in energy. As the quality and quantity of cross section data increased and as interest in fast reactors shifted toward the large 1000 MWe class, it became apparent that the tools for averaging cross sections must also improve. Significant improvements were indeed made through codes such as those previously noted, but an important step is the verification of the improved methods by comparison with critical experiments.

It is not always possible to identify specific inaccuracies in cross sections or methods by measurements from individual critical assemblies due to the multiplicity of effects involved in experimental work. One can, however, by examining a large class of experiments, perhaps observe trends which may yield helpful information. Many comparisons of calculation versus measurement obtained in the Zero Power Reactors (ZPR) have been made for reactor parameters such as k_{eff}, critical mass, reaction rates, central worths, and Doppler effect. The multiplication factor,

critical mass, and reaction rate ratio comparisons between calculation and experiment should be the simpler parameters to investigate in order to assess the current theory for handling heterogeneity. Reactivity comparisons would contain additional complexities in both theory and experiment which could conceal errors due to heterogeneity.

The effect of heterogeneity on the multiplication factor has been studied analytically by various means for essentially all the critical assemblies. Some studies[73,74] have obtained a detailed breakdown due to heterogeneous effects, but although such analytic studies can estimate the heterogeneous effects on k_{eff}, experimental verification is generally limited to the total calculated deviation from criticality. One is quite interested in the effect of heterogeneity on k_{eff}, but comparison of the calculated multiplication factor to experiment is probably not the best area for assessment of heterogeneity computational methods. Such studies do, however, estimate the relative magnitudes of the effects, and comparison to criticality gives some general insight into the accuracy of the methods.

Comparisons between calculated and experimental critical mass were performed by Pond and Till[75] for ZPR-9 assemblies with polyethylene-moderated spectra of varying softness. Their analysis did not point out any specific errors that could be attributed to heterogeneity, but the discrepancy between calculation and experiment did tend to increase as the softness of the spectrum increased. Calculated parameters were obtained using ENDF/B cross sections with the MC^2 code, or the ERIC-2 code and the RABBLE code accounting for heterogeneity in the resonance region. Additional assemblies of ZPR-9 were analyzed by LeSage and Robinson[76] with

no corrections for spatial self-shielding, yielding poor agreement with measured critical masses. Studies for ZPR-6 Assembly 6,[77] a large uranium oxide core, by Karam and Marshall[78] showed the sensitivity of the calculated critical mass as a function of the spatial weighting of the cross sections. Calculated masses were from approximately 10 to 50% higher than the experimental value. Similar results were shown for ZPR-6 Assembly 5.[79]

Heterogeneous effects should be easier to isolate in reaction rates and reaction rate ratios since there should be less compensating mechanisms occurring than for critical mass calculations. The economics of large fast breeder reactors depend in part on the value of the capture-to-fission ratios in the fissile isotopes and the capture in the fertile isotopes. Heterogeneous effects on these reaction rates would then seem quite important. A survey of experimental data from several assemblies shows systematic discrepancies with the calculated data for some important reaction rates and reaction rate ratios.

Analyses of plutonium fueled ZPR-3 assemblies by Hess and Palmer[35] show a trend of calculations underpredicting the fission ratios relative to ^{235}U. Some of their results are noted in Table 1. This trend for fission ratios, and the opposite trend for capture-to-fission ratios, is also seen in studies by Till, et al.,[80] for other assemblies of ZPR-3 and ZPR-9. Similar results have been seen for ZPR-6 Assemblies 5[79] and 6.[81] Studies of the heterogeneous effects due to changes in loading pattern have also included experiments which included drawers filled with fuel rods as opposed to the usual plate loading. Studies by Lewis, et al.,[82] on ZPR-6 Assembly 7 using rodded assemblies typical of a UO_2-PuO_2 fueled LMFBR showed discrepancies between calculated and measured reaction rates much

Table 1. Fission Ratios for Assemblies of ZPR-3

Fission Ratio Relative to ^{235}U	Assembly					
	48	48B	49	50	53	59
^{238}U						
Experiment	0.0307	0.0297	0.0345	0.0251	0.0254	0.0325
Calculated	0.0290	0.0278	0.0324	0.0237	0.0239	0.0293
Calc/Exp	0.946	0.936	0.938	0.945	0.942	0.902
^{239}Pu						
Experiment	0.976	0.964	0.986	0.903	0.928	0.942
Calculated	0.907	0.902	0.934	0.839	0.822	0.830
Calc/Exp	0.929	0.936	0.947	0.929	0.885	0.881

Table 2. Reaction Rate Ratios for Rodded and Plate Loadings of ZPR-6 Assembly 7

Ratio	Experiment		Calculated		Calc/Exp	
	Rodded	Plate	Rodded	Plate	Rodded	Plate
$^{238}\sigma_f/^{235}\sigma_f$	0.02347	0.02202	0.02044	0.02004	0.871	0.910
$^{238}\sigma_c/^{235}\sigma_f$	0.1360	0.1343	0.1433	0.1426	1.054	1.062

the same as found for the normal plate loading. Table 2 shows some of their results for both the rodded and plate loadings. The trend of over-predicting the ^{238}U capture rate and underpredicting the ^{238}U fission rate relative to fission in ^{235}U is again evident. This trend has been observed in other critical and subcritical facilities.[83,84]

The presence of these trends has prompted several attempts at resolution. Recent experimental evidence in assemblies with relatively soft neutron spectra[85-87] indicates that ENDF/B-I predicts too few neutrons below 2 keV and above 2 MeV. Similar evidence was also found in depleted uranium blocks.[88] Spectral index reaction ratios, primarily $^{238}\sigma_f/^{235}\sigma_f$ and $^{238}\sigma_c/^{235}\sigma_f$, also show[89] that the actual neutron spectrum is flatter, i.e., more neutrons at the low and at the high energy regions than calculations predict. The $^{238}\sigma_c/^{235}\sigma_f$ ratio is poorly predicted (10-15% too high) by ENDF/B--Version III.[33] Frick and Neill in a recent paper[90] proposed that the $^{238}U(n,\gamma n')$ reaction might be responsible for the discrepancy between the measured and calculated neutron spectrum at low neutron energies. They incorporated this reaction in their analysis of STSF-7 which is similar to ZPR-3 Assembly 11 and obtained good agreement with experiment. Hummel and Stacey[91] applied the same technique to ZPR-6 Assembly 7, a dilute, demo-size critical assembly, and concluded that this reaction does not make significant difference on the important parameters.

The concern over the confidence with which one can predict heterogeneity effects in a critical assembly relates to the establishment of the major physics parameters of large fast power reactors. Since the power reactor design appears more homogeneous in a neutronic sense than the critical assemblies, there has been a justifiable concern for many

years of the ability to transform the experimental data to the power reactor condition. In a recent study of heterogeneity effects in ZPPR Assembly 2, Davey[92] noted this concern particularly in light of the use of sophisticated calculations whose accuracy was difficult to assess. He points out that experiments with rodded zones will give valuable experimental measurements of heterogeneity while further analytic study continues.

A possible source of the current discrepancy between measured and calculated reactor parameters such as $^{238}\sigma_c/^{235}\sigma_f$ and the low energy portion of the neutron spectrum may be due to using inappropriate methods for treating heterogeneity effects in the resonance region. The current methods used to analyze almost all the integral data from the critical facilities are based on equivalence theory and the flat-flux reciprocity relation. Although a few more accurate methods are available, practical limitations often restrict their use. Trends such as those noted above have been noted to be far outside experimental uncertainty[93] and the systematic discrepancies provide a rather strong criticism of the current methods of cross section averaging. Towards possible resolution of such discrepancies, the remainder of this work sets forth a general method of determining effective resonance cross sections for heterogeneous media. This method has the potential of accurately accounting for detailed spatial and spectral effects while retaining a simple formulation through which practical insight into specific areas may be gained.

CHAPTER III

THEORY

To obtain effective cross sections which include heterogeneous effects, the underlying theory must adequately treat the flux variations in space and energy near resonances. Current methods of determining effective cross sections for heterogeneous media are largely based on theory which applies restrictive assumptions on both the spatial and energy dependence of the flux. These restrictions result in what is widely known as the flat-flux approximation and equivalence theory.[1,5,7,9,14] In order to obtain cross section averages which are free from such restrictions, this work presents a generalized method of determining effective cross sections for heterogeneous media. This approach not only yields a less restrictive method of determining cross section averages but, also, due to its general nature, allows direct assessment of the restrictions present in current methods.

General Development

The fundamental definition of effective, or average, cross section is given by

$$\langle \sigma_x \rangle = \frac{\int_V \int_{\Delta E} \sigma_x(\vec{r},E)\phi(\vec{r},E)\,dE\,dV}{\int_V \int_{\Delta E} \phi(\vec{r},E)\,dE\,dV}, \qquad (3\text{-}1)$$

where $\sigma_x(\vec{r},E)$ is the reaction cross section for the nuclide of interest

which is to be averaged over an appropriate energy and volume range. $\phi(\vec{r},E)$ is the real flux and $\langle\sigma_x\rangle$ is the effective cross section of type x which, when multiplied by the flux integral, conserves the real reaction rate. The flux integral in the denominator can also serve as a normalizing function consistently defining the effective cross section for use in subsequent calculations. Spatial dependence is included in the reaction cross section to imply the possible variation in atom density over the volume integration. For a volume which contains a uniform concentration of the nuclide, and denoting this volume as V_i, the effective cross section is written as

$$\langle\sigma_x\rangle_i = \frac{\int_{\Delta E} \sigma_x(E)\bar{\phi}_i(E)\,dE}{\int_{\Delta E} \bar{\phi}_i(E)\,dE} , \qquad (3\text{-}2)$$

where the spatially averaged flux at energy E, $\bar{\phi}_i(E)$ has been introduced.

$$\bar{\phi}_i(E) = \frac{1}{V_i}\int_{V_i} \phi(\vec{r},E)\,dV . \qquad (3\text{-}3)$$

Knowing the energy dependence of the reaction cross section, a knowledge of the flux spectrum or an approximation to it is required to determine the effective cross section. The flux can be obtained from knowledge of the collision density contained in the slowing-down equation for heterogeneous media. The collision density may be written in accordance with the integral transport equation as given by Irving,[61]

$$\Sigma_t(\vec{r},E)\phi(\vec{r},E,\hat{\Omega}) = \int_{V'} T(\vec{r}'\rightarrow\vec{r};E,\hat{\Omega})\chi(\vec{r}',E,\hat{\Omega})\,dV' \quad , \tag{3-4}$$

where

$\phi(\vec{r},E,\hat{\Omega})$ = angular neutron flux at position $\vec{r}$, energy E, in the direction $\hat{\Omega}$,

$\Sigma_t(\vec{r},E)$ = total macroscopic cross section at position $\vec{r}$, energy E,

$\chi(\vec{r},E,\hat{\Omega})$ = emergent particle density, or source of neutrons emerging from position $\vec{r}$ with energy E and direction $\hat{\Omega}$,

$T(\vec{r}'\rightarrow\vec{r};E,\hat{\Omega})$ = transport kernel, or probability of a neutron at position $\vec{r}'$, energy E and direction $\hat{\Omega}$, having its next collition at position $\vec{r}$,

$$T(\vec{r}'\rightarrow\vec{r};E,\hat{\Omega}) = \Sigma_t(\vec{r},E)\,e^{-\int_{\vec{r}'}^{\vec{r}}\Sigma_t(s,E)\,ds}\,\frac{\delta\left(\hat{\Omega} - \frac{(\vec{r}-\vec{r}')}{|\vec{r}-\vec{r}'|}\right)}{|\vec{r}-\vec{r}'|^2} \quad . \tag{3-5}$$

The volume integration in Eq. 3-4 is over all space, and the delta function is in the transport kernel in order to include only those sources which, when headed in the direction $\hat{\Omega}$ from $\vec{r}'$, can reach position $\vec{r}$.

The neutron source distribution, $\chi(\vec{r},E,\hat{\Omega})$ consists of all sources of neutrons due to elastic scattering, inelastic scattering, fission, external sources, or any other applicable mechanism. Writing only the elastic scattering portion explicitly, the neutron source distribution density may be expressed as

$$\chi(\vec{r},E,\hat{\Omega}) = \int_{E'}\int_{\hat{\Omega}'} \Sigma_s(\vec{r};E'\hat{\Omega}'\rightarrow E,\hat{\Omega})\phi(\vec{r},E',\hat{\Omega}')\,d\hat{\Omega}'\,dE' + Q(\vec{r},E,\hat{\Omega}) \quad , \tag{3-6}$$

where

$\Sigma_s(\vec{r};E',\hat{\Omega}'\rightarrow E,\hat{\Omega})$ = differential elastic scattering cross section at $\vec{r}$, for an incident neutron of energy E' and direction $\hat{\Omega}'$, emerging from the collision with energy E and direction $\hat{\Omega}$,

$Q(\vec{r},E,\hat{\Omega})$ = source of neutrons, other than elastic scattering, emerging from position $\vec{r}$ with energy E and direction $\hat{\Omega}$.

To perform the cross section averaging noted in Eq. 3-1, the total flux $\phi(\vec{r},E)$ is desired rather than the angular flux. To obtain this, Eq. 3-4 is integrated over all directions to yield

$$\Sigma_t(\vec{r},E)\phi(\vec{r},E) = \int_{V'}\int_{\hat{\Omega}} T(\vec{r}'\rightarrow\vec{r};E,\hat{\Omega})\chi(\vec{r}',E,\hat{\Omega})\,d\hat{\Omega}dV' \ , \tag{3-7}$$

since

$$\phi(\vec{r},E) = \int_{\hat{\Omega}}\phi(\vec{r},E,\hat{\Omega})\,d\hat{\Omega} \ . \tag{3-8}$$

The volume integration can be expressed as a sum of integrals over individual volumes V_j which make up the system to give

$$\Sigma_t(\vec{r},E)\phi(\vec{r},E) = \sum_j \int_{V_j}\int_{\hat{\Omega}} T(\vec{r}'\rightarrow\vec{r};E,\hat{\Omega})\chi(\vec{r}',E,\hat{\Omega})\,d\hat{\Omega}dV' \ . \tag{3-9}$$

One can then define

$$P_j(r,E) = \frac{\int_{V_j}\int_{\hat{\Omega}} T(\vec{r}'\rightarrow\vec{r};E,\hat{\Omega})\chi(\vec{r}',E,\hat{\Omega})\,d\hat{\Omega}dV'}{\int_{V_j}\int_{\hat{\Omega}}\chi(\vec{r}',E,\hat{\Omega})\,d\hat{\Omega}dV'} \tag{3-10}$$

which is the number of neutrons from sources in V_j which have their next collision at position $\vec{r}$, divided by the total source in V_j. This is merely the average probability that a neutron from sources in V_j will have its next collision at $\vec{r}$. With the use of Eq. 3-10 one may rewrite Eq. 3-9 as

$$\Sigma_t(\vec{r},E)\phi(\vec{r},E) = \sum_j P_j(\vec{r},E) \int_{V_j}\int_{\hat{\Omega}} \chi(\vec{r}',E,\hat{\Omega})\, d\hat{\Omega}dV' \ . \tag{3-11}$$

The above expression may be further simplified by introducing the average source strength of volume V_j,

$$\bar{\chi}_j(E) = \frac{1}{V_j}\int_{V_j}\int_{\hat{\Omega}} \chi(\vec{r}',E,\hat{\Omega})\, d\hat{\Omega}dV' \ , \tag{3-12}$$

which then yields

$$\Sigma_t(\vec{r},E)\phi(\vec{r},E) = \sum_j P_j(\vec{r},E)\bar{\chi}_j(E)V_j \ . \tag{3-13}$$

For the case in which the volume of interest for cross section averaging is V_i, the total collision rate in the volume is obtained by integrating Eq. 3-13 over V_i. The result is

$$\Sigma_{t_i}\bar{\phi}_i(E)V_i = \sum_j \bar{\chi}_j(E)V_j \int_{V_i} P_j(\vec{r},E)\, dV \ , \tag{3-14}$$

where the total cross section is assumed to be space independent within V_i and the spatially averaged flux has been introduced from Eq. 3-3.

Based on the interpretation of $P_j(r,E)$, the factor $\int_{V_i} P_j(\vec{r},E)$ can be described as the average probability that a neutron from sources in V_j will make its next collision in V_i. This is simply the escape probability from V_j to V_i which may be written as

$$\int_{V_i} P_j(\vec{r},E)dV = P_{j\to i}(E) \ . \tag{3-15}$$

For the case of $j = i$, the above interpretation is simply the i^{th} volume non-escape probability. Writing this term explicitly, one gets

$$\int_{V_i} P_i(\vec{r},E)dV = P_{i\to i}(E) \ . \tag{3-16}$$

It should be noted that, since $P_i(\vec{r},E)$ is the probability that neutrons from V_i will collide at point $\vec{r}$, then the integral over all space will be unity provided that leakage from the reactor system is considered. First writing the integral over all space and then expressing it as a summation of integrals,

$$\int_{-\infty}^{\infty} P_i(\vec{r},E)dV = 1 \ , \tag{3-17}$$

or

$$\int_{V_i} P_i(\vec{r},E)dV + \sum_{j\neq i} \int_{V_j} P_i(\vec{r},E)dV = 1 \ . \tag{3-18}$$

One can then identify the i^{th} region non-escape probability to be

$$P_{i\to i}(E) = 1 - \sum_{j\neq i} P_{i\to j}(E) \ , \tag{3-19}$$

where one of the $P_{i\to j}(E)$ is the probability of a neutron in V_i completely escaping the reactor. The collision rate in V_i can now be written as

$$\Sigma_{t_i}(E)\bar{\phi}_i(E)V_i = \left(1 - \sum_j P_{i\to j}(E)\right)\bar{X}_i(E)V_i + \sum_j P_{j\to i}(E)\bar{X}_j(E)V_j \ , \qquad (3\text{-}20)$$

where the summation is over all volumes other than V_i.

The collision rate expression developed above is a general basis for developing effective cross sections for heterogeneous media. The expression is completely general with only the restriction that cross sections are space independent within each volume V_j. The same expression may be obtained by a simple neutron balance, but the above approach gives the required formulation of the escape probabilities in order that Eq. 3-20 be exact. Most current methods of obtaining effective cross sections for heterogeneous media also begin with this collision rate expression, but various restrictions on spatial effects are immediately imposed.

Reciprocity Relations

In order to solve the collision rate expression given by Eq. 3-20 the sources and escape probabilities must be determined. However, before attempting to obtain each escape probability, additional development using the reciprocity properties of the transport equation can allow escape probabilities to be related to each other.

The use of reciprocity relations in current heterogeneous methods is described in several references.[1-9,27,63,64,71] After development of a generalized reciprocity relation without restrictive assumptions, comparisons to the more generally used relation will be made.

The general, energy-dependent reciprocity property of the transport equation as noted by Bell[1] is

$$\int_V\int_E\int_{\hat{\Omega}} S(\vec{r},E,\hat{\Omega})\phi^*(\vec{r},E,\hat{\Omega})\,d\hat{\Omega}dEdV = \int_V\int_E\int_{\hat{\Omega}} S^*(\vec{r},E,\hat{\Omega})\phi(\vec{r},E,\hat{\Omega})\,d\hat{\Omega}dEdV, \quad (3\text{-}21)$$

where ϕ and ϕ^* are the real and adjoint flux solutions of the real and adjoint energy dependent transport equations with arbitrary external sources,

$$L\phi = -S \quad \text{and} \quad L^*\phi^* = -S^*. \quad (3\text{-}22)$$

L and L* are the transport operator and adjoint operator, respectively, and S and S* are real and adjoint sources. This relation can be used to determine relationships between escape probabilities by defining the arbitrary sources as

$$\begin{aligned} S &= \chi(\vec{r},E,\hat{\Omega})\,\delta(E-E_o) \quad , \quad \text{for r in } V_i, \\ &= 0 \qquad\qquad\qquad\quad , \quad \text{otherwise;} \end{aligned} \quad (3\text{-}23)$$

$$\begin{aligned} S^* &= \Sigma_d(\vec{r},E,\hat{\Omega})\,\delta(E-E_o) \quad , \quad \text{for r in } V_j, \\ &= 0 \qquad\qquad\qquad\quad , \quad \text{otherwise.} \end{aligned} \quad (3\text{-}24)$$

E_o is some arbitrary energy of interest and δ is the Dirac delta function. The general interpretation of $\Sigma_d(\vec{r},E,\hat{\Omega})$ is an arbitrary detector response function; in this case the response of interest is a collision in V_j, so $\Sigma_d(\vec{r},E,\hat{\Omega}) = \Sigma_{t_j}(E)$. With these sources, Eq. 3-21 then becomes

$$\int_{V_i}\int_{\hat{\Omega}} \chi(\vec{r},E_o,\hat{\Omega})\phi^*(\vec{r},E_o,\hat{\Omega})\,d\hat{\Omega}dV = \int_{V_j}\int_{\hat{\Omega}} \Sigma_{t_j}(E_o)\phi(\vec{r},E_o,\hat{\Omega})\,d\hat{\Omega}dV \ . \quad (3\text{-}25)$$

Equation 3-25 is now divided by $\int_{V_i}\int_{\hat{\Omega}} \chi(\vec{r},E_o,\hat{\Omega})\,d\hat{\Omega}dV$ which after rearranging yields

$$\frac{\int_{V_i}\int_{\hat{\Omega}} \chi(\vec{r},E_o,\hat{\Omega})\phi^*(\vec{r},E_o,\hat{\Omega})\,d\hat{\Omega}dV}{\int_{V_i}\int_{\hat{\Omega}} \chi(\vec{r},E_o,\hat{\Omega})\,d\hat{\Omega}dV} = \frac{\int_{V_j}\int_{\hat{\Omega}} \Sigma_{t_j}(E_o)\phi(\vec{r},E_o,\hat{\Omega})\,d\hat{\Omega}dV}{\int_{V_i}\int_{\hat{\Omega}} \chi(\vec{r},E_o,\hat{\Omega})\,d\hat{\Omega}dV} \ . \quad (3\text{-}26)$$

Inspection of the right-hand side of Eq. 3-26 shows that it is the collision rate at energy E_o in volume V_j due to a source χ only in volume V_i, divided by that total source strength. This is the same as the escape probability from V_i to V_j at energy E_o. On the left-hand side of the above equation one can also note that the ratio of the integrals could be interpreted as an average adjoint flux with the source χ as the weighting function. Thus with

$$P_{i\to j}(E_o) = \frac{\int_{V_j}\int_{\hat{\Omega}} \Sigma_{t_j}(E_o)\phi(\vec{r},E_o,\hat{\Omega})\,d\hat{\Omega}dV}{\int_{V_i}\int_{\hat{\Omega}} \chi(\vec{r},E_o,\hat{\Omega})\,d\hat{\Omega}dV} \ , \quad (3\text{-}27)$$

and defining

$$\hat{\phi}_i^*(E_o) = \frac{\int_{V_i}\int_{\hat{\Omega}} \chi(\vec{r},E_o,\hat{\Omega})\phi^*(\vec{r},E_o,\hat{\Omega})\,d\hat{\Omega}dV}{\int_{V_i}\int_{\hat{\Omega}} \chi(\vec{r},E_o,\hat{\Omega})\,d\hat{\Omega}dV} , \qquad (3\text{-}28)$$

one can write Eq. 3-26 as

$$\hat{\phi}_i^*(E_o) = P_{i\to j}(E_o) . \qquad (3\text{-}29)$$

Thus the escape probability is obtained for an arbitrary source shape in one volume in terms of a weighted average of the adjoint flux solution due to a uniform source in another volume. Since the only restriction on the volumes is that the cross section of each be space independent, a volume may have arbitrary shape, even be subdivided, and the above expression still holds.

The same development which led to Eq. 3-29 can be applied reversing the roles of V_i and V_j, or the indices may be reversed in Eq. 3-29 since it is general to yield

$$\hat{\phi}_j^*(E_o) = P_{j\to i}(E_o) . \qquad (3\text{-}30)$$

The ratio of Eq. 3-30 to Eq. 3-29 then yields a generalized reciprocity relation,

$$\frac{P_{j\to i}(E_o)}{P_{i\to j}(E_o)} = \frac{\hat{\phi}_j^*(E_o)}{\hat{\phi}_i^*(E_o)} . \qquad (3\text{-}31)$$

Thus one may eliminate half the escape probabilities in the collision rate expression (Eq. 3-20) by use of the above relation.

In comparison to the generalized reciprocity relation of Eq. 3-31, it is useful to examine the generally used reciprocity relation. Let the neutron source be isotropic and uniform in space,

$$\chi(\vec{r},E_o,\hat{\Omega}) = \frac{1}{4\pi V_i} , \qquad \vec{r} \text{ in } V_i \text{ only.} \tag{3-32}$$

Equation 3-25 then becomes

$$\frac{1}{4\pi V_i}\int_{V_i}\int_{\hat{\Omega}}\phi^*(\vec{r},E_o,\hat{\Omega})\,d\hat{\Omega}dV = \int_{V_j}\int_{\hat{\Omega}}\Sigma_{t_j}(E_o)\phi(\vec{r},E_o,\hat{\Omega})\,d\hat{\Omega}dV . \tag{3-33}$$

The left-hand side of Eq. 3-33 is just the volume average of the adjoint flux, $\bar{\phi}_i^*(E_o)$, and by also introducing the volume average of the real flux, Eq. 3-33 becomes

$$\bar{\phi}_i^*(E_o) = 4\pi V_j \Sigma_{t_j}(E_o)\bar{\phi}_j(E_o) . \tag{3-34}$$

An analogous development yields

$$\bar{\phi}_j^*(E_o) = 4\pi V_i \Sigma_{t_i}(E_o)\bar{\phi}_i(E_o) . \tag{3-35}$$

Inspection of Eq. 3-28 shows that for a uniform source, the source weighted adjoint flux is equal to the volume averaged adjoint flux, so for the flat source case Eq. 3-31 becomes

$$\frac{P_{j\to i}(E_o)}{P_{i\to j}(E_o)} = \frac{\overline{\phi}^*_j(E_o)}{\overline{\phi}^*_i(E_o)} = \frac{V_i\Sigma_{t_i}(E_o)\overline{\phi}_i(E_o)}{V_j\Sigma_{t_j}(E_o)\overline{\phi}_j(E_o)} . \tag{3-36}$$

However, Bell[1] notes that the average flux in one volume due to a uniform source in another volume is equal to the average flux in the second volume due to a uniform source in the first volume. That is,

$$\overline{\phi}_i(E_o) = \overline{\phi}_j(E_o) . \tag{3-37}$$

From this, Eq. 3-36 reduces to the generally used flat-flux reciprocity relation

$$P_{j\to i}(E_o)V_j\Sigma_{t_j}(E_o) = P_{i\to j}(E_o)V_i\Sigma_{t_i}(E_o) . \tag{3-38}$$

Comparing the generalized reciprocity relation of Eq. 3-31 with the flat-flux reciprocity relation of Eq. 3-38, one can readily introduce a parameter

$$f_{ij}(E) = \frac{\hat{\phi}^*_j(E)V_j\Sigma_{t_j}(E)}{\hat{\phi}^*_i(E)V_i\Sigma_{t_i}(E)} , \tag{3-39}$$

which can be used to rewrite the generalized reciprocity relation as

$$\frac{P_{j\to i}(E)V_j\Sigma_{t_j}(E)}{P_{i\to j}(E)V_i\Sigma_{t_i}(E)} = f_{ij}(E) . \tag{3-40}$$

In this form the new parameter can be interpreted as a nonuniformity

parameter which is unity when the neutron source is flat. Introducing this parameter into the collision rate expression (Eq. 3-20), the result is

$$\Sigma_{t_i}(E)\bar{\phi}_i(E) = \left(1 - \sum_j P_{i\to j}(E)\right) \bar{\chi}_i(E) + \sum_j f_{ij}(E) P_{i\to j}(E) \frac{\Sigma_{t_i}(E)}{\Sigma_{t_j}(E)} \bar{\chi}_j(E). \tag{3-41}$$

This expression may then be used for arbitrary nonuniform sources, and for uniform sources it correctly reduces to the flat-flux approximation.

Escape Cross Section

The collision rate expression of Eq. 3-41 can be simplified by expressing the escape probability in a form similar to that introduced by Wigner in his work on lumped absorbers.[11] Wigner noted that, when the dimensions of a region were large compared to the mean free path, the escape probability for a uniformly distributed source could be expressed as

$$P_{esc} = \frac{A}{4V\Sigma_t(E)}, \tag{3-42}$$

where A is the surface area and V is the volume of the region. For very small regions the escape probability will approach unity, so Wigner proposed a "rational approximation" for intermediate cases given by

$$P_{esc} = \frac{1}{1 + \frac{4V\Sigma_t(E)}{A}}. \tag{3-43}$$

Noting that the factor A/4V has the units of macroscopic cross section, an artificial escape cross section could be defined,

$$\Sigma_e = \frac{A}{4V} , \tag{3-44}$$

with which the rational approximation becomes

$$P_{esc} = \frac{\Sigma_e}{\Sigma_t(E) + \Sigma_e} . \tag{3-45}$$

The validity of Wigner's rational approximation has been questioned several times noting that it generally underpredicts the exact escape probability for a uniform source.[1,5,31,51] However, the simplicity of it has been so advantageous that it is widely used. Correction factors have been applied to the escape cross section for isolated regions[31,51,52] and close-packed lattices[26,27,53]; nevertheless, the accuracy of the approximation is still limited.[51,52,94] The primary restriction that causes limitation is that the escape cross section, even with corrections, be a constant. However, by defining an energy-dependent escape cross section as that which preserves the correct escape probability, the simplicity of the form of Wigner's rational approximation can be introduced into the generalized development.

Similar to Eq. 3-45, introduce an energy dependent escape cross section $\Sigma_e^{ij}(E)$ such that the escape probability from V_i to V_j is given by

$$P_{i\to j}(E) = \frac{\Sigma_e^{ij}(E)}{\Sigma_{t_i}(E) + \Sigma_e^{ij}(E)} . \tag{3-46}$$

The escape cross section is thus defined as

$$\Sigma_e^{ij}(E) = \frac{\Sigma_{t_i}(E)P_{i\to j}(E)}{1 - P_{i\to j}(E)} . \tag{3-47}$$

The escape probability as given by Eq. 3-46 can now be substituted into the collision rate expression shown in Eq. 3-41. For the case of a two-region problem, with either one region isolated within another one or a repeating arrangement of two volumes, Eq. 3-41 reduces to

$$\Sigma_{t_i}(E)\bar{\phi}_i(E) = \frac{\Sigma_{t_i}(E)}{(\Sigma_{t_i}(E) + \Sigma_e^{ij}(E))} \bar{X}_i(E) \tag{3-48}$$

$$+ f_{ij}(E) \frac{\Sigma_e^{ij}(E)}{(\Sigma_{t_i}(E) + \Sigma_e^{ij}(E))} \frac{\Sigma_{t_i}(E)}{\Sigma_{t_j}(E)} \bar{X}_j(E) .$$

From this equation one can readily solve for the spatial average of the flux as

$$\bar{\phi}_i(E) = \frac{\bar{X}_i(E) + f_{ij}(E) \frac{\Sigma_e^{ij}(E)}{\Sigma_{t_j}(E)} \bar{X}_j(E)}{\Sigma_{t_i}(E) + \Sigma_e^{ij}(E)} . \tag{3-49}$$

One has thus obtained a generalized expression for the flux which is simple in form but which can include detailed spatial effects as well as spectral effects.

To again demonstrate the generality of this approach it may be easily shown that it correctly reduces to equivalence theory under the

usual assumptions. The basic assumptions of equivalence theory and their implications in this approach are:

1. Narrow resonance approximation -- $\bar{\chi}(E) = \Sigma_s/E$,
2. Flat-flux approximation -- $f_{ij}(E) = 1$,
3. Wigner's rational approximation -- Σ_e = constant

Also imposing constant scattering cross section and no absorption in the moderator region, Eq. 3-49 becomes

$$\bar{\phi}_i(E) = \frac{(\Sigma_{s_i} + \Sigma_e)}{(\Sigma_{t_i}(E) + \Sigma_e)} \frac{1}{E} , \tag{3-50}$$

which yields the usual equivalence properties.[1,14] Here Σ_e appears as merely an addition to the scattering cross section, so the heterogeneous case can be made equivalent to a homogeneous case by merely augmenting the scattering cross section by Σ_e. It should be noted, however, that only after imposing the above assumptions does the general method reduce to equivalence theory.

To determine cross section averages, Eq. 3-49 can be substituted into Eq. 3-2 to yield

$$\langle \sigma_x \rangle_i = \frac{\int_{\Delta E} \sigma_x(E) \dfrac{\left(\bar{\chi}_i(E) + f_{ij}(E) \dfrac{\Sigma_e^{ij}(E)}{\Sigma_{t_i}(E)} \bar{\chi}_j(E)\right)}{(\Sigma_{t_i}(E) + \Sigma_e^{ij}(E))} dE}{\int_{\Delta E} \dfrac{\left(\bar{\chi}_i(E) + f_{ij}(E) \dfrac{\Sigma_e^{ij}(E)}{\Sigma_{t_i}(E)} \bar{\chi}_j(E)\right)}{(\Sigma_{t_i}(E) + \Sigma_e^{ij}(E))} dE} . \tag{3-51}$$

One thus has the basis of a generalized method of generating effective resonance cross sections with freedom from restrictive assumptions, but which can also easily and correctly include approximations. The simple form and general nature of this method should allow easy assessment of the influence of any of the parameters, and this property yields two distinct contributions. First, since each parameter has an analog in current methods, sophisticated analysis could be used to determine parameters of the flux expression, thus allowing evaluation of the magnitude and sources of restrictions in current methods. Secondly, with an understanding of the effects of the various parameters involved, a characterization of the parameters could be used along with optional inclusion of the standard approximations to yield a general method of cross section averaging. This method could then be used in favor of the more time-consuming methods, and the parameterization could be applied in much the same way as self-shielding factors and polynomial fits are used to account for resonance effects in current methods.[60,95] Standard approximations could be included by merely adjusting the appropriate parameter in the general expression. To investigate the potential of this general method both of these areas are examined in the remainder of this work. A detailed assessment and a parameterization of the effect of spatial non-uniformity in the slowing-down source on average cross sections in the resolved resonance range is undertaken. The methods which are used to apply the general theory to this area are covered in the following chapter.

CHAPTER IV

COMPUTATIONAL APPROACH

In order to utilize the general method of cross section averaging described in the previous chapter, methods must be devised to investigate the fundamental parameters. Determination of the fluxes and sources is required to subsequently obtain escape probabilities and the nonuniformity parameters f(E) and $\Sigma_e(E)$. Current methods either do not have the capabilities to investigate these heterogeneous effects or are not readily adaptable for such analyses. Consequently, a method of determining the flux and source distributions was developed which would also yield the nonuniformity parameters. Although the preceding development which led to the nonuniformity parameters included the use of both an adjoint flux solution and a real flux solution, determination of these parameters can be made with just the real solution. Solution of the integral transport equation for the real neutron flux and source is then the basis of the following method. Whenever appropriate, available techniques were utilized and current methods were also implemented for comparison.

For the purposes of this work the computational development was limited to the study of heterogeneous effects in a one-dimensional slab model of a two-region cell. This should be adequate for the determination of the nonuniformity factors and assessment of the general method. The computational procedure can be outlined with the following

steps. The neutron flux and source solutions to the integral transport equation as expressed by Eqs. 3-4 and 3-6 are first obtained for an infinitely repeating lattice of two-region cells. After obtaining the source distribution, the components of the flux distribution due to the source in one region, then the other, are obtained. This approach allows determination of the escape probabilities as given by Eq. 3-27. From the escape probabilities the nonuniformity factors f(E) and $\Sigma_e(E)$ can then be obtained by Eq. 3-40 and Eq. 3-47, respectively.

For an infinite, repetitive lattice in slab geometry, the integral transport equation can be written as

$$\phi(x,E) = \int_{x'=-\infty}^{\infty} \int_{R=|x-x'|}^{\infty} \frac{e^{-\frac{R}{|x-x'|}\int_{x'}^{x} \Sigma_t(S,E)\,dS}}{2R} \chi(x',E)\,dR\,dx' \qquad (4\text{-}1)$$

where x and x′ are spatial positions and R is the chord shown in Figure 1. Equation 4-1 was obtained from Eqs. 3-4 and 3-5 by dividing through by the total cross section and integrating over all angles. For the source, the scattering and external components were assumed to be isotropic, and integration of Eq. 3-6 over angle yields

$$\chi(x,E) = \int_{E'} \Sigma_S(x,E'\rightarrow E)\phi(x,E')\,dE' + Q(x,E) \ . \qquad (4\text{-}2)$$

Equation 4-1 can be simplified by introducing the optical thickness

$$\tau(x,x',E) = \int_{x'}^{x} \Sigma_t(s,E)\,ds \ , \qquad (4\text{-}3)$$

$$R^2 = \left|\vec{r}-\vec{r}'\right|^2 = \rho^2 + \left|x-x'\right|^2$$

$$dV' = 2\pi\rho d\rho dx' = 2\pi R dR dx'$$

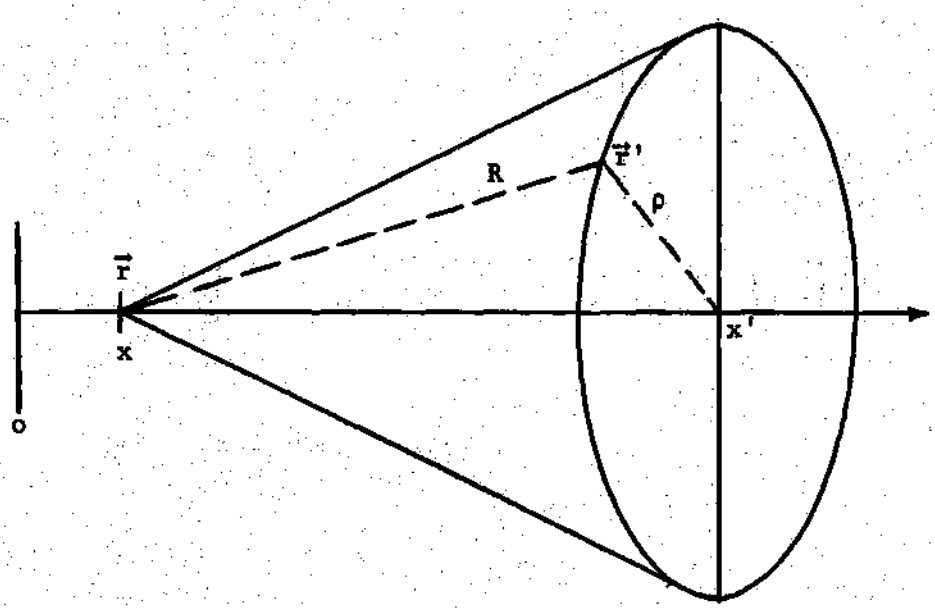

Figure 1. Coordinate System for One-Dimensional Slab Integral Transport Theory

and rearranging to yield

$$\phi(x',E) = \int_{x'=-\infty}^{\infty} \frac{\chi(x',E)}{2} \int_{R=|x-x'|}^{\infty} e^{-\frac{R}{|x-x'|}\tau(x,x',E)} \frac{dR}{R} dx'. \quad (4\text{-}4)$$

The general form of the exponential integral function is given by[1]

$$E_n(z) = z^{n-1} \int_z^{\infty} e^{-u} u^{-n} du , \quad (4\text{-}5)$$

and by change of variable in the inside integral of Eq. 4-4 one obtains

$$\phi(x,E) = \int_{x'=-\infty}^{\infty} \frac{\chi(x',E)}{2} E_1[\tau(x,x',E)]dx'. \quad (4\text{-}6)$$

The objective of the computational method is then to solve the coupled equations, Eqs. 4-6 and 4-2, for energies near a resonance throughout a unit cell.

The spatial integration in Eq. 4-6 includes all space for an infinitely repeating lattice of unit cells, and for a two-region cell the repeating lattice is shown schematically in Figure 2. The origin of the coordinate system is defined at the center of one region denoted as V_1 with thickness T_1; the other region V_2 has thickness T_2. The unit cell can then be described as region V_1 with adjacent half-thicknesses of region V_2. For the cell centered at the origin the spatial extent is from $x = -b$ to b, where $b = 1/2(T_1+T_2)$. V_1 is within this range from $x = -a$ to a, where $a = 1/2\ T_1$.

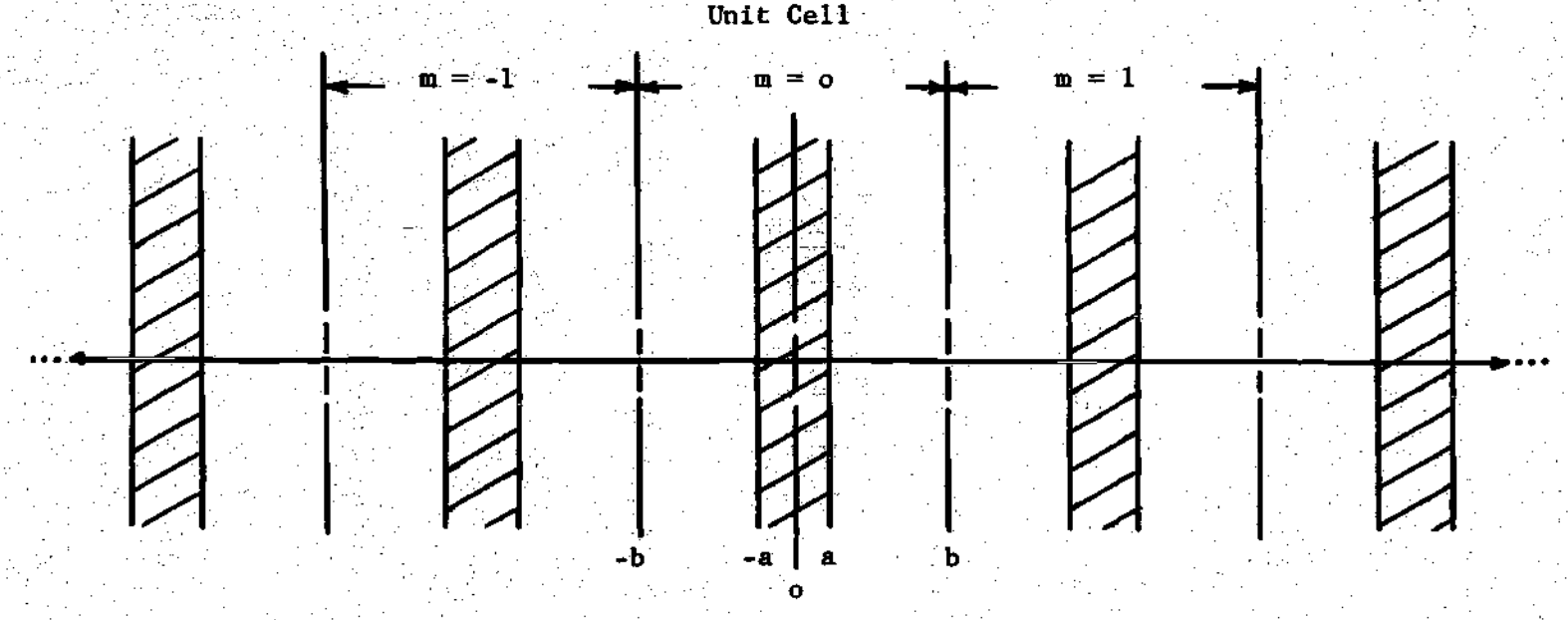

Figure 2. Schematic of Infinitely Repeating Two-Region Cell Lattice

The repeating nature of the lattice can be used to express the spatial integration of Eq. 4-6 as a sum of integrals over the individual cells. Assigning an index m to each unit cell, with m = 0 referring to the cell centered at the origin, one can define the center of the m^{th} cell as $x = X_m$, where

$$X_m = m2b \ . \tag{4-7}$$

Equation 4-6 can then be expressed as

$$\phi(x,E) = \sum_{m=-\infty}^{\infty} \int_{X_m-b}^{X_m+b} \frac{\chi(x',E)}{2} E_1[\tau(x,x',E)]dx' \ . \tag{4-8}$$

By introducing the change of variable $y = x'-X_m$ this expression becomes

$$\phi(x,E) = \sum_{m=-\infty}^{\infty} \int_{-b}^{b} \frac{\chi(y+m2b,E)}{2} E_1[\tau(x,y+2mb,E)]dy \ . \tag{4-9}$$

The periodic nature of the source distribution throughout the lattice, however, requires for any y values

$$\chi(y+m2b,E) = \chi(y,E) \ . \tag{4-10}$$

This periodic condition can be inserted into Eq. 4-9 and the remaining integral divided to yield

$$\phi(x,E) = \sum_{m=-\infty}^{\infty} \left\{ \int_{o}^{b} \frac{\chi(y,E)}{2} E_1[\tau(x,y+m2b,E)]dy \right. \tag{4-11}$$

$$\left. + \int_{-b}^{o} \frac{\chi(y,E)}{2} E_1[\tau(x,y+m2b,E)]dy \right\} .$$

By a change of variables, y=-y, in the second term above, and use of a symmetry condition about the center of the cell,

$$\chi(-y,E) = \chi(y,E), \qquad 0 \leq y \leq b , \tag{4-12}$$

the flux expression becomes

$$\phi(x,E) = \sum_{m=-\infty}^{\infty} \int_{o}^{b} \frac{\chi(y,E)}{2} \{E_1[\tau(x,y+m2b,E)] \tag{4-13}$$

$$+ E_1[\tau(x,-y+m2b,E)]\}dy .$$

The infinite integral of Eq. 4-6 has thus been changed to an integration over half the unit cell. The above expression can be simplified farther by defining the transport kernel for an infinite lattice in slab geometry as

$$T(x,x',E) = \sum_{m=-\infty}^{\infty} \{E_1[\tau(x,x'+m2b,E)] + E_1[\tau(x,-x'+m2b,E)]\} . \tag{4-14}$$

Using the kernel expression, Eq. 4-13 becomes

$$\phi(x,E) = \int_{o}^{b} \frac{\chi(x',E)}{2} T(x,x',E)dx' . \tag{4-15}$$

Provided one knows the source distribution in the above expression the integration could be carried out to obtain the flux distribution. The two distributions are interdependent, however, and the solutions must be obtained simultaneously. Let us investigate the source distribution and examine the elastic scattering component. Assuming inelastic scattering, the differential scattering cross section in Eq. 4-2 can be expressed as

$$\Sigma_S(x,E'\to E) = \frac{\Sigma_S(x,E')}{(1-\alpha)E'} , \quad \text{for } E \leq E' \leq E/\alpha , \tag{4-16}$$

$$= 0, \text{ otherwise.}$$

$\Sigma_S(x,E')$ is the total elastic scattering cross section at energy E', and

$$\alpha = \left(\frac{A-1}{A+1}\right)^2 , \tag{4-17}$$

where A is the atomic weight of a particular isotope. Assuming the presence of several isotopes and indicating each with an index i, the elastic scattering source can be more adequately formulated and Eq. 4-2 becomes

$$\chi(x,E) = \sum_i \int_E^{E/\alpha_i} \frac{\Sigma_{Si}(x,E')}{(1-\alpha_i)E'} \phi(x,E')dE' + Q(x,E) . \tag{4-18}$$

To solve Eqs. 4-15 and 4-18 together a discrete mesh of spatial and energy points is imposed. These meshes are simply

$$x = x_n, \qquad n = 1,\ldots,N,$$

and

$$E = E_g, \qquad g = 1,\ldots,G,$$

where $x_1 = 0$, $x_N = b$, and one of the points $x_K = a$; for the energy mesh E_1 is the highest energy of interest and the remaining values decrease in energy. Between the energy mesh points the scattering rate for each isotope is assumed to be a linear function of energy, that is,

$$\Sigma_{Si}(x,E)\phi(x,E) = \frac{(E-E_g)\Sigma_{Si}(x,E_{g-1})\phi(x,E_{g-1}) + (E_{g-1}-E)\Sigma_{Si}(x,E_g)\phi(x,E_g)}{E_{g-1} - E_g} . \tag{4-19}$$

Above the energy E_1, the asymptotic flux spectrum is assumed,

$$\Sigma_{Si}(x,E)\phi(x,E) = \Sigma_{Si}(x,E_1)\phi(x,E_1)\frac{E_1}{E} , \qquad E \geq E_1 . \tag{4-20}$$

Between the spatial mesh points the source distribution is assumed to be a linear function of position,

$$\chi(x,E) = \frac{(x-x_n)\chi(x_{n+1},E) + (x_{n+1}-x)\chi(x_n,E)}{x_{n+1} - x_n} , \tag{4-21}$$

so the integral transport problem becomes the determination of the flux and source at the space-energy nodes -- x_n, E_g. The energy mesh approach noted above is modeled after the treatment used in the GAROL code and the spatial mesh treatment reflects that used in the RABID code. The use of them together here is felt to capitalize on the most advantageous aspects of both codes. The spatial treatment in GAROL is inadequate for examining detailed heterogeneous effects, and the energy treatment in RABID has been

previously noted to cause certain problems.

By imposing the energy mesh the integration required for the source determination can be carried out. For the elastic scattering contribution to E_g due to just one isotope one can write

$$\chi_i(x,E_g) = \int_{E_g}^{E_g/\alpha_i} \frac{\Sigma_{Si}(x,E')}{(1-\alpha_i)E'} \phi(x,E')dE' \qquad (4\text{-}22)$$

$$= \sum_{g'=g}^{p_i+1} \int_{E_g}^{E_{g'-1}} \frac{\Sigma_{Si}(x,E')}{(1-\alpha_i)E'} \phi(x,E')dE'$$

$$+ \int_{E_{p_i}}^{E_g/\alpha_i} \frac{\Sigma_{Si}(x,E')}{(1-\alpha_i)E'} \phi(x,E')dE'$$

where $E_{p_i} \leq E_g/\alpha_i \leq E_{p_i-1}$. A schematic diagram of the energy scale is given in Figure 3 showing the appropriate mesh points. For the case when $p_i=1$, that is $E_g/\alpha_i > E_1$, the asymptotic form of Eq. 4-20 is substituted into the second integral to yield

$$\Sigma_{Si}(x,E)\ \phi(x,E)\ E_1\left(\frac{1}{E_{p_i}} - \frac{\alpha_i}{E_g}\right).$$

By using Eq. 4-19 the evaluation of the first integral of Eq. 4-22 can be obtained; the resulting form is

$$\int_{E_g}^{E_{g'-1}} \Sigma_{Si}(x,E')\phi(x,E')\ \frac{dE'}{E'} = \Sigma_{Si}(x,E_{g'-1})\phi(x,E_{g'-1}) \qquad (4\text{-}23)$$

(continued)

$$\times \left(1 - \frac{E_{g'} \ln E_{g'-1}/E_{g'}}{E_{g'-1} - E_{g'}}\right) + \Sigma_{Si}(x,E_{g'})\phi(x,E_{g'})\left(\frac{E_{g'-1} \ln E_{g'-1}/E_{g}}{E_{g'-1} - E_{g'}} - 1\right) .$$

The second integral of Eq. 4-22 can be similarly evaluated to yield

$$\int_{E_{p_i}}^{E_g/\alpha_i} \Sigma_{Si}(x,E')\phi(x,E') \frac{dE'}{E'} = \Sigma^*_{Si}(x,E_g/\alpha_i)\phi^*(x,E_g/\alpha_i) \qquad (4\text{-}24)$$

$$\times \left(1 - \frac{E_{p_i} \ln E_g/\alpha_i E_{p_i}}{E_g/\alpha_i - E_{p_i}}\right) + \Sigma_{Si}(x,E_{p_i})\phi(x,E_{p_i})\left(\frac{E_g/\alpha_i \ln E_g/\alpha_i E_{p_i}}{E_g/\alpha_i - E_{p_i}} - 1\right)$$

where the starred factors merely denote that they represent the evaluation of Eq. 4-19 at $E = E_g/\alpha_i$. The expressions given above can be simplified somewhat by defining the coefficients

$$\beta_g = 1 - \frac{E_{g+1} \ln E_g/E_{g+1}}{E_g - E_{g+1}} , \qquad (4\text{-}25)$$

and

$$\gamma_g = \frac{E_{g-1} \ln E_{g-1}/E_g}{E_{g-1} - E_g} - 1 , \qquad (4\text{-}26)$$

and the special coefficients

$$\beta^*_{p_i g} = 1 - \frac{E_{p_i} \ln E_g/\alpha_i E_{p_i}}{E_g/\alpha_i - E_{p_i}} \qquad (4\text{-}27)$$

and

$$\gamma^*_{p_i g} = \frac{E_g/\alpha_i \ln E_g/\alpha_i E_{p_i}}{E_g/\alpha_i - E_p} - 1 . \qquad (4\text{-}28)$$

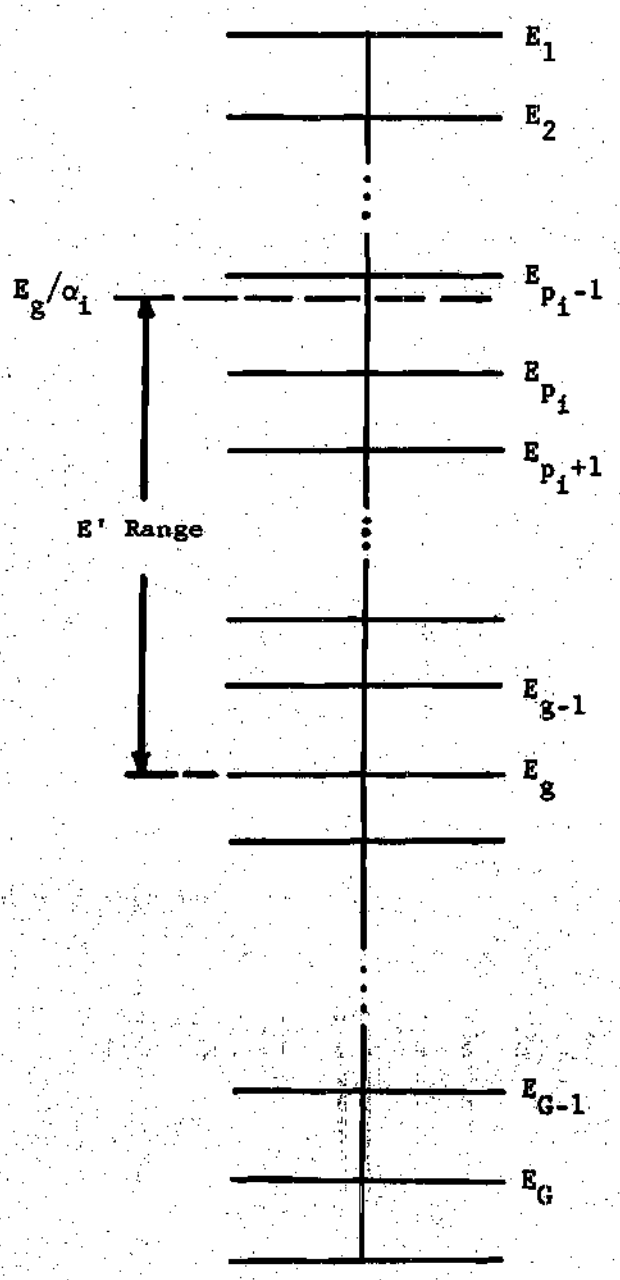

Figure 3. Schematic Energy Mesh Structure for Elastic Scattering Treatment

Then by combination of like terms, Eq. 4-22 can be expressed as

$$\chi_i(x,E_g) = \frac{1}{1-\alpha_i}\left\{\Sigma_{Si}(x,E_g)\phi(x,E_g)\gamma_g + \sum_{g'=g-1}^{p_i+1}\Sigma_{Si}(x,E_{g'})\right. \tag{4-29}$$

$$\times \phi(x,E_{g'})(\beta_{g'}+\gamma_{g'}) + \Sigma_{Si}(x,E_{p_i})\phi(x,E_{p_i})(\beta_{p_i}+\gamma^*_{p_i g})$$

$$\left. + \Sigma^*_{Si}(x,E_g/\alpha_i)\phi^*(x,E_g/\alpha_i)\beta^*_{p_i g}\right\} .$$

Then the total source is given by

$$\chi(x,E_g) = \sum_i \chi_i(x,E_g) + Q(x,E_g) . \tag{4-30}$$

The spatial integral of Eq. 4-15 can be obtained by imposing the spatial mesh and inserting the shape given by Eq. 4-21. The flux at one of the space points is then given by

$$\phi(x_n,E) = \frac{1}{2}\sum_{n'=1}^{N-1}\left\{\frac{[x_{n'+1}\chi(x_{n'},E) - x_{n'}\chi(x_{n'+1},E)]}{x_{n'+1}-x_{n'}}\right. \tag{4-31}$$

$$\times \int_{x_{n'}}^{x_{n'+1}} T(x_n,x',E)\,dx' + \frac{[\chi(x_{n'+1},E) - \chi(x_{n'},E)]}{x_{n'+1}-x_{n'}}$$

$$\left. \times \int_{x_{n'}}^{x_{n'+1}} x' T(x_n,x',E)\,dx'\right\} .$$

Although the process is tedious, the kernel integrations noted above can be carried out, and for energy E_g the integrals are denoted as the coeffi-

cients

$$Z^1_{n',ng} = \int_{x_{n'}}^{x_{n'+1}} T(x_n, x', E_g)\,dx' \tag{4-32}$$

$$= \frac{1}{\Sigma_t(x_{n'}, E_g)} \Big\{ \epsilon_{n',n} \{ E_2[\epsilon_{n',n}(\tau(x_{n'}, E_g) - \tau(x_n, E_g))]$$

$$- E_2[\epsilon_{n',n}(\tau(x_{n'+1}, E_g) - \tau(x_n, E_g))]\} + E_2[\tau(x_{n'}, E_g)$$

$$+ \tau(x_n, E_g)] - E_2[\tau(x_{n'+1}, E_g) + \tau(x_n, E_g)] + \epsilon_{n',n} \sum_{m=0}^{\infty} \sum_{j=1}^{4}$$

$$\delta_j \{ E_2[m\tau_o(E_g) + \alpha_{n',nj}(E_g)] - E_2[m\tau_o(E_g) + \alpha_{n'+1,nj}(E_g)] \} \Big\}$$

and

$$Z^2_{n',ng} = \int_{x_{n'}}^{x_{n'+1}} x' T(x_n, x', E_g)\,dx' \tag{4-33}$$

$$= \frac{1}{\Sigma_t(x_{n'}, E_g)^2} \Big\{ E_3[\epsilon_{n',n}(\tau(x_{n'}, E_g) - \tau(x_n, E_g))] - E_3[\epsilon_{n',n}$$

$$\times (\tau(x_{n'+1}, E_g) - \tau(x_n, E_g))] + \epsilon_{n',n} \Sigma_t(x_{n'}, E_g) \{ x_{n'} E_2$$

$$\times E_2[\epsilon_{n',n}(\tau(x_{n'}, E_g) - \tau(x_n, E_g))] - x_{n'+1} E_2[\epsilon_{n',n}(\tau(x_{n'+1}, E_g)$$

$$- \tau(x_n, E_g))]\} + E_3[\tau(x_{n'}, E_g) + \tau(x_n, E_g)] - E_3[\tau(x_{n'+1}, E_g)$$

$$+ \tau(x_n, E_g)] + \Sigma_t(x_{n'}, E_g) \{ x_{n'} E_2[\tau(x_{n'}, E_g) + \tau(x_n, E_g)]$$

(continued)

$$- x_{n'+1} E_2[\tau(x_{n'+1},E_g) + \tau(x_n,E_g)]]$$

$$+ \sum_{m=o}^{\infty} \sum_{j=1}^{4} \{E_3[m\tau_o(E_g) + \alpha_{n',nj}(E_g)] - E_3[m\tau_o(E_g)$$

$$+ \alpha_{n'+1,nj}(E_g)] + \delta_j \Sigma_t(x_{n'},E_g)[x_{n'} E_2[m\tau_o(E_g) + \alpha_{n',nj}(E_g)]$$

$$- x_{n'+1} E_2[m\tau_o(E_g) + \alpha_{n'+1,nj}(E_g)]]\}$$

In the above expressions

$$\tau(x_n,E_g) = \tau(o,x_n,E_g) \ , \tag{4-34}$$

$$\tau_o(E_g) = \tau(o,b,E_g) \ , \tag{4-35}$$

$$\epsilon_{n'n} = +1 \ , \qquad n' \geq n \ , \tag{4-36}$$

$$= -1 \ , \qquad n' < n \ ,$$

$$\delta_j = +1 \ , \qquad j = 1, 4, \text{ or } 5 \ , \tag{4-37}$$

$$= -1 \ , \qquad j = 2 \text{ or } 3 \ ,$$

and

$$\alpha_{n'nj}(E_g) = \tau_o(E_g) + \delta_j \tau(x_{n'},E_g) + \delta_{j+1} \tau(x_n,E_g) \ . \tag{4-38}$$

Development of the above integrals is covered in more detail in Appendix A. With these coefficients the flux expression of Eq. 4-31 can be stated

$$\phi(x_n,E) = \frac{1}{2}\sum_{n'=1}^{N-1}\frac{1}{x_{n'+1}-x_{n'}}\left\{\left[x_{n'+1}\chi(x_n,E) - x_{n'}\chi(x_{n'+1},E)\right] Z^1_{n',ng}\right. \tag{4-39}$$

$$\left. + \left[\chi(x_{n'+1},E) - \chi(x_{n'},E)\right] Z^2_{n',ng}\right\} .$$

Since the cell is made up of two regions with a discontinuity in cross section occurring at the interface, the source distribution will be discontinuous there. The flux distribution will be continuous at the interface but the spatial derivative can be discontinuous. To handle this discontinuity and to avoid any ambiguity in identifying the proper cross sections to apply near the boundary, Eq. 4-39 can be rewritten as

$$\phi_{ng} = \frac{1}{2}\sum_{L=1}^{2}\sum_{n'=A_L}^{B_L}\frac{1}{x_{n'+1}-x_{n'}}\left\{\left[x_{n'+1}\chi_{n'+L-1,g} - x_{n'}\chi_{n'+L,g}\right]Z^1_{n',ng}\right. \tag{4-40}$$

$$\left. + \left[\chi_{n'+L,g} - \chi_{n'+L-1,g}\right]Z^2_{n',ng}\right\}$$

A simple notation has been introduced here: $\phi_{ng} = \phi(x_n,E_g)$ and $\chi_{n+L-1,g} = \chi(x_n,E_g)$ for x_n in region L. The source can be double valued at the interface; and $A_1 = 1$, $B_1 = K-1$, $A_2 = K$, $B_2 = N-1$. Using the simpler notation, the source expression from Eqs. 4-29 and 4-30 becomes

$$\chi_{n+L-1,g} = \sum_i \left\{\frac{1}{(1-\alpha_i)}\left[\Sigma^{Lg}_{Si}\phi_{ng}\gamma_g + \sum_{g'=g-1}^{P_i+1}\Sigma^{Lg'}_{Si}\phi_{ng'}(\beta_{g'}+\gamma_{g'})\right.\right. \tag{4-41}$$

$$\left.\left. + \Sigma^{Lp_i}_{Si}\phi_{np_i}(\beta_{p_i} + \gamma^*_{p_ig}) + (\Sigma^{Lg}_{Si}\phi_{ng})^*\beta^*_{p_ig}\right]\right\} + Q_{n+L-1,g} ,$$

where $\Sigma_{Si}^{Lg} = \Sigma_{Si}(x_n, E_g)$ for x_n in region L, and the starred term again denotes evaluation of Eq. 4-19 at $E = E_g/\alpha_i$.

Evaluation of the kernels given in Eqs. 4-32 and 4-33 is performed similar to that used in the RABID code.[71] To evaluate a single exponential integral function, $E_n(z)$, a series expansion[96] is used for E_1, and higher ordered functions are obtained by a recursion relation.[1] The error for an evaluation is typically less than 10^{-6}. To determine the infinite sums of the exponential integral functions two approaches are used. If either α or τ_o as used in Eqs. 4-32 or 4-33 is small, a Euler-MacLaurin summation formula as used in RABID is evaluated. For the second order summation the error is less than $\tau_o^7/10080\alpha^6$; for the third order summation the error is less than $\tau_o^7/50400\alpha^5$. Since $\alpha \geq \tau_o$ is required for accuracy then, the first few terms of the sum are evaluated singly and then the summation formula used. When α and τ_o are not small a method of evaluating the infinite sum using special Gaussian quadratures developed by Olson[97] is used. This approach is found in RABID and other codes and has been implemented here. The resulting maximum error in kernel evaluation should be less than 1/30%. Since differences of the various functions also exist, Taylor series expansions are also used when arguments get very close.

With the collision kernels and other coefficients, using Eqs. 4-40 and 4-41, the flux and source solutions can be obtained by an iterative approach. From an initial flux guess an approximation of the source can be obtained from Eq. 4-41. Based on this source an improved flux solution can be obtained from Eq. 4-40. This process is then repeated until acceptable flux and source solutions are obtained. From the physical nature of

this problem the flux solution at a given energy does not depend on the flux at lower energies. However, determination for a lower energy can take advantage of any improvements in the higher energy solutions during the iteration process. A boundary condition at the highest energy is required, and the iteration process can step down in energy from there to determine the final solution. Although the above approach is inherently stable, there is the possibility that problems can occur, because with the integral approach any small errors will tend to accumulate. To eliminate this problem a kernel normalization and a neutron conservation relation are used.

As noted by Lewis[68] the known solution to the flux for the case of no absorption can be used to normalize the collision kernel. For no absorption or external sources the source will be proportional to Σ_s/E and the corresponding flux solution will be $1/E$, with both being uniform in space. Substituting these solutions into Eq. 4-40 one obtains

$$\frac{1}{E_g} = \frac{1}{2} \sum_{L=1}^{2} \sum_{n'=A_L}^{B_L} \frac{\Sigma_s^{Lg}}{E_g} Z_{n',ng}^{1} \quad . \tag{4-42}$$

In the above case $\Sigma_t = \Sigma_s$ and for any case the kernel values depend only on Σ_t; however, by replacing Σ_s in the above expression by Σ_t, a normalization condition even for cases with absorption can be written as

$$\frac{1}{2} \sum_{L=1}^{2} \Sigma_t^{Lg} \sum_{n'=A_L}^{B_L} Z_{n',ng}^{1} = 1 \; ; \qquad n = 1,N, \; g = 1,G. \tag{4-43}$$

This normalization process then tends to eliminate small errors in the kernel calculations or point out larger errors.

Since the geometry under investigation is an infinite array of unit cells, neutron conservation requires that there be no net loss of neutrons across the cell boundaries. This property can be used to compensate for small errors in the flux calculation. Since no leakage can occur all source neutrons must be accounted for by collisions, and this is expressed as

$$\int_V \Sigma_t(x,E)\phi(x,E)dx = \int_V \chi(x,E)dx \ , \qquad (4\text{-}44)$$

where the integration is over both regions of the cell and applies for every energy. The above expression can also be stated as

$$\sum_{L=1}^{2} \Sigma_t^{Lg} \bar{\phi}_{Lg} V_L = \sum_{L=1}^{2} \bar{\chi}_{Lg} V_L \ , \qquad (4\text{-}45)$$

where $\bar{\phi}_{Lg}$ is the average flux in region L for energy E_g and $\bar{\chi}_{Lg}$ is the corresponding average source. By determination of these averages from the flux and source solutions, Eq. 4-45 can be evaluated to see if neutron conservation exists. If, due to some error, the relation is not satisfied, a correction to the flux solution can be made which will yield the correct conservation. Lewis[68] suggests an approach which attributes the deviation from conservation to the flux depression in or near the fuel region. One can then add a corrective term to the flux which will vanish when there is no depression. The corrected flux can be defined as

$$\phi'_{ng} = \phi_{ng} + \Delta(\phi_{Ng} - \phi_{ng}) \ , \qquad (4\text{-}46)$$

where Δ is defined such that for the corrected flux the conservation relation (Eq. 4-45) is met. To satisfy this condition the correction factor Δ can be written in terms of the uncorrected fluxes as

$$\Delta = \frac{\sum_{L=1}^{2} (\bar{\chi}_{Lg} - \Sigma_t^{Lg} \bar{\phi}_{Lg}) V_L}{\sum_{L=1}^{2} \Sigma_t^{Lg} (\phi_{Ng} - \bar{\phi}_{Lg}) V_L} . \tag{4-47}$$

This approach should yield acceptable corrections provided that Δ is small compared to the average flux within each region.

With the determination of the final flux and source solutions, the escape probabilities and nonuniformity factors can then be obtained. The escape probabilities can be determined by obtaining the flux solution in one region due to the source in the other region. This can be stated by

$$P_{1\to 2}(E) = \frac{\int_{V_2} \Sigma_{t_2}(E) \phi^1(x,E)\,dx}{\int_{V_1} \chi(x,E)\,dx} , \tag{4-48}$$

or

$$P_{1\to 2}(E_g) = \frac{\Sigma_t^{2g} \bar{\phi}_{2g}^1 T_2}{\bar{\chi}_{1g} T_1} , \tag{4-49}$$

where $\bar{\phi}_{2g}^1$ is the average flux in region 2 due only to sources in region 1. The flux solution, and hence the average, are determined from Eq. 4-40 by restricting the summation over region to just L=1, then only the region 1 portion of the final source is allowed to contribute. By restricting the

region summation to L=2 the other escape probability is determined and can be written as

$$P_{2\to1}(E_g) = \frac{\Sigma_t^{1g}\,\bar{\phi}_{1g}^{2}\,T_1}{\bar{\chi}_{2g}\,T_2} \,. \tag{4-50}$$

The escape cross section can then be expressed by

$$\Sigma_e(E_g) = \frac{\Sigma_t^{1g}\,P_{1\to2}(E_g)}{1-P_{1\to2}(E_g)} \,, \tag{4-51}$$

or by dividing by the atom density of the resonance absorber, N_r, an escape cross section per atom of absorber can be defined by

$$\sigma_e(E_g) = \Sigma_e(E_g)/N_r \,. \tag{4-52}$$

Finally, the expression for the nonuniformity factor f(E) can be obtained by using Eqs. 3-49 and 3-50 to reduce the general relation of Eq. 3-40 from the form

$$f(E_g) = \frac{P_{2\to1}(E_g)\,\Sigma_t^{2g}\,T_2}{P_{1\to2}(E_g)\,\Sigma_t^{1g}\,T_1} \tag{4-53}$$

to

$$f(E_g) = \frac{\bar{\phi}_{1g}^{2}\,\bar{\chi}_{1g}\,T_1}{\bar{\phi}_{2g}^{1}\,\bar{\chi}_{2g}\,T_2} \,. \tag{4-54}$$

The methods and steps outlined above were implemented into a computer code to determine the detailed effects of heterogeneity due to an isolated resonance for a material in region 1 of the two-region, slab cell configuration. The code also includes the ability to handle precalculated kernels, arbitrary external source, flux guess and boundary condition, and Doppler broadened cross sections with interference scattering. The highest energy point is required to be at least E_o/α^3, where E_o is the resonance energy and α is for the resonance isotope. Thirty mesh points each are allowed for energy and space with arbitrary spacing. To obtain a reasonable mesh, energy spacing is determined by inspection after generating the resonance cross sections. The spatial mesh selection is quite important due to the spatial averaging that is to be performed. To assure that spatial points are selected which will yield acceptable resolution for all energies an approximate solution is examined. For the case of a flat source of neutrons in one region the first collision flux shape in the other region is given by

$$\phi(x,E) = \phi_o \{E_2[\Sigma_t(E)(a+x)] + E_2[\Sigma_t(E)(a-x)]\} , \qquad (4\text{-}55)$$

$$0 \le x \le a .$$

This type relation can then be studied and used to obtain an estimate of the flux depression and the spatial mesh required to adequately describe it. The above relation can also be used to yield a good approximation of the flux shape between space points which can be used in the spatial averaging. Specifically, the shape between points is assumed to be

described by

$$\frac{\phi(x,E_g) - \phi_{ng}}{\phi_{n+1,g} - \phi_{ng}} = \frac{F(x,E_g) - F(x_n,E_g)}{F(x_{n+1},E_g) - F(x_n,E_g)} , \qquad (4\text{-}56)$$

where $x_n \le x \le x_{n+1}$, and

$$F(x,E_g) = E_2[\Sigma_t(E_g)(a+x)] + E_2[\Sigma_t(E_g)(a-x)] . \qquad (4\text{-}57)$$

This type approach in the averaging process may then offset some of the adverse effects of inadequate spatial mesh.

Since only one isolated resonance is examined in the computation, the cross sections for the non-resonance materials are assumed to be constant. Any degree of absorption is allowed for these materials though. The resonance cross sections include s-wave scattering only and are determined from

$$\sigma_c(E) = \sigma_o \frac{\Gamma_c}{\Gamma_t} \sqrt{\frac{E_o}{E}} \; \psi(\xi,y) , \qquad (4\text{-}58)$$

$$\sigma_s(E) = \sigma_o \frac{\Gamma_n}{\Gamma_t} \psi(\xi,y) + (\sigma_p \sigma_o g \frac{\Gamma_n}{\Gamma_t})^{\frac{1}{2}} \chi(\xi,y) + \sigma_p , \qquad (4\text{-}59)$$

where

σ_o = peak height of resonance

$$= \frac{2.60385 \times 10^6}{E_o} \left(\frac{A+1}{A}\right)^2 g \frac{\Gamma_n}{\Gamma} ,$$

Γ_c, Γ_n, Γ_t = capture, neutron, and total width, respectively,

σ_p = potential scattering cross section,

$\xi = \Gamma_t/\Gamma_D$; $\Gamma_D = \left(\frac{4k\theta E_o}{A}\right)^{\frac{1}{2}}$,

$y = \frac{2}{\Gamma_t}(E-E_o)$,

g = statistical spin factor,

$\psi(\xi,y)$ = symmetric Doppler shape function,

$\chi(\xi,y)$ = nonsymmetric Doppler shape function.

All parameters are standard; k is Boltzmann's constant and θ is absolute temperature. The nonsymmetric function is not to be confused with the previously defined source distribution. Routines for evaluating the shape functions were obtained from the ERIC-2 code[56] and the RABBLE code.[64]

Through the methods and procedures outlined above the spatial nonuniformity effects in a heterogeneous lattice can be examined in detail. The nonuniformity effects can then be expressed in terms of a simple flux expression, which for the average flux in region 1 of the two-region cell is given by

$$\bar{\phi}_1(E) = \frac{\bar{\chi}_1(E) + f(E)\frac{\Sigma_e(E)}{\Sigma_{t2}(E)}\bar{\chi}_2(E)}{\Sigma_{t1}(E) + \Sigma_e(E)} . \qquad (4\text{-}60)$$

To perform cross section averaging, however, these effects must be expressed for a wide energy range including many resonances and in the following chapter the advantageous manner in which the generalized method allows extension to various energies and different resonances is brought out. With a representation of the nonuniformity effects over the appropriate energy range the cross section averaging can then be carried out.

To perform the cross section averaging using the general method, a separate computer code was written. The energy integration is performed resonance by resonance using a Romberg numerical quadrature.[98] Any number of neighboring resonances are allowed to contribute to the total cross section and nonresonance materials can have broad group dependent cross sections. The exact flat treatment and equivalence theory are also available as special cases of the general method. For the exact flat treatment f(E) is set equal to unity and the escape cross section is determined from

$$\Sigma_e^{flat}(E) = \frac{\Sigma_{t1}(E)\, P_{1\to 2}^{flat}(E)}{1 - P_{1\to 2}^{flat}(E)} . \qquad (4\text{-}61)$$

For this case the escape probability for a flat source can be written[9]

$$P_{1\to 2}^{flat}(E) = \frac{P_{esc}(E)(1-C)}{1 - (1-2\Sigma_{t1}(E)T_1 P_{esc}(E))C} , \qquad (4\text{-}62)$$

with

$$P_{esc}(E) = \frac{1}{\Sigma_{t1}(E)T_1}\left[0.5 - E_3(\Sigma_{t1}(E)T_1)\right] , \qquad (4\text{-}63)$$

and the Dancoff correction is given by[28]

$$C = 2E_3(\Sigma_{t2}T_2) . \qquad (4\text{-}64)$$

For equivalence theory f(E) is also unity and Σ_e is constant. The value

of Σ_e is determined by the procedure given by Travelli[53] for a slab lattice, where

$$\Sigma_e \approx \frac{1.09}{2T_1} (1-C) \ , \tag{4-65}$$

with

$$1-C = \gamma_B + 1.7\gamma_B^4 (1-\gamma_B) \ , \tag{4-66}$$

and

$$\gamma_B = \left(1 + \frac{1}{2\Sigma_{t2}T_2}\right)^{-1} \ . \tag{4-67}$$

In each of the above cases the intermediate resonance approximation as obtained from ERIC-2[56] is used for the resonance absorber and the NR approximation for other materials. Within the same general method then there are three different degrees of treating heterogeneity, and with these three treatments available together, comparisons can be made on a consistent basis and the relative effects of heterogeneity by the different treatments readily assessed.

CHAPTER V

RESULTS

Using the methods outlined in the previous chapters, calculations were performed to assess the characteristics of the general method and the effect of nonuniformity on effective resonance cross sections. First, briefly, the behavior of the escape cross section for an exact treatment of a flat source of neutrons is examined. The exact flat case forms a basis of comparison to later treatment of nonuniformity, and differences as compared to the constant escape cross section of equivalence theory are noted. Next, the behavior of the nonuniformity parameter f(E) and escape cross section $\sigma_e(E)$ are determined for resonances of ^{238}U for a two-region cell of ZPR-6 Assembly 5[79] using the integral transport theory method of Chapter IV. The same method is then used for a parametric assessment of the nonuniformity parameters for the resolved resonance range of ^{238}U to characterize the parameters required for cross section averaging. Effective cross sections are then obtained using the general method, and comparisons are made between the nonuniform treatment and more approximate treatments. Results of comparative calculations using other, independent computational methods are also included.

Escape Cross Section for Flat Source

A major advantage of the general cross section averaging method which has been set forth in this work is the ability to handle various degrees of approximations within the same framework. This ability allows

the comparison of different treatments to be made on a consistent basis. One examination which can form a useful basis of comparison for the following analysis of nonuniform source effects is the behavior of the escape cross section reflecting the exact treatment of the escape probability for a flat source of neutrons. This behavior can also be compared to the constant value of the escape cross section used in equivalence theory.

For a flat source of neutrons the escape cross section is given by Eq. 4-61; the required escape probability and Dancoff factor are given by Eqs. 4-62 and 4-64, respectively. The behavior of the escape cross section for a flat source was examined for an equivalent two-region cell for the core region of ZPR-6 Assembly 5. A complete description of the plate loading pattern for Assembly 5 is given in Reference 79. There are several ^{238}U plates distributed throughout the actual cell, twelve 1/8 inch plates and two 1/16 inch plates; the two-region cell is a single 1/8 inch plate with the associated outer region representing a proportional homogenization of the other types of plates. The resulting cell description is given below:

^{238}U Plate Thickness	0.3175 cm
Outer Region Thickness	1.0264 cm
^{238}U Atom Density	0.04783×10^{24} cm^{-3}

A schematic of the equivalent cell is given in Figure 4. A detailed composition of the outer region is not required for determination of escape probability and escape cross section; a constant macroscopic cross section of 0.35 cm^{-1} is used in the Dancoff correction. Additional cell description is given with the integral transport theory results.

The escape cross section around three different ^{238}U resonances was

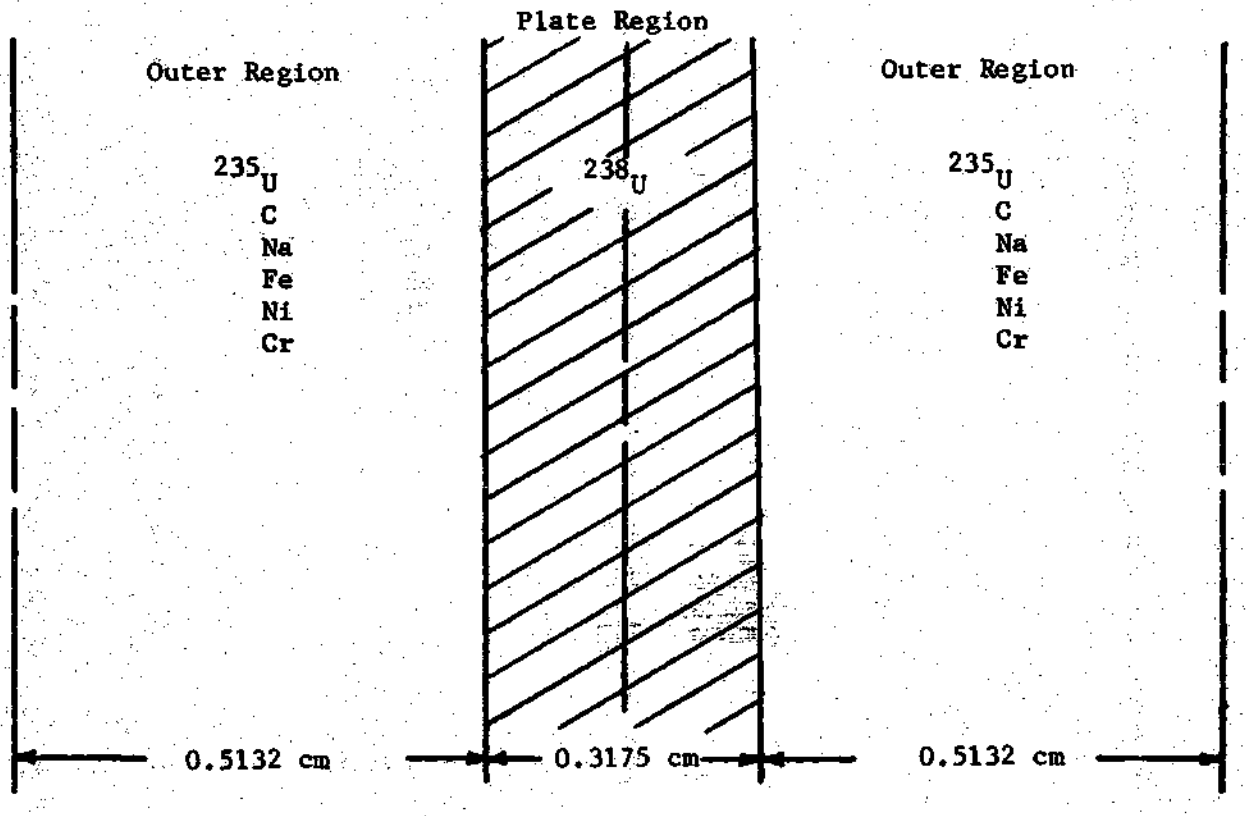

Figure 4. Equivalent Two-Region Cell for ZPR-6 Assembly 5

examined. The three resonances represent a large, moderate, and weak resonance; the resonance parameters of these resonances are given in Table 3. The total microscopic cross section for each of the resonances is given in Figure 5. Interference scattering and Doppler broadening to room temperature (293°K) are included. The accompanying escape probabilities from plate to outer region and escape cross sections for these resonances are shown in Figures 6 and 7, respectively. Figure 7 also shows the constant values for escape cross section as given by the rational approximation and Eq. 4-65.

Table 3. Selected ^{238}U Resonance Parameters

Peak Energy(eV)	Neutron Width(eV)	Capture Width(eV)	Total Width(eV)
189.6	0.1690	0.0247	0.1937
518.3	0.0555	0.0244	0.0799
1098.1	0.0170	0.0235	0.0405

By its definition the escape cross section depends on the total cross section and escape probability. The escape probability is a strong function of the total cross section, decreasing as the cross section increases. The combined behavior of the two functions yields the behavior given in Figure 7 which is larger than the constant value used for equivalence theory by as much as 15%. For the rational approximation, the Levine factor of 1.09 is not used in determining the constant escape cross section value from Eq. 4-65, and the Dancoff correction includes only the

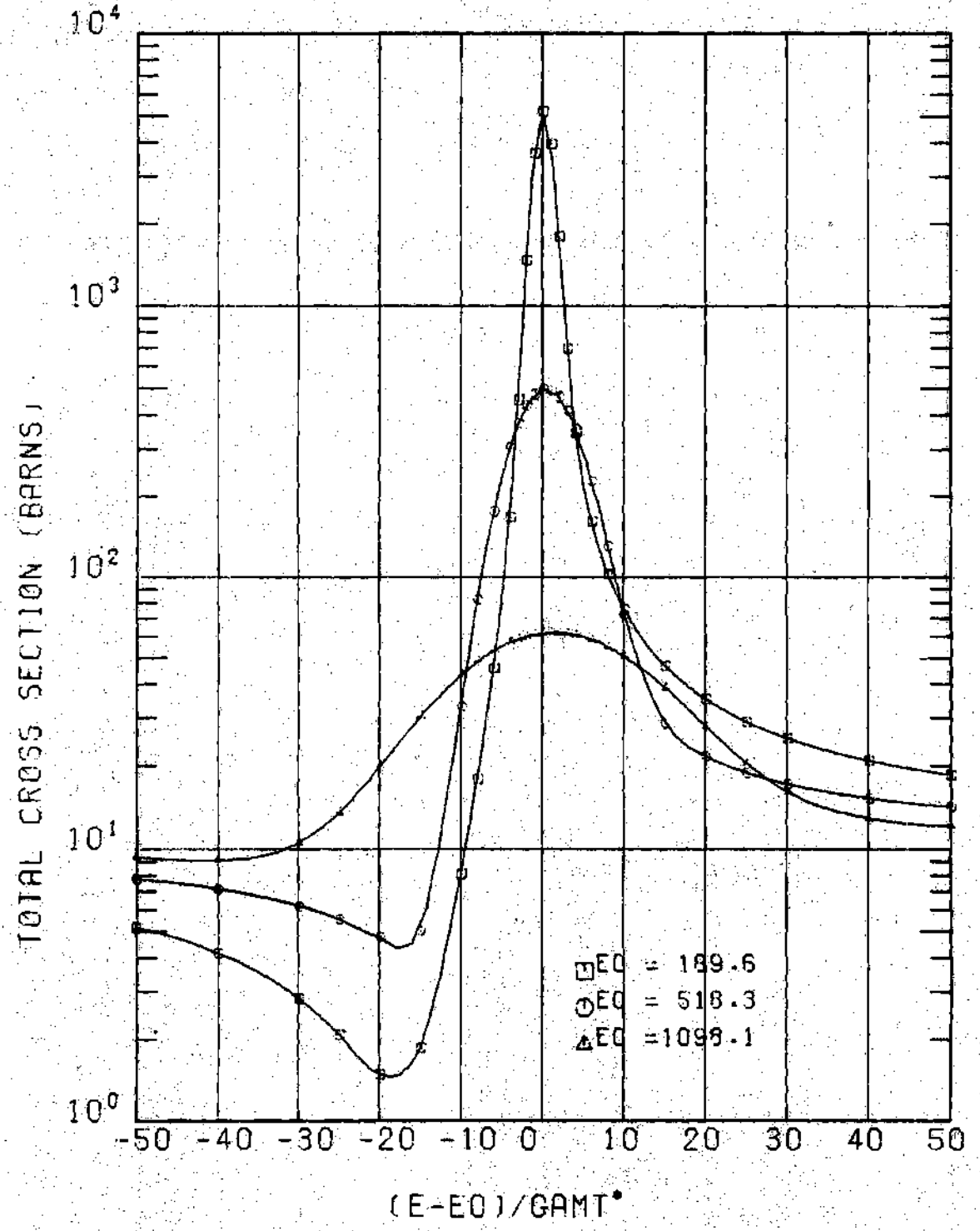

Figure 5. ^{238}U **Resonance Cross Sections at 293°K**
(*GAMT refers to Γ_t)

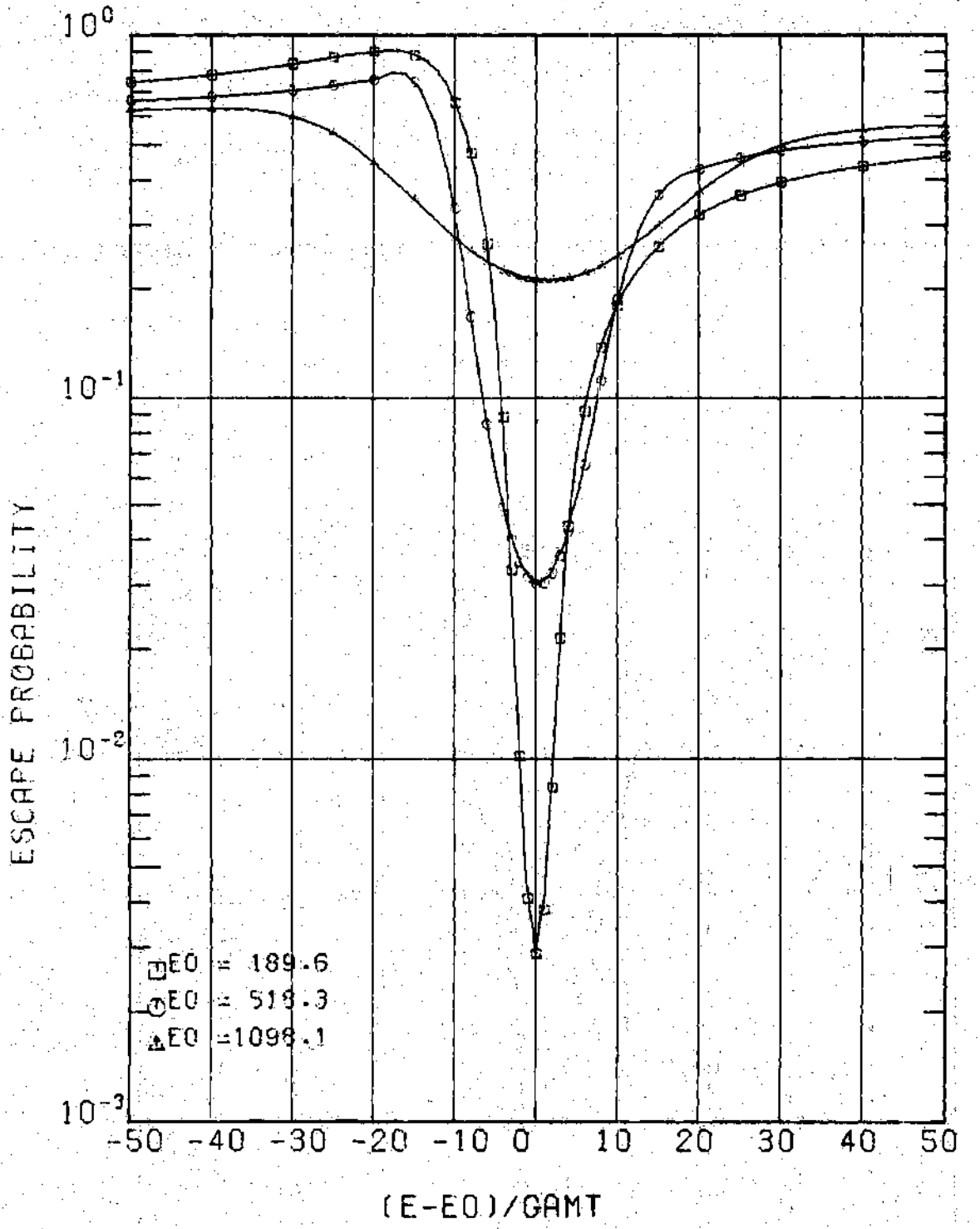

Figure 6. Escape Probabilities for ^{238}U Resonances in Assembly 5 Cell for a Flat Neutron Source

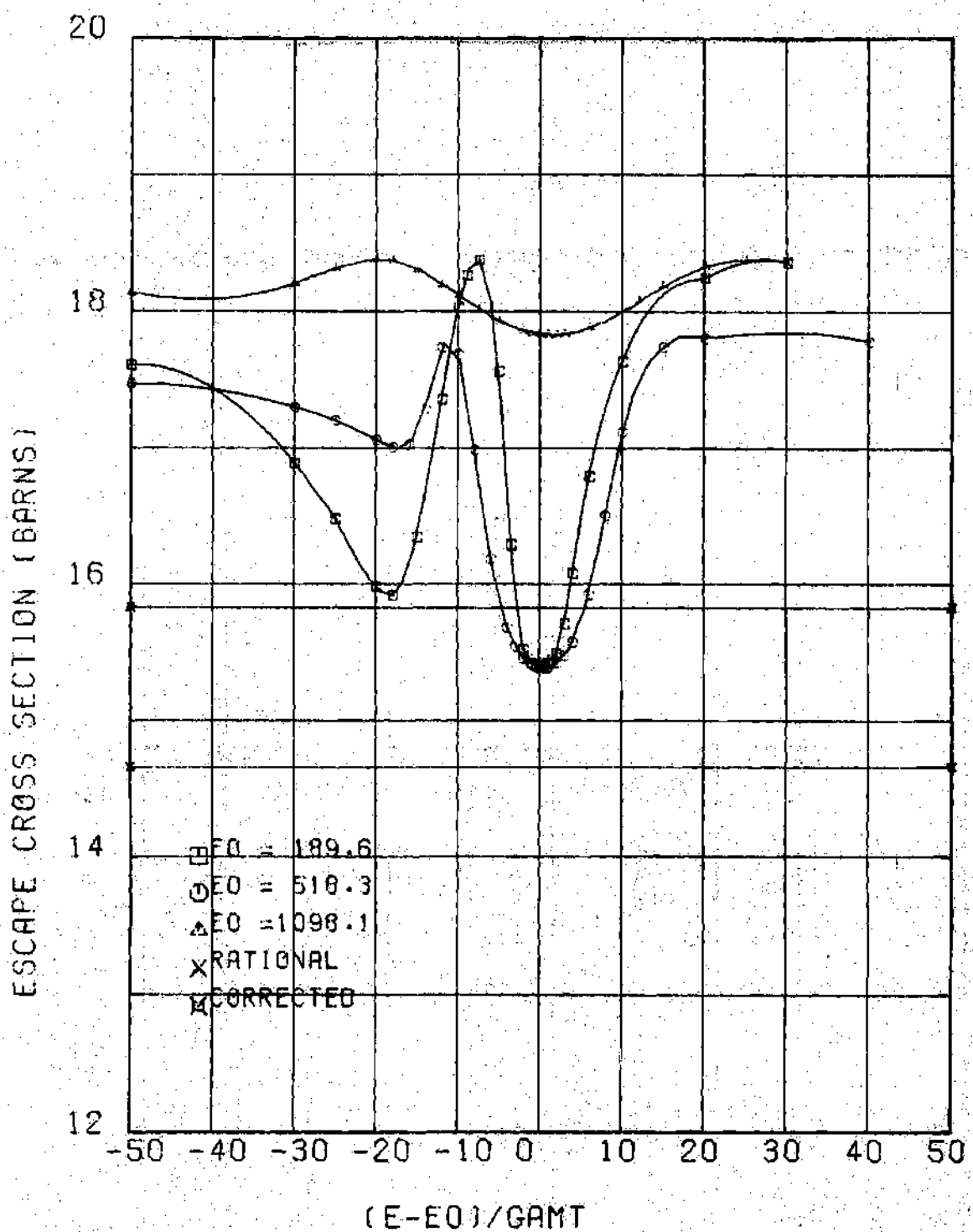

Figure 7. Escape Cross Sections for ^{238}U Resonances for a Flat Neutron Source

first term of Eq. 4-66. As shown in Figure 7 this results in an underprediction of the exact value. The Levine corrected constant including the improved Dancoff correction yields a more acceptable value around the resonance peak, but still tends to underpredict overall. Subsequent analysis will show additional deviations from the exact flat shape as well as the constant values due to nonuniformity in the neutron source.

Integral Transport Theory Analysis

In order to determine the degree of nonuniformity in the neutron source and the effect on the parameters of the general method, the two-region cell of Assembly 5 just described was analyzed by the integral transport theory method of Chapter IV. First of all, calculations for the three resonances examined above were made with comparisons to the exact treatment of the escape probability for a flat source. Then a parametric study of the nonuniformity effects for a sequence of artificial resonances which represent the resolved range for ^{238}U was performed to obtain data necessary for cross section averaging.

In the integral transport theory analysis the cell is described from the center of the ^{238}U plate to the center of the outer region as previously shown in Figure 4. The various nuclides present are noted in the figure; the atom density of ^{238}U is as previously noted and the composition of the outer region is given in Table 4. Cross sections for the outer region nuclides were obtained from an MC^2 equivalence theory calculation. The broad group cross section for the group in which the resonance occurred was used over the range of the calculation for that resonance.

Table 4. Outer Region Composition for Two-Region Cell of ZPR-6 Assembly 5

Nuclide	Concentration (10^{24} cm^{-3})
^{235}U	0.00202
C	0.01693
Na	0.01205
Fe	0.01184
Ni	0.00148
Cr	0.00313

The energy-dependent fluxes at the center of the plate, at the plate/outer region interface, and at the center of the outer region, or edge of the cell, for the three resonances of ^{238}U are shown in Figures 8-10. In each case the flux is normalized to unity, and uniform across the cell, at E_o/α^3 or $E_o + 50\Gamma_t$, whichever is larger. The magnitude of the flux depression in the plate and the accompanying depression in the outer region is seen in each case. The depression of the flux in the plate for the 189.6 eV resonance is seen to be quite large and Figure 11 shows the spatial flux profile for this resonance at a few energy points. It is such flux depressions that yield nonuniformity in the neutron source as can be seen in Figure 12. The source nonuniformity is also reflected in the nonuniformity factor f(E) shown in Figure 13 for each of the three resonances. Recall that f(E) is unity for a flat source, which shows that the slowing-down source through the 1098.1 eV resonance is flat. For the 518.3 eV resonance there is some nonuniformity and a larger amount for the 189.6 eV resonance.

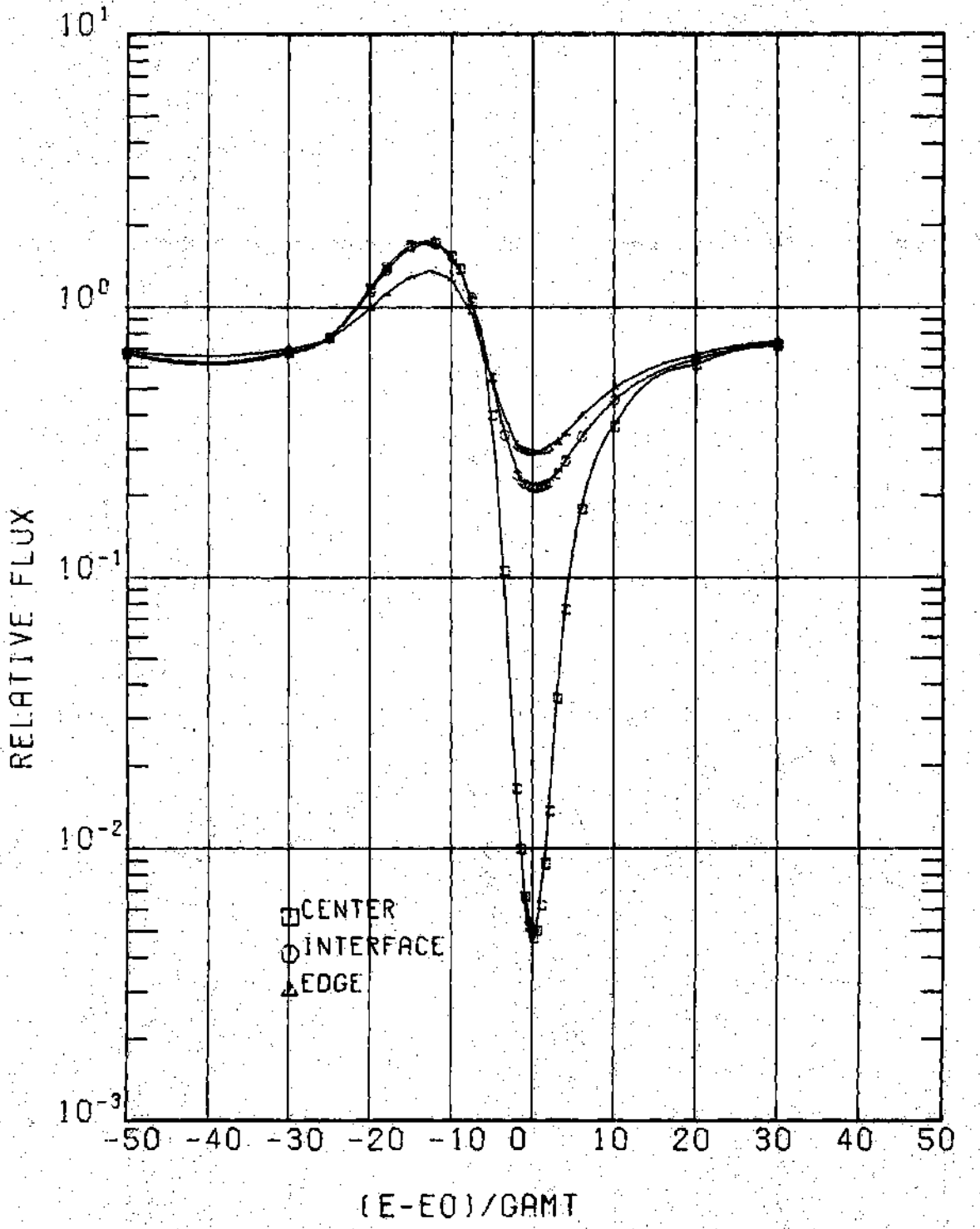

Figure 8. Energy Dependent Flux Around 189.6 eV Resonance

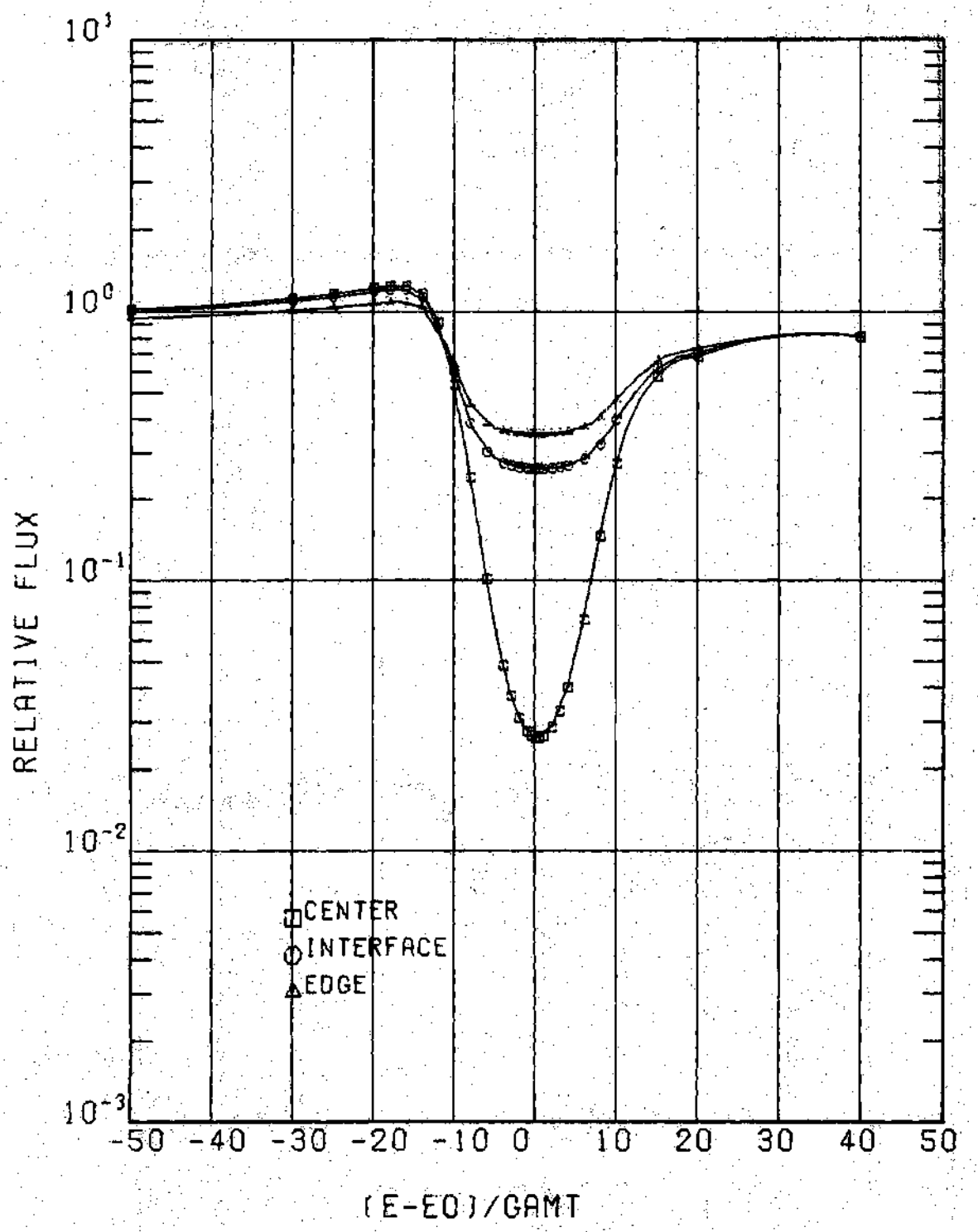

Figure 9. Energy Dependent Flux Around 518.3 eV Resonance

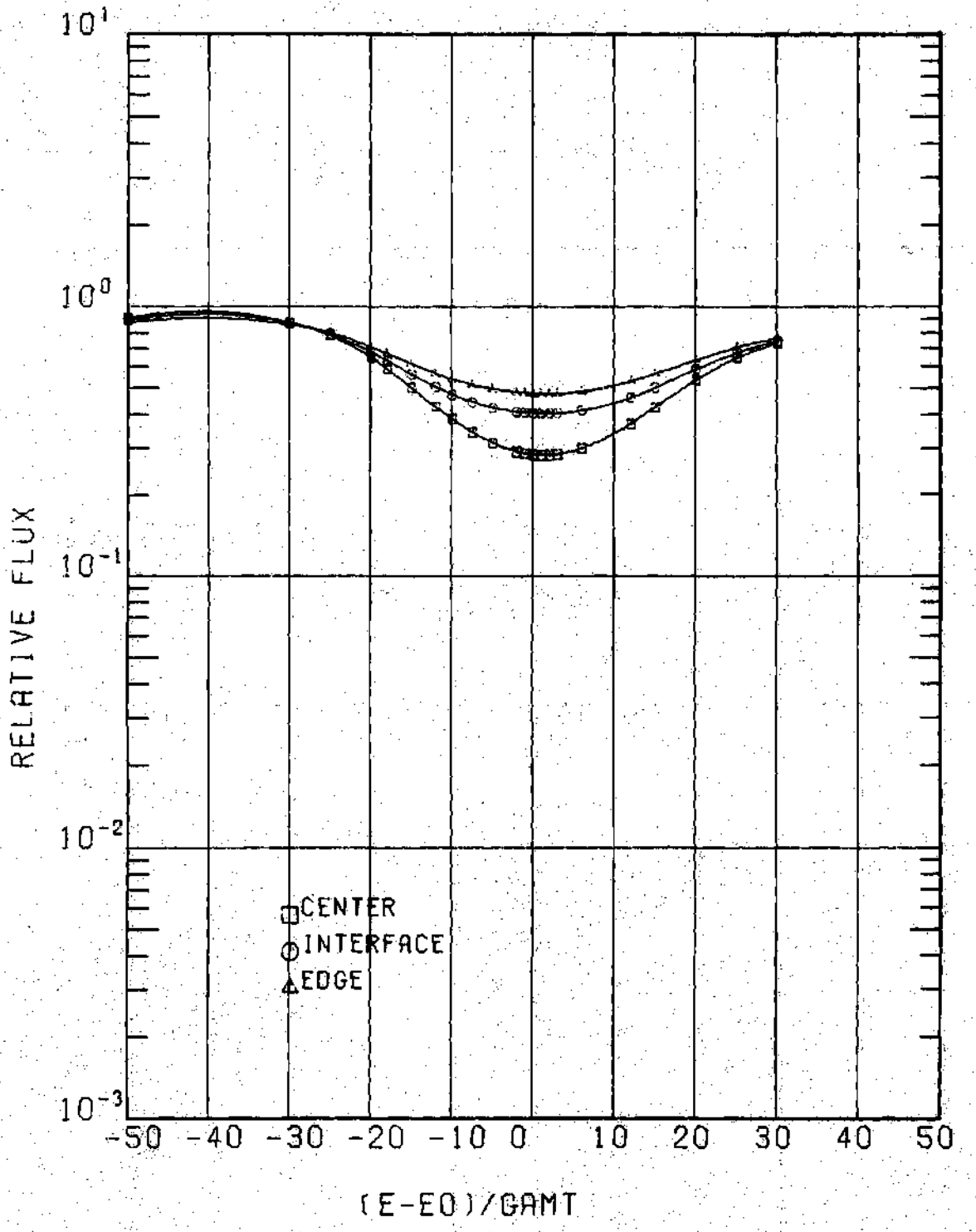

Figure 10. Energy Dependent Flux Around 1098.1 eV Resonance

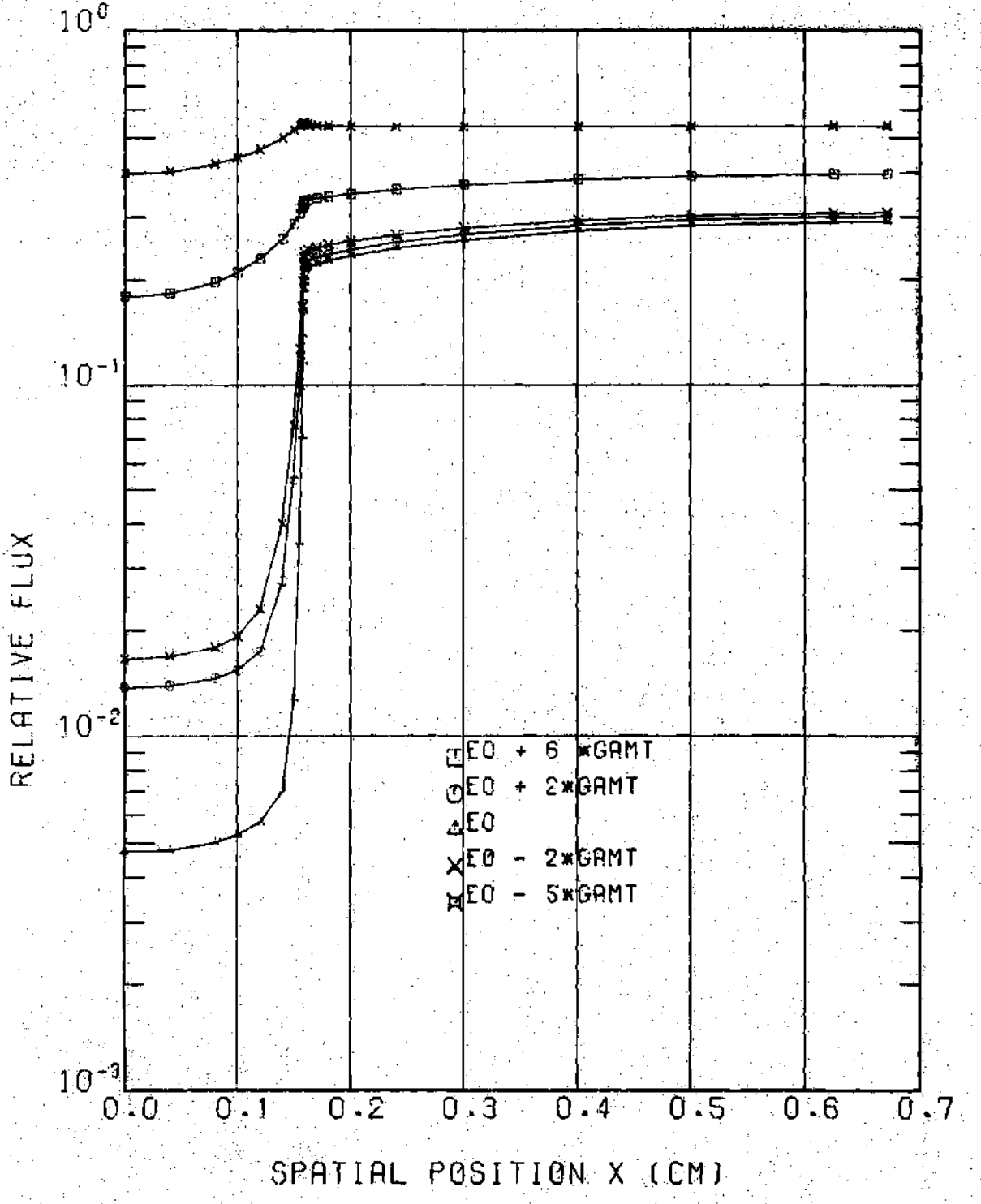

Figure 11. Spatially Dependent Flux for 189.6 eV Resonance

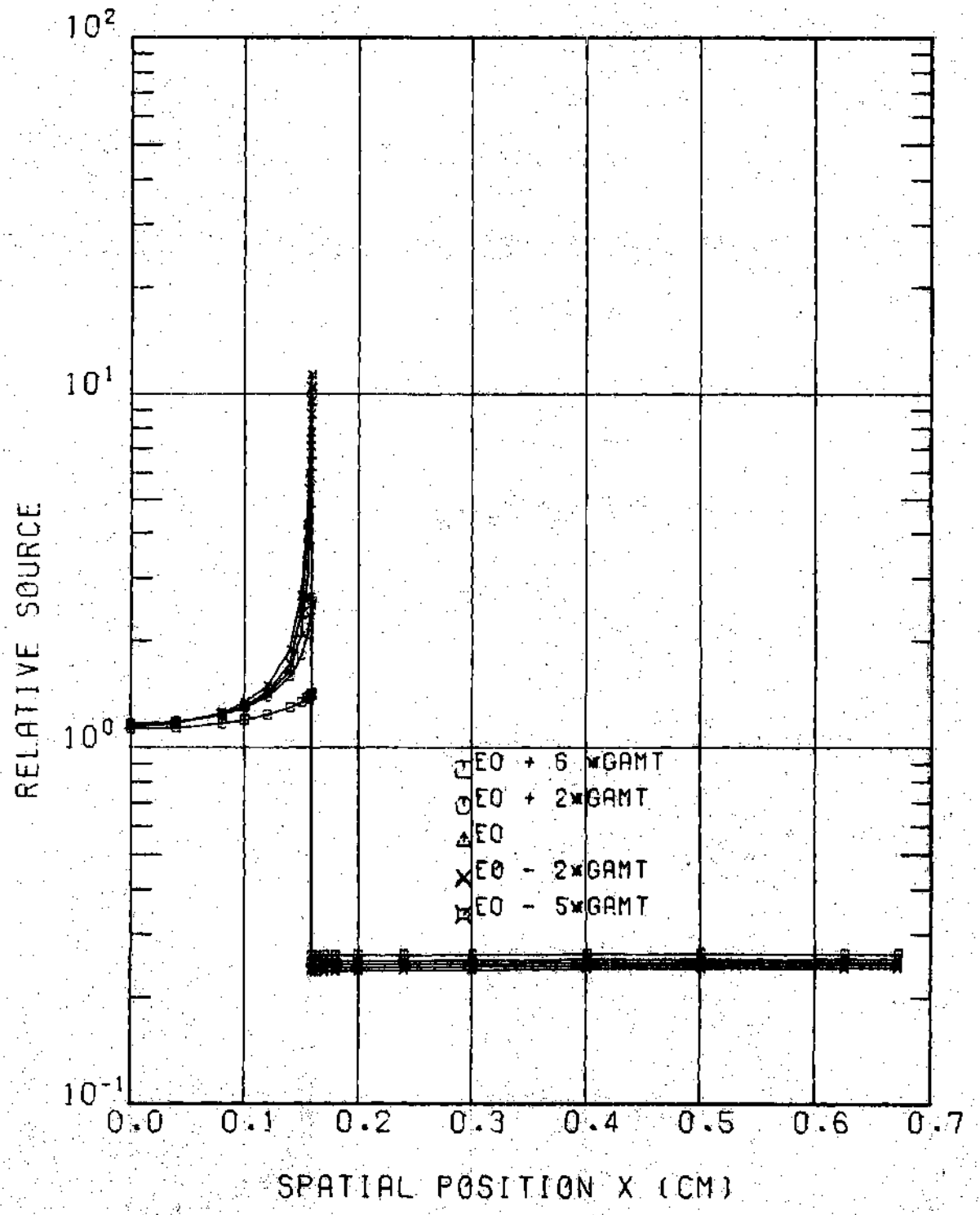

Figure 12. Spatially Dependent Source for 189.6 eV Resonance

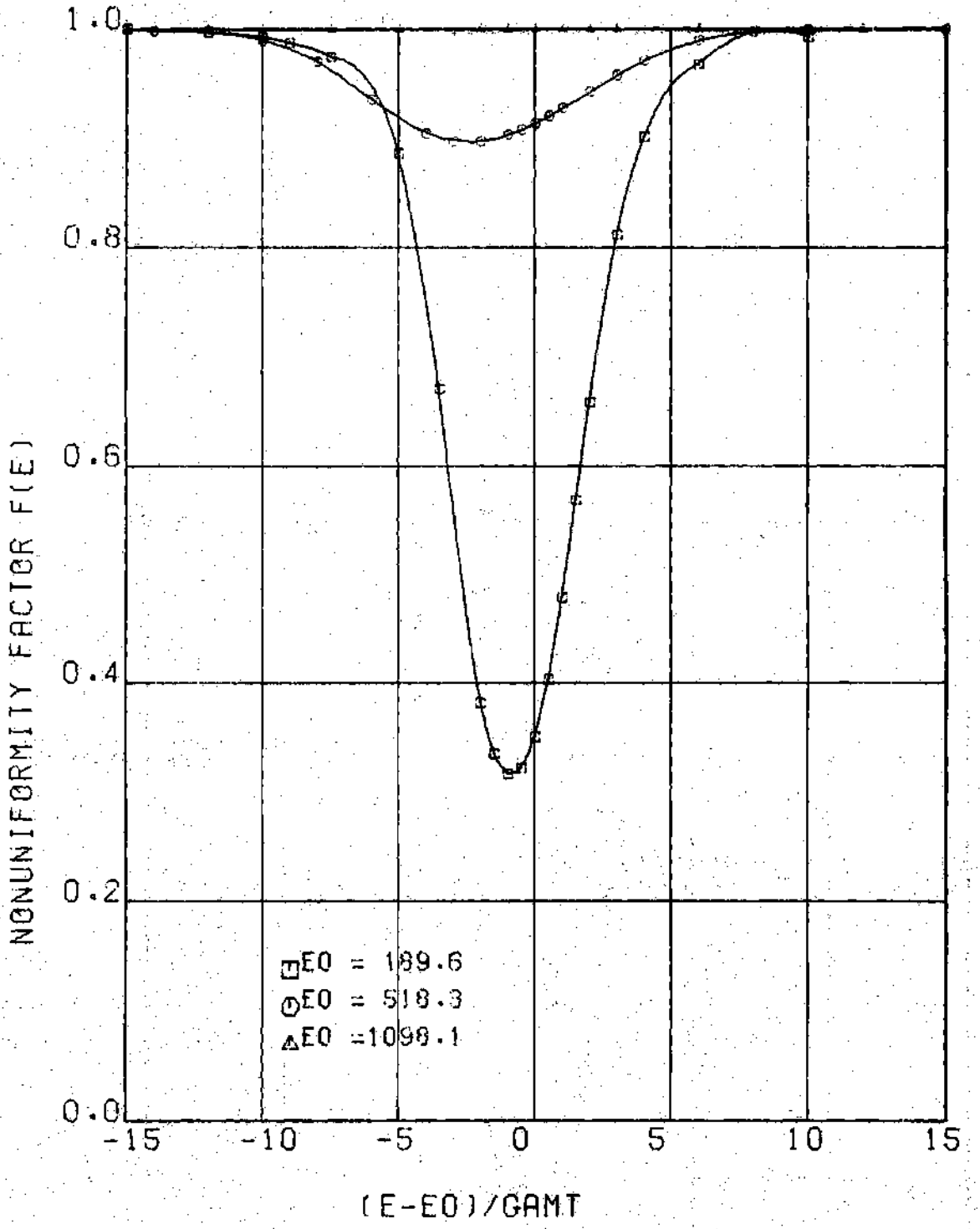

Figure 13. Nonuniformity Factor f(E) for ^{238}U Resonances

The nonuniformity of the neutron source is also reflected in the shape of the escape cross section as determined by the escape probability for the nonuniform source. Escape cross sections for the three resonances are given in Figure 14. Comparison to Figure 7, which is for a flat source, shows no difference for the 1098.1 eV resonance, but differences of over a factor of three near the center of the 189.6 eV resonance. Careful inspection shows, in Figure 14 and more obviously in Figure 13, that the effect of nonuniformity is not symmetric about the center of the resonance. For these cases the minimum value of f(E) occurs below the center of the resonance because the slowing-down source below the center has been affected by a larger portion of the resonance than has an equally spaced point above the center. Interference scattering and the accompanying smaller cross section values also affect the shape below the center as the flux and source recover rapidly.

Choosing the strong 189.6 eV resonance, it is instructive to investigate the impact of nonuniformity on the general flux expression given by Eq. 4-60. In that expression the escape cross section appears in the numerator multiplied by f(E) and in the denominator added to the total cross section. Although the escape cross section reflecting the nonuniform source is greater than three times the exact flat value near the center of the resonance, the net difference when comparing the sums with the large total cross section value is only about 1%. The difference between the nonuniform treatment and the exact flat treatment as reflected in the numerator can be seen by comparing $f(E) \times \sigma_e(E)$ for the nonuniform case to the escape cross section for a flat source. For this particular resonance,

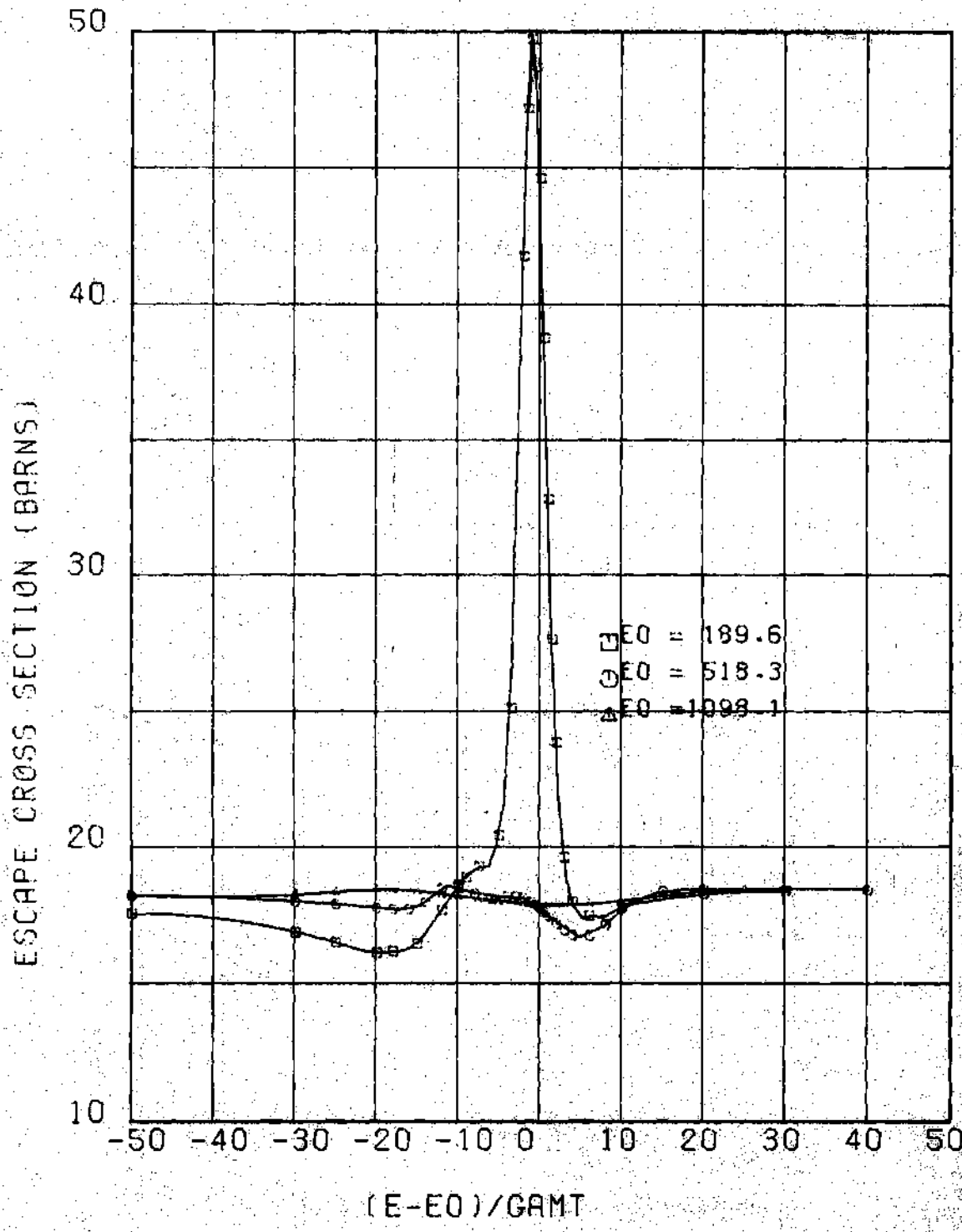

Figure 14. Escape Cross Sections for ^{238}U Resonances

the product of the factors for the nonuniform case near the center of the resonance is only 3% higher than the escape cross section for a flat source. Hence the effect of nonuniformity of f(E) and $\sigma_e(E)$ combine to compensate, yielding a net result very similar to that for a flat source.

The compensating effect can perhaps be seen more clearly by examination of the escape probability, rather than the artificial escape cross section. The reaction rate balance given in the collision density equation of Eq. 3-41 provides a mechanism for comparing the difference due to nonuniform or flat source treatment. For the same source magnitudes with the two treatments, differences in the collision rate expression can be due only to the escape probability and f(E). The specific comparisons to be made are for the term $1-P_{1\to2}(E)$ and for $f(E) \times P_{1\to2}(E)$ for the two treatments. Such comparisons can be made by examination of Figure 15 which gives the escape probabilities for the nonuniform source and flat source as well as f(E) times the escape probability for the nonuniform source. The escape probability for the nonuniform source is seen to be significantly greater than that for the flat source near the center of the resonance, but at such points both values are much less than unity. When the nonuniform escape probability is multiplied by f(E) one also sees that compensation results, yielding values very much the same as the exact flat case.

A more detailed assessment of the effects of nonuniformity on the escape probabilities and parameters of the general method, and the potential effects on cross section averaging, requires investigation over a larger number of resonances than just the three cases noted above. In order to perform such an assessment then, a parametric evaluation was

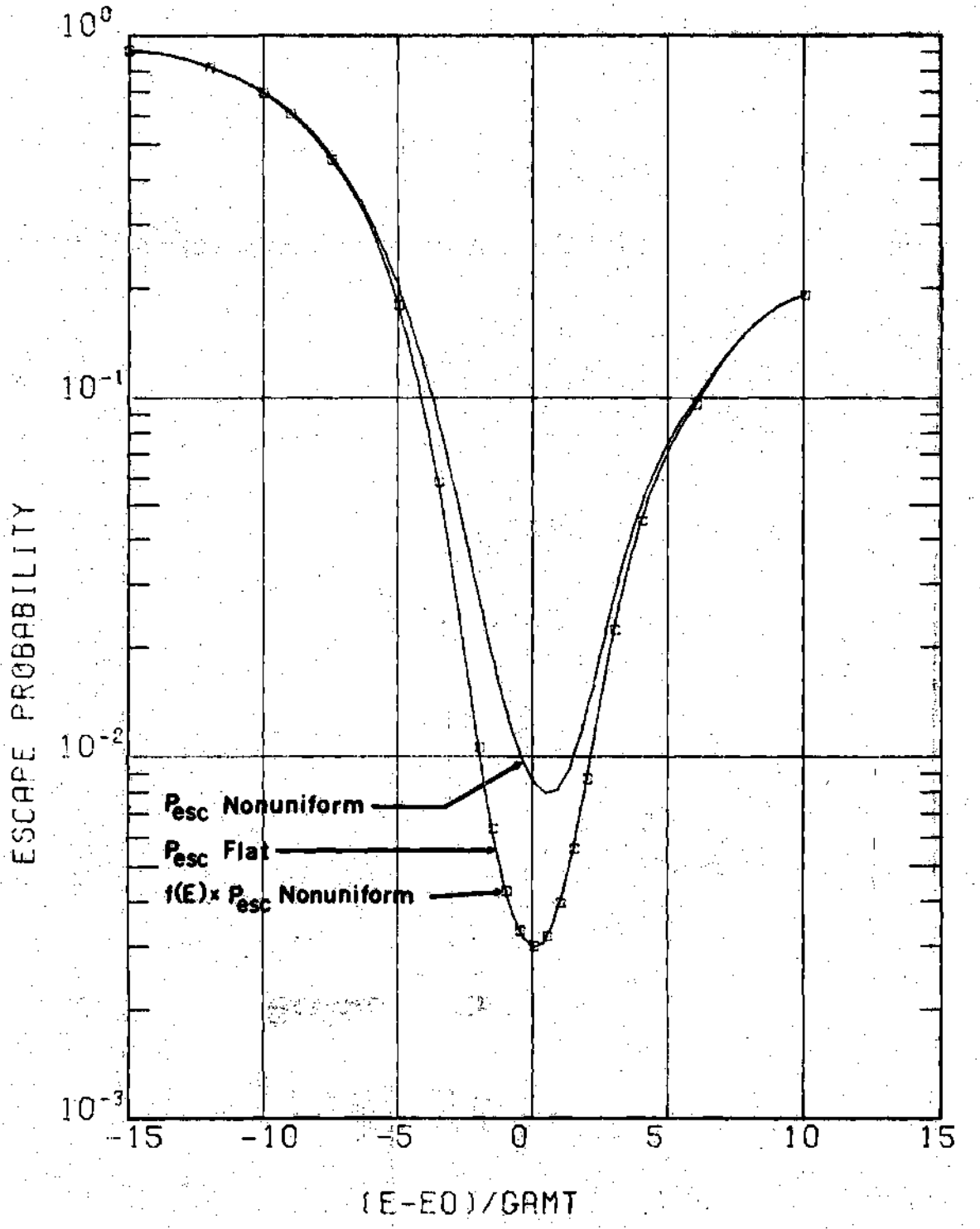

Figure 15. Escape Probability Comparisons for Flat and Nonuniform Sources Around 189.6 eV Resonance

carried out using artificial resonances which represented the resolved range for ^{238}U. An entire analysis of the 199 resolved s-wave resonances of ^{238}U as given in ENDF/B-III would be prohibitive, but studies of a parametric nature over selected resonance parameters can be used to obtain data for the actual resonances.

The resonance parameters from which combinations were used for the parametric evaluation of nonuniformity effects in the two-region cell of Assembly 5 are given in Table 5. Four different peak energies and six different neutron widths are given; a constant capture width of 0.0235 eV was used for each combination.

Table 5. Resonance Parameters for Parametric Study of Nonuniformity in Two-Region Cell of ZPR-6 Assembly 5

Peak Energy (eV)	Neutron Width (eV)
100.	0.002
400.	0.010
1000.	0.050
2000.	0.100
	0.200
	0.400

During the parametric study every combination of resonance parameters was not investigated. Calculations for some resonances showed little effect, so smaller resonances at the same energy were not evaluated. There were also two combinations with Γ_n = 0.4 eV, at 100. eV and 400. eV, which yield resonances significantly larger than any actually occurring in those

energy ranges. With these guidelines, sixteen resonance calculations were performed as noted in the matrix of Table 6. These cases should reasonably represent the resolved resonance range of ^{238}U.

Table 6. Parametric Cases Investigated for Nonuniformity Effects in Two-Region Cell of ZPR-6 Assembly 5

Neutron Width (eV)	Peak Energy (eV)			
	100.	400.	1000.	2000.
0.002	x			
0.010	x	x		
0.050	x	x	x	
0.100	x	x	x	x
0.200	x	x	x	x
0.400			x	x

The effects of nonuniformity determined by the parametric study as reflected by the parameter f(E) are shown for the various neutron widths for the four peak energies in Figures 16-19. Substantial deviation from unity for the larger neutron widths at lower energies is obvious. A summary of the effects on this parameter is shown in Figure 20, which gives the minimum value of f(E) as a function of neutron width for the various peak energies. The same results are also shown in Figure 21 as a function of peak energy. A comparison of escape probabilities for the nonuniform sources and for a flat source at the peak energy of the resonance is shown in Table 7. The compensation effect is also shown in the table by

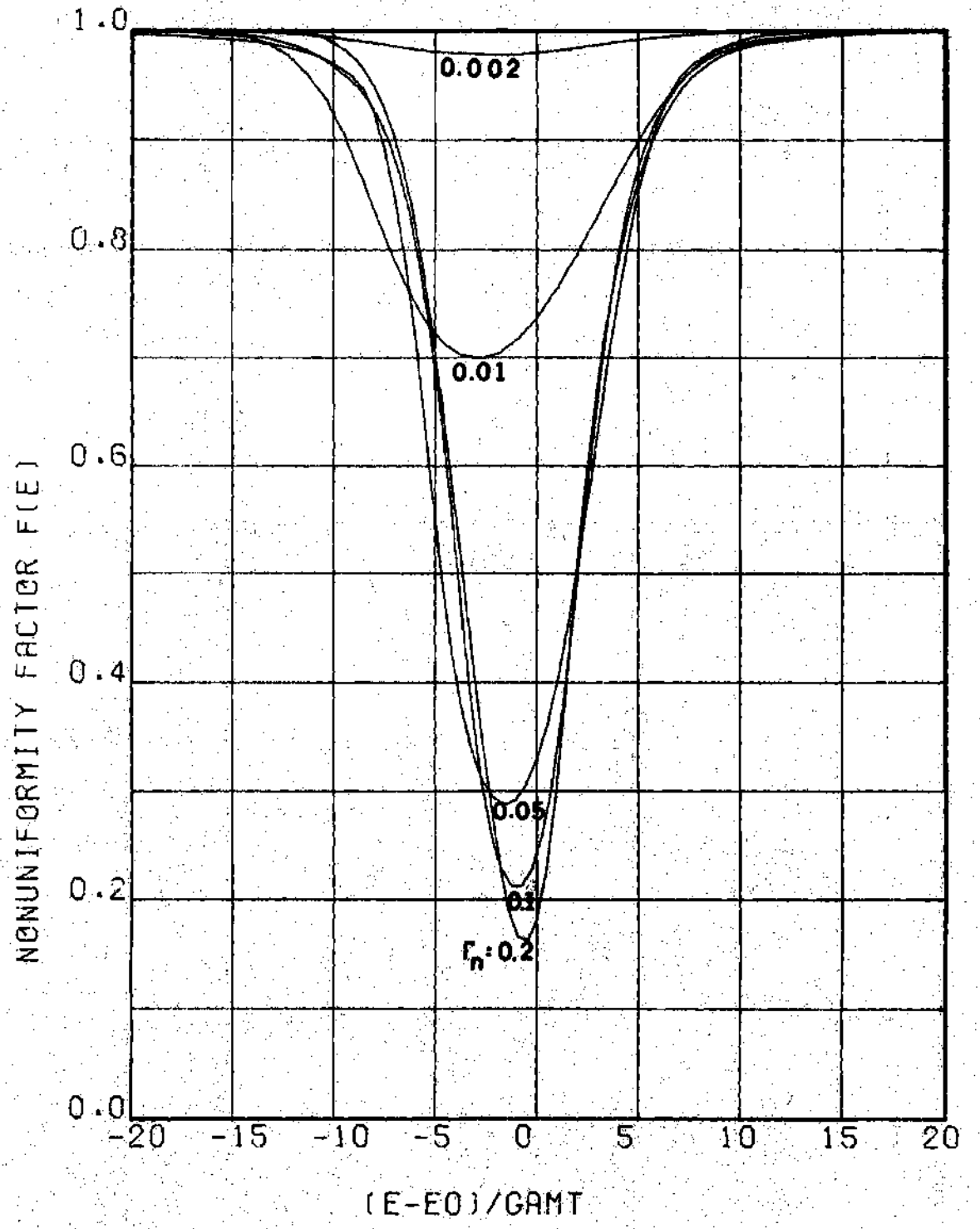

Figure 16. Nonuniformity Factor f(E) for Various Neutron Widths at E_o = 100 eV

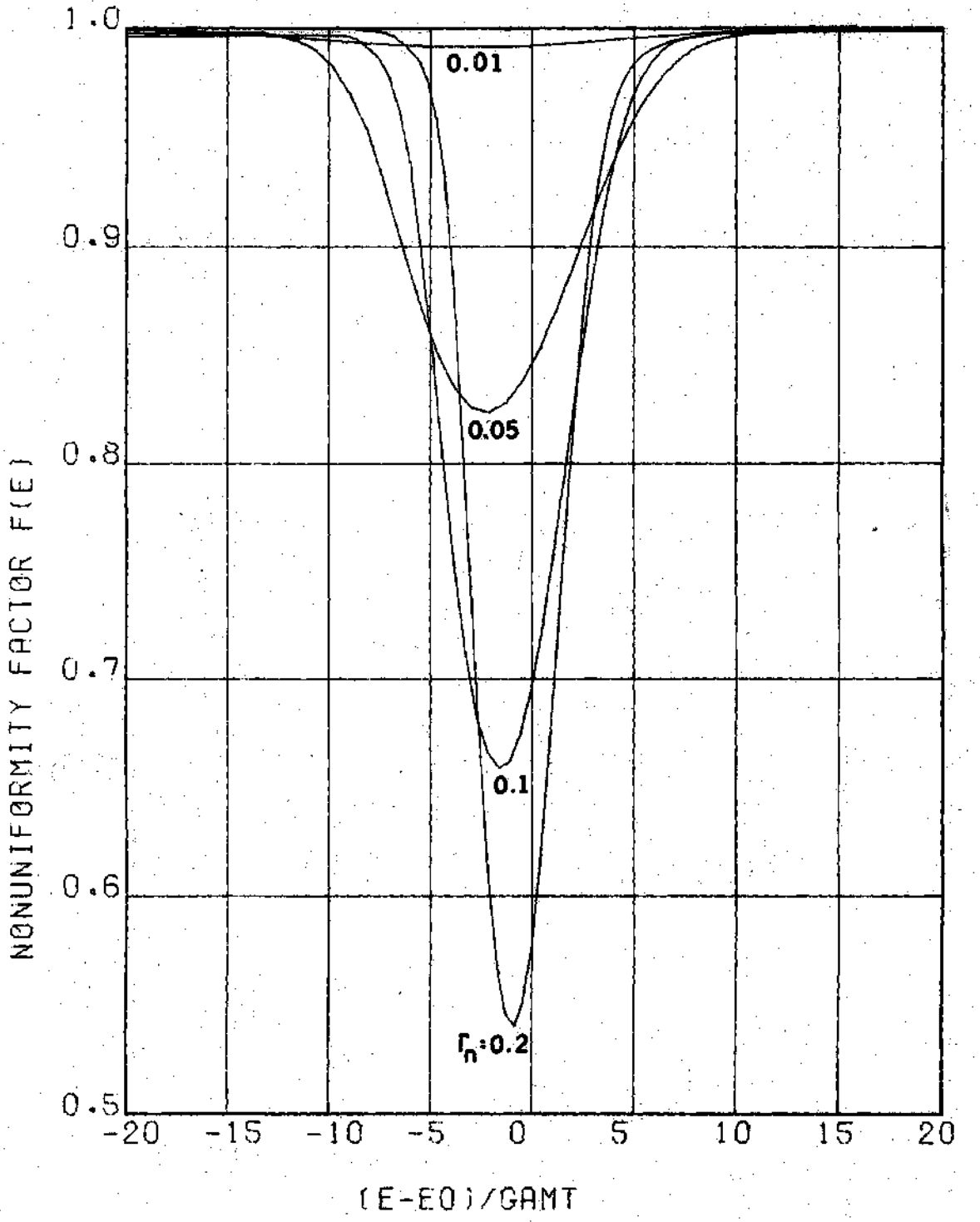

Figure 17. Nonuniformity Factor f(E) for Various Neutron Widths at E_o = 400 eV

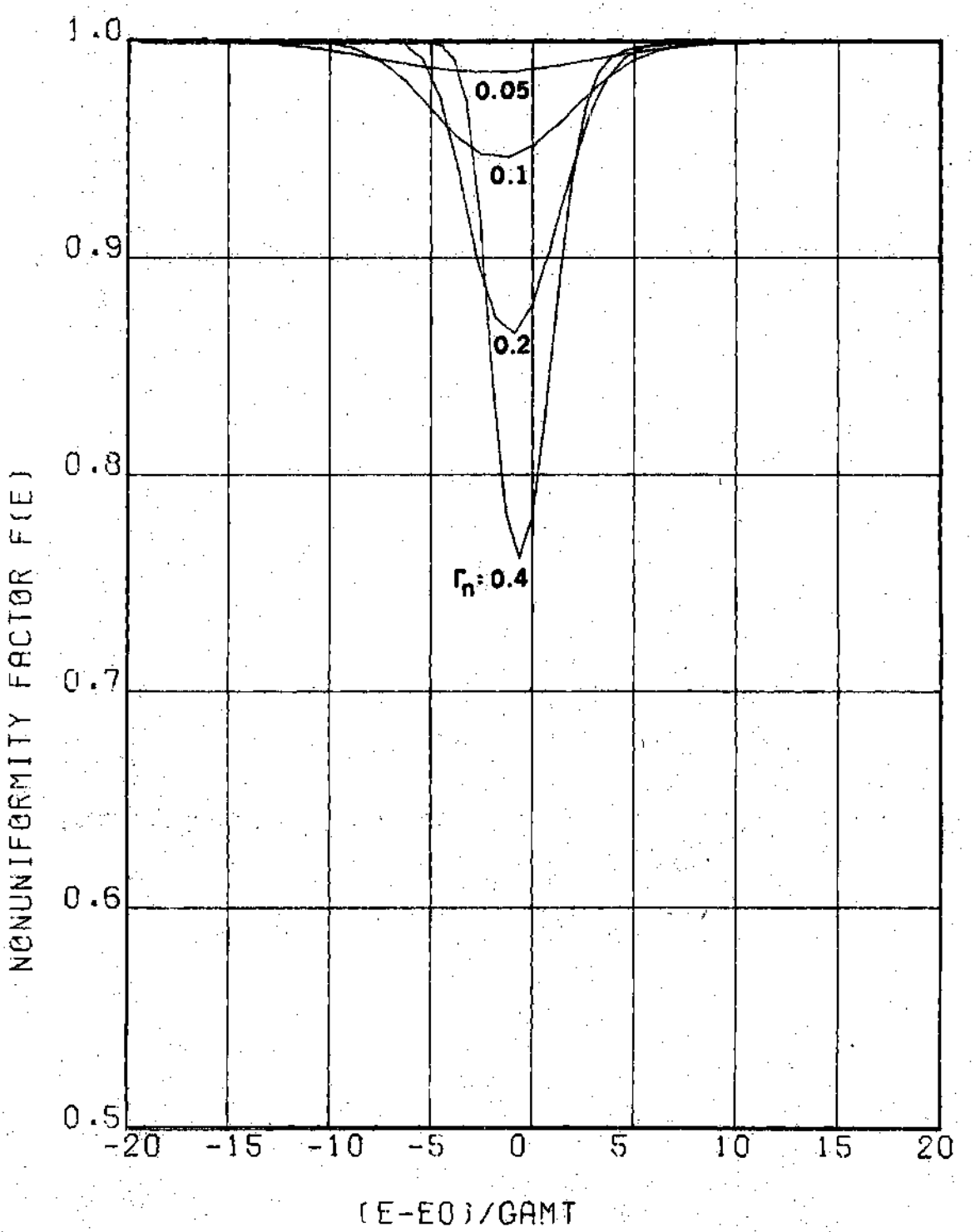

Figure 18. Nonuniformity Factor f(E) for Various Neutron Widths at E_o = 1000 eV

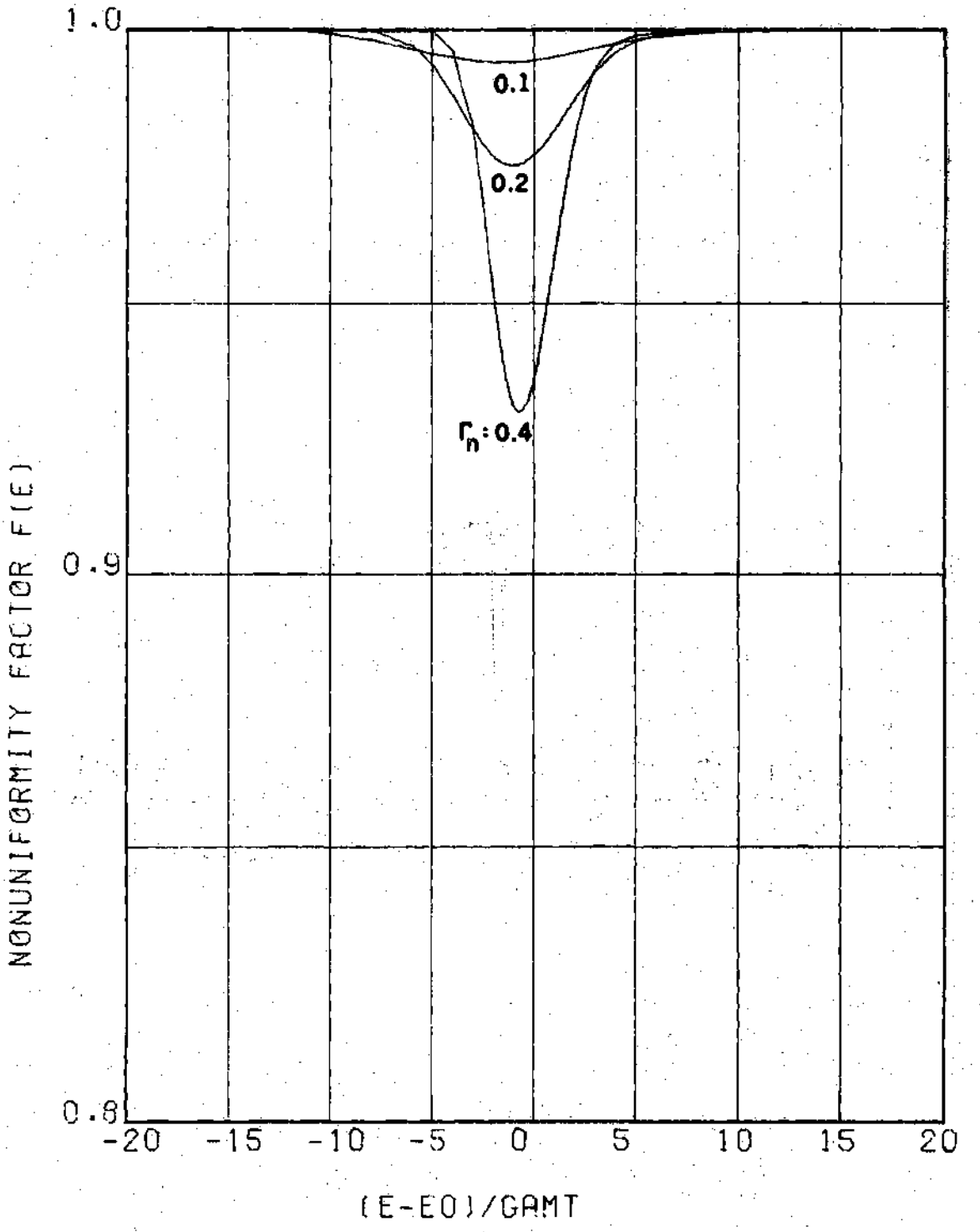

Figure 19. Nonuniformity Factor f(E) for Various Neutron Widths at E_o = 2000 eV

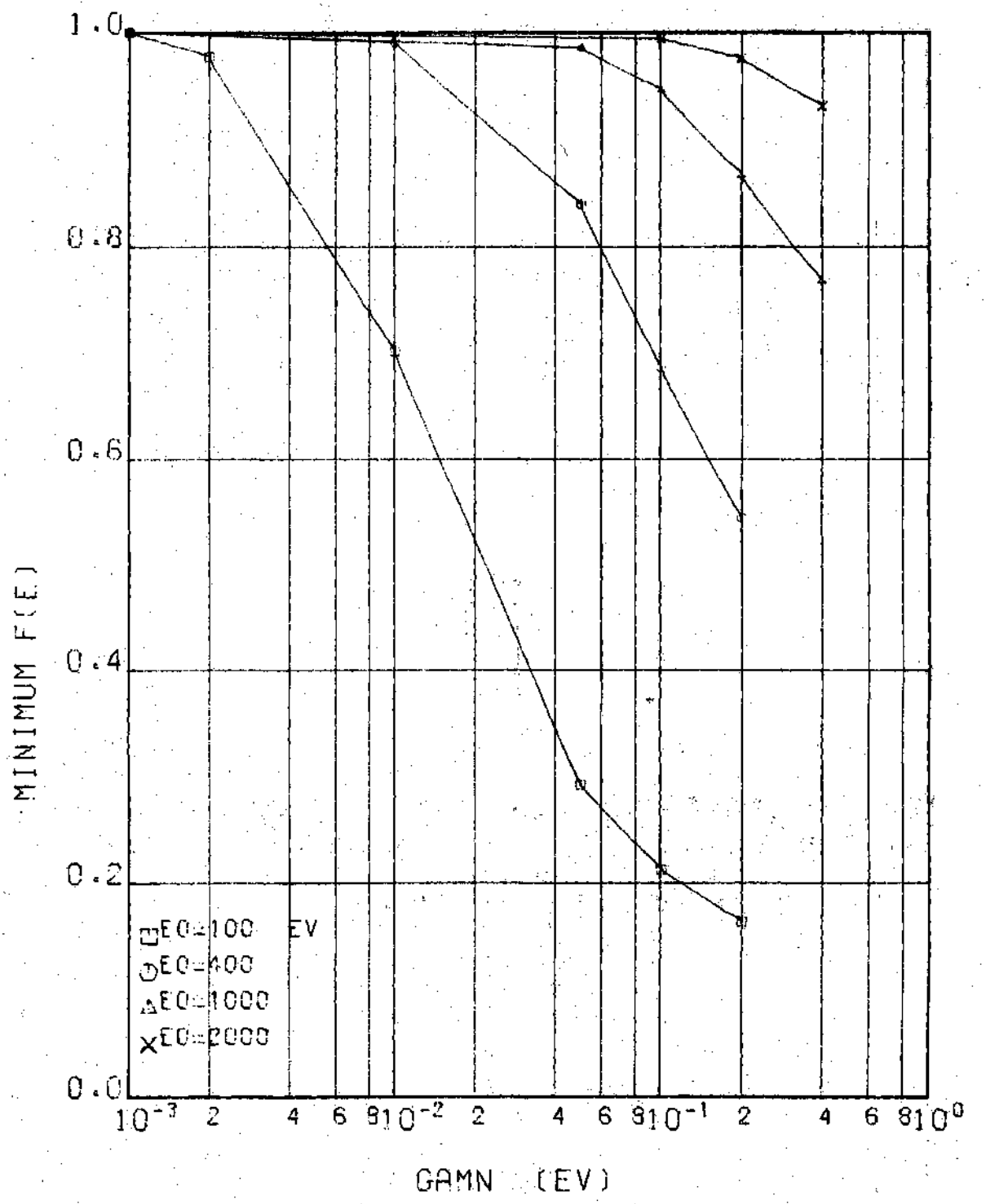

Figure 20. Minimum Values of f(E) as a Function of Neutron Width

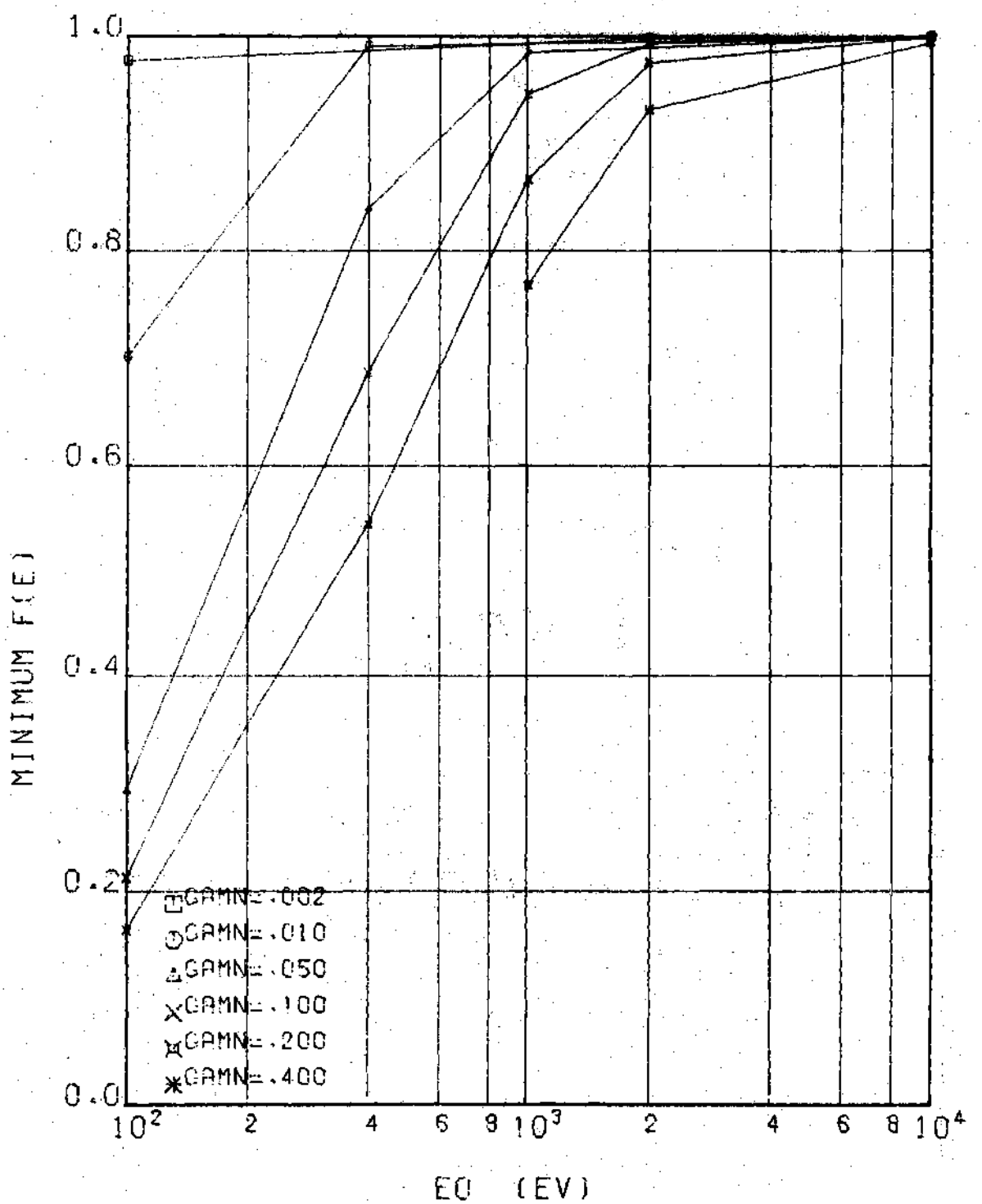

Figure 21. Minimum Values of f(E) as a Function of Peak Energy

Table 7. Escape Probability at the Resonance Peak Energy for Parametric Cases

E_o (eV)	Γ_n (eV)	P_{esc} Nonuniform	P_{esc} Flat	$f(E) \times P_{esc}$ Nonuniform
100.	0.002	7.321-2	7.170-2	7.177-2
	0.010	2.068-2	1.527-2	1.534-2
	0.050	1.035-2	3.406-3	3.442-3
	0.100	7.936-3	1.918-3	1.937-3
	0.200	6.490-3	1.186-3	1.193-3
400.	0.010	1.019-1	1.011-1	1.012-1
	0.050	2.713-2	2.293-2	2.293-2
	0.100	1.771-2	1.231-2	1.231-2
	0.200	1.209-2	6.966-3	7.005-3
1000.	0.050	8.157-2	8.048-2	8.054-2
	0.100	4.566-2	4.345-2	4.352-2
	0.200	2.719-2	2.388-2	2.395-2
	0.400	1.789-2	1.395-2	1.402-2
2000.	0.100	1.147-1	1.141-1	1.141-1
	0.200	6.550-2	6.400-2	6.407-2
	0.400	3.906-2	3.653-2	3.661-2

Note: Read values such as 7.321-2 as 7.321×10^{-2}.

comparison of f(E) times the escape probability of the nonuniform source to the exact flat escape probability.

Additional examination of the parametric cases gave a basis for the compensating effect. It was observed that the probability of neutrons within the outer region escaping into the plate region was never more than 1% different from that for a flat source. This observation can be used to restate the general reciprocity relation of Eq. 4-53 to the form

$$f(E) = \frac{P_{1\to 2}^{flat}(E)}{P_{1\to 2}^{Nonuniform}(E)} \tag{5-1}$$

This expression is possible due to the fact that the numerator of Eq. 4-53 can be replaced by $P_{1\to 2}^{flat}(E)\,\Sigma_{t1}(E)V_1$ according to the flat-flux reciprocity relation of Eq. 3-38. The excape cross section can then be rewritten as

$$\sigma_e(E) = \frac{\sigma_{t1}(E)P_{1\to 2}^{flat}(E)}{f(E) - P_{1\to 2}^{flat}(E)}. \tag{5-2}$$

With this simplification the effect of nonuniformity is completely contained in f(E).

In order to extend the data for f(E) from the parametric study to the actual resonances of ^{238}U an interpolation in energy and neutron width was used. The parametric data were first fitted to a consistent mesh of 41 points from $-50\Gamma_t$ to $50\Gamma_t$ about the resonance peak energy. This was necessary because different energy meshes were used in the integral transport calculations, tailored to the particular cross section behavior. A cubic spline interpolation was used to go from the specific meshes to the

consistent mesh; 25 points in the consistent mesh were used between $\pm 5\Gamma_t$. From the data in the consistent mesh structure a logarithmic interpolation in energy and neutron width between parametric points was used to obtain f(E) for the actual resonances from the parametric data. Based on the shapes shown in Figures 20 and 21, the logarithmic interpolation appears adequate. As additional input for interpolation, f(E) was assumed to be unity at Γ_n = .001 eV and at E_o = 10000. eV. As a check on the fitting, results were compared to the calculations for the three actual ^{238}U resonances previously noted. A comparison of the fitted to the calculated results for the 189.6 eV resonance is given in Figure 22. The smooth curve represents the fitted data and the points are from actual calculation. Agreement between the two shapes is excellent with a maximum difference of about 6% at the minimum value. This deviation is most likely due to the use of a constant capture width of 0.0235 eV in the parametric study, whereas the actual capture width for this resonance is 0.0247 eV. Comparisons between fitted and actual data for the other two smaller resonances is better; a maximum difference of 0.5% was found for the 518.3 eV resonance and less than 0.01% for the 1098.1 eV resonance.

Cross Section Averaging

Having fitted the nonuniformity parameter f(E) to the actual ^{238}U resonances, cross section averages were obtained by the methods noted in Chapter IV. By the same method, averages were calculated using equivalence theory and the exact escape probability treatment for a flat source. For the purpose of cross section averaging the outer region source was assumed to have the asymptotic 1/E shape for all cases. For equivalence theory

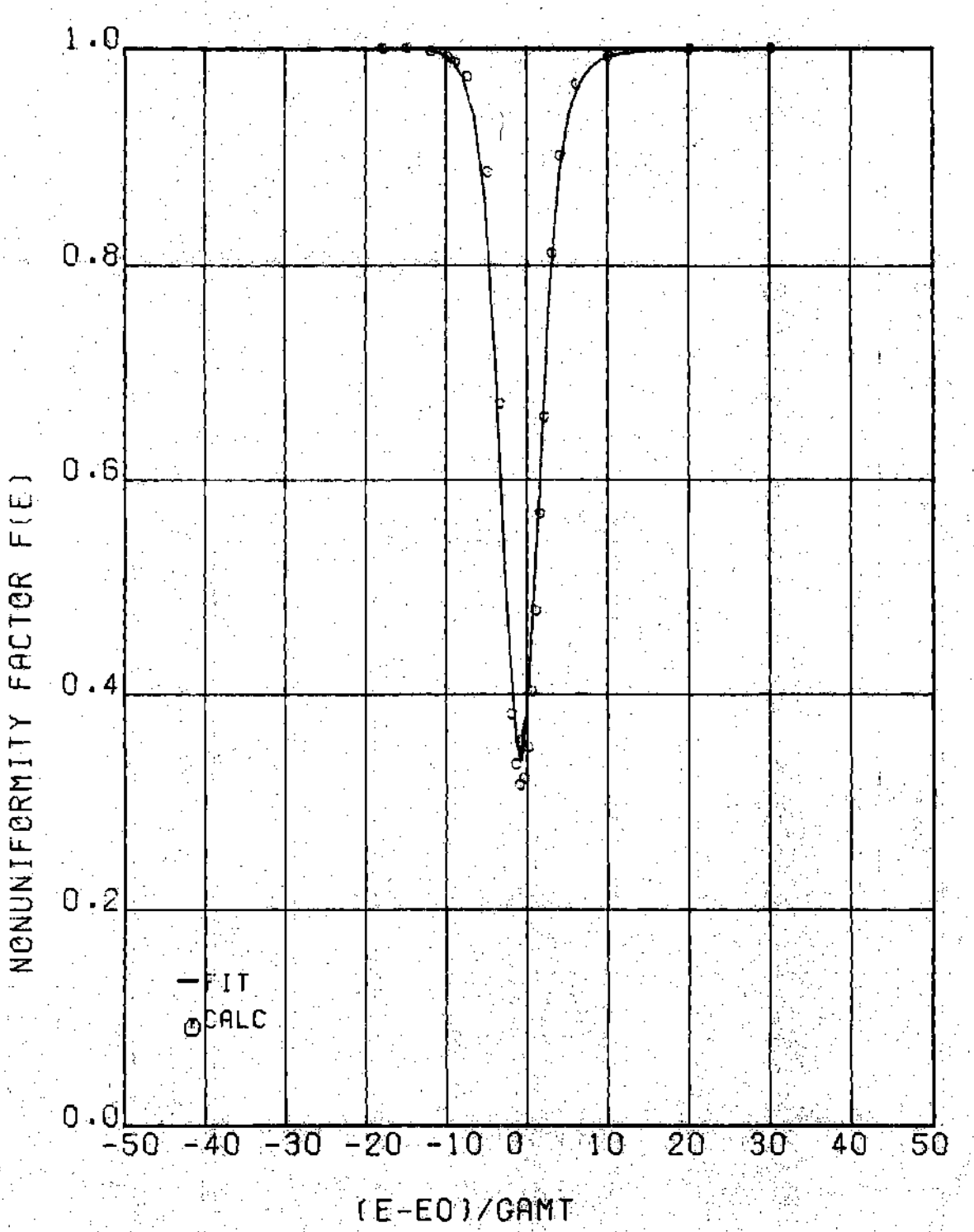

Figure 22. Comparison of Fitted and Calculated f(E) Shape

and the exact flat treatment the plate source was treated by the NR approximation. For the nonuniform source treatment the plate region source was determined by iterative solution of the collision rate expression with the NR approximation as an initial guess.

Cross section averages for the three treatments noted above are given in Table 8 for the two-region cell of Assembly 5. Only the resolved s-wave resonances of ^{238}U were included; the energy structure and indices of the broad groups are the same as in Reference 79; the upper bound of group 15 is 4307. eV. From the tabulated results, it can be seen that there is very little difference between the three treatments of heterogeneity. Equivalence theory results are seen to be consistently the smallest, exact flat the largest, with the nonuniform treatment between then; the maximum difference is hardly more than 1% though. The compensating effects which occur in the nonuniform treatment have been noted to tend toward the exact flat treatment, and any remaining effects appear to give slight reductions which tend toward the equivalence theory results.

Table 8. Effective Resonance Cross Sections for the Two-Region Cell of ZPR-6 Assembly 5 (Barns)

Group	E_{lo}(eV)	Equivalence Theory	Exact Flat	Nonuniform
15	2612.	0.3875	0.3925	0.3886
16	2035.	0.5202	0.5275	0.5214
17	1234.	0.5318	0.5425	0.5350
18	961.	0.6443	0.6539	0.6466
19	582.9	0.8005	0.8121	0.8021
20	275.4	0.6871	0.6987	0.6894
21	101.3	1.1224	1.1305	1.1218
22	29.02	1.7327	1.7427	1.7318
23	13.71	2.7702	2.7852	2.7696

In order to obtain independent assessment of the nonuniformity effect on the effective cross sections and to verify the magnitude of the cross sections, comparative calculations were performed. Equivalence theory calculations were performed using the MC^2 module of the Argonne Reactor Computation (ARC) System,[57] and integral transport theory calculations were made with the latest version of the RABBLE code.[65,66] RABBLE runs were made first with only the two regions of the Assembly 5 cell, then each region was divided into five subregions to determine the effect of nonuniformity.

Before meaningful comparisons could be made between the MC^2 and RABBLE results and the above data, certain differences had to be accounted for. First of all, MC^2 includes both s- and p-wave resonances in the resolved resonance range. It also includes unresolved resonances and a background capture cross section. The unresolved resonances affect only group 15 and the contribution to the total capture cross section is specified. The amount of the background capture cross section is also specified. The breakdown of the resolved resonance component is not specified so the fraction attributed to just s-wave had to be determined. The RABBLE code was used to determine this contribution by calculating the average capture cross sections with and without the p-wave resonances. The net amount associated with the p-wave resonances was from about 0.1 barns in the higher group to 0.007 barns in Group 23. The resulting cross section comparison for just the s-wave component is given in Table 9.

There are several areas of difference between the MC^2 and RABBLE data themselves as well as to the results of Table 8; however, taken as a total, there is general agreement among the various calculations. One

Table 9. Comparative Cross Sections for Two-Region Cell of ZPR-6 Assembly 5 (Barns)

Group	MC^2 Equivalence Theory	RABBLE (2 Regions)	RABBLE (10 Subregions)
15	0.3936	0.4094	0.4072
16	0.6228	0.5619	0.5515
17	0.5489	0.5682	0.5591
18	0.6705	0.7186	0.7092
19	0.8081	0.9056	0.8880
20	0.7242	0.8028	0.7927
21	0.9988	1.3028	1.2899
22	1.2661	1.6410	1.6227
23	2.1474	2.6402	2.6109

can also note that the two RABBLE calculations show little change in the cross section when more spatial resolution is included. There is a significant difference in the cross section for group 16 from MC^2 as opposed to the other calculations and this difference is probably due to the large sodium resonance. Sodium was handled by broad group cross sections only in the RABBLE calculations. For the data reflected in Table 8 the use of an asymptotic outer region source requires only a total macroscopic cross section, so sodium is not handled separately. The use of a fine-group weighting spectrum within the broad group structure of MC^2 could also yield differences and has a significant effect in the lower energy groups. Inspection of the MC^2 data showed that the fine-group spectrum drops almost five orders of magnitude over the last three broad groups. Recalculation of the equivalence theory result for Group 23 from Table 8 using the MC^2 fine groups and flux weighting resulted in a value of 2.272 barns which is in much better agreement with the MC^2 result. Additional comparisons did

not show the fine group weighting to be responsible for all differences, but the combination of such differences in treatment as the fine group weighting, unresolved resonances, background capture, light element treatment, and resonance overlap could easily be responsible for the remaining differences between the results.

Common to both sets of results just presented is the conclusion that source nonuniformity within the cell has little effect on the effective cross sections and should hence have little impact on reactor integral parameters. The differences that can be seen in the comparisons can be more easily attributed to the methods of obtaining the spectra of the source and flux rather than the effects of the spatial distribution on the escape probability. This is not to say that the spatial flux distribution has no effect, but that the net effect on cross section averages is rather insensitive to nonuniformity in the source through the escape probability. In order to put this premise to additional tests, RABBLE calculations were made for various other types of cells, first with two regions, then with several subregions. The first cell in these additional tests was for ZPR-6 Assembly 6,[81] a plate critical with 1/4 inch U_3O_8 plates. The next cells were hypothetical cells of pin geometry for the core and blanket region of a large LMFBR; a typical cell for a light water reactor (LWR) was also examined. A brief description of the various cells is given in Table 10.

Since the intent of these calculations was to explore the nonuniformity effect on ^{238}U capture cross sections, other materials were handled with broad group cross sections or 1/v cross sections. This treatment may be poor for Na, ^{235}U, and Pu isotopes, but it does afford

Table 10. Cell Descriptions for Additional Assessment of Nonuniformity

ZPR-6 Assembly 6	LMFBR Core	LMFBR Blanket	LWR
Plate Region	**Pin Region**	**Pin Region**	**Pin Region**
Thickness: 0.635 cm	Radius: 0.2921 cm	Radius: 0.9525 cm	Radius: 0.479 cm
Composition (10^{24} cm^{-3})	Composition (10^{24} cm^{-3})	Composition (10^{24} cm^{-3})	Composition (10^{24} cm^{-3})
^{238}U 0.0233	^{238}U 0.0184	^{238}U 0.0223	^{238}U 0.0362
^{235}U 0.00017	^{235}U 0.00013	^{235}U 0.00005	^{235}U 0.00106
O 0.0627	O 0.0446	O 0.0396	O 0.0745
	^{239}Pu 0.00285		
Outer Region	^{240}Pu 0.00081	**Outer Region**	**Outer Region**
Thickness: 2.365 cm		Radius: 1.239 cm	Radius:
Composition (10^{24} cm^{-3})	**Outer Region**	Composition (10^{24} cm^{-3})	Composition (10^{24} cm^{-3})
^{238}U 0.00109	Radius: 0.5236 cm	Na 0.0139	Zr 0.00069
^{235}U 0.00141	Composition (10^{24} cm^{-3})	Fe 0.0212	H 0.00716
Na 0.0116	Na 0.0133	Ni 0.0042	O 0.0120
O 0.00175	Fe 0.0187	Cr 0.0062	
Fe 0.0179	Ni 0.0037		
Ni 0.0017	Cr 0.0049		
Cr 0.0035			

a consistent basis for comparison. The resulting cross section averages are noted in Table 11. Inspection again shows little difference due to the improved spatial treatment of the source. By two independent methods and for different types of cells, it has then been found that nonuniformity has little effect on average cross sections. Differences of only about 1% can be located. From differences of this magnitude the effect on reactor integral parameters is judged to be small, and nonuniformity treatment does not appear to be the source of current discrepancies between calculations and experiment.

Table 11. ^{238}U Capture Cross Sections for Additional Cell Descriptions (barns)

Group	ZPR-6 Assembly 6 Cell		LMFBR Core Cell		LMFBR Blanket Cell		LWR Cell	
	2 Regions	10 Subregions	2 Regions	10 Subregions	2 Regions	10 Subregions	2 Regions	10 Subregions
15	0.475	0.473	0.587	0.587	0.453	0.455	0.378	0.378
16	0.670	0.666	0.870	0.874	0.613	0.616	0.486	0.487
17	0.682	0.679	0.936	0.941	0.638	0.642	0.498	0.500
18	0.852	0.849	1.216	1.223	0.792	0.797	0.618	0.620
19	1.101	1.096	1.688	1.701	1.014	1.021	0.756	0.759
20	0.989	0.985	1.579	1.591	0.911	0.917	0.666	0.668
21	1.576	1.568	2.536	2.554	1.461	1.468	1.254	1.257
22	--	--	2.869	2.881	1.843	1.849	--	--
23	--	--	4.685	4.701	2.869	2.880	--	--

CHAPTER VI

CONCLUSIONS AND RECOMMENDATIONS

From the studies carried out in this work, two primary conclusions are reached. First, through the use of a generalized reciprocity relation and an energy dependent escape cross section, a method for cross section averaging can be obtained which is simple in form, correctly accounts for nonuniformity, and can include the more standard approximations. Secondly, the effect on nonuniformity in the source yields little effect on cross section averages and should yield little difference in calculated reactor integral parameters from current methods.

The small effect on cross sections has been shown both through the general method and independent calculations; however, the reasons for such a small effect can only adequately be found through examination of the parameters of the general method. Although significant differences occur between the escape probabilities, or escape cross sections, for a nonuniform source treatment as compared to a flat source treatment, compensating changes occur in the reciprocity relation for the nonuniform case which combine to yield results similar to the flat source treatment. Although this result seems to reduce the value of having a method which can handle nonuniformity effects, it is perhaps only through such a method that the compensating phenomena can be investigated. It also tends to point out that, if improved treatment of escape probabilities are to be used, the correct reciprocity relation must be specifically employed to

avoid erroneous interpretation.

Although the results of this study show that the use of the escape probability for a flat source of neutrons appears adequate for the determination of effective cross sections, it does not give sufficient indication of how the energy dependence of the sources should be handled. For example, in all cases of the general method, the asymptotic spectrum for the source in the outer region was used, and this treatment could partially be responsible for the similarity of results. Inspection of the integral transport theory results shows that this treatment may not be adequate, and in this area additional study is recommended.

Since this study has not shown that improved methods for cross section averaging including nonuniform effects can explain differences between current calculations and experiments, one must necessarily address the adequacy of the differential cross section data. G. de Saussure[99] has pointed out that, although a precision of 2% in the capture cross section of ^{238}U is required for acceptable uncertainties in reactor integral parameters, the present uncertainty is of the order of 15%. He points out systematic differences between several recent experiments and the ENDF/B-III evaluation which are apparent throughout the resolved resonance range. The best approach to resolution of these differences is probably to perform additional measurements with different techniques, but it is unlikely that these measurements will yield the 2% precision required by the reactor designers. Anticipated differences in the differential data, or differences between the competition for scattering and absorption could possibly resolve current discrepancies. In this light, one must continue to

use the best evaluated data and methods available with input from critical experiments which specifically examine such effects as heterogeneous self-shielding.

APPENDIX A

COLLISION KERNELS

In order to carry out the kernel integrations indicated in Eqs. 4-32 and 4-33, the optical thickness $\tau(x,x',E)$ must be uniquely defined. For x' in the range (o,b) the optical thickness from the origin is given by

$$\tau(o,x',E) = \Sigma_t^1(E)\ x', \qquad o \leqq x \leqq a, \tag{A-1}$$

$$= \Sigma_t^1(E)a + \Sigma_t^2(E)(x'-a), \qquad a \leqq x' \leqq b.$$

Since the optical thickness is just the scalar distance between two points measured in units of the neutron mean free path, one can state

$$\tau(x,x',E) = \left|\tau(o,x,E) - \tau(o,x',E)\right|, \tag{A-2}$$

$$\tau(x,-x',E) = \tau(o,x,E) + \tau(o,x',E)\ , \tag{A-3}$$

$$\tau(x,x',E) = \tau(x',x,E)\ . \tag{A-4}$$

The optical thickness arguments of Eq. 4-14 can then be written

$$\tau(x,x'+m2b,E) = \left|\tau(o,x,E) - \tau(o,x'+m2b,E)\right|\ , \tag{A-5}$$

$$= \left|\tau(o,x,E) - \tau(o,x',E)\right|\ , \qquad m = 0\ ,$$

$$= m\tau_o(E) - \tau(o,x,E) + \tau(o,x',E) \ , \quad m > 0 \ ,$$

$$= |m|\tau_o(E) + \tau(o,x,E) - \tau(o,x',E) \ , \ m < 0 \ .$$

From this a more general expression may be written for any m,

$$\tau(x,x'+m2b,E) = \left|m\tau_o(E) - \tau(o,x,E) + \tau(o,x',E)\right| \ . \qquad \text{(A-6)}$$

In similar fashion the complementary argument may be expressed,

$$\tau(x,-x'+m2b,E) = \left|m\tau_o(E) - \tau(o,x,E) - \tau(o,x',E)\right| \ . \qquad \text{(A-7)}$$

Equation 4-14 can then be expressed with these forms and broken up to yield

$$T(x,x',E) = \sum_{m=-\infty}^{\infty} \{E_1[\left|m\tau_o(E) - \tau(o,x,E) + \tau(o,x',E)\right|] \qquad \text{(A-8)}$$

$$+ E_1[\left|m\tau_o(E) - \tau(o,x,E) - \tau(o,x',E)\right|]\}$$

$$= E_1[\left|\tau(o,x,E) - \tau(o,x',E)\right|] + E_1[\tau(o,x,E) + \tau(o,x',E)]$$

$$+ \sum_{m=1}^{\infty} \{E_1[\left|m\tau_o(E) - \tau(o,x,E) + \tau(o,x',E)\right|]$$

$$+ E_1[\left|m\tau_o(E) - \tau(o,x,E) - \tau(o,x',E)\right|]\}$$

$$+ \sum_{n=1}^{\infty} [E_1[\left|-n\tau_o(E) - \tau(o,x,E) + \tau(o,x',E)\right|]$$

(continued)

$$+ E_1[|-n\tau_o(E) - \tau(o,x,E) - \tau(o,x',E)|]\} .$$

The first two terms of the above expression represent the evaluation at $m = 0$, the next set of terms is the summation for $m \geq 1$, and the latter terms are for the summation $m \leq -1$, using $n = -m$. Since $\tau(o,x,E) \leq \tau_o(E)$ the signs within the absolute value indication can be determined for the terms in summation. Combining the two summations and beginning the sum at $m = 0$, Eq. A-8 can be written

$$T(x,x',E) = E_1[|\tau(o,x,E) - \tau(o,x',E)|] + E_1[\tau(o,x,E) + \tau(o,x',E)] \tag{A-9}$$

$$+ \sum_{m=0}^{\infty} \{E_1[m\tau_o(E) + \tau_o(E) - \tau(o,x,E) + \tau(o,x',E)]$$

$$+ E_1[m\tau_o(E) + \tau_o(E) - \tau(o,x,E) - \tau(o,x',E)]$$

$$+ E_1[m\tau_o(E) + \tau_o(E) + \tau(o,x,E) - \tau(o,x',E)]$$

$$+ E_1[m\tau_o(E) + \tau_o(E) + \tau(o,x,E) + \tau(o,x',E)]\}.$$

By using the notation of Eqs. 4-34 to 4-38 the kernel expression can be written for $x = x_n$, $x' = x_{n'}$, and $E = E_g$ as

$$T(x_n,x_{n'},E_g) = E_1[\epsilon_{n',n}(\tau(x_{n'},E_g) - \tau(xm,E_g))] \tag{A-10}$$

$$+ E_1[\tau(x_{n'},E_g) + \tau(x_n,E_g)]$$

$$+ \sum_{m=o}^{\infty} \sum_{j=1}^{4} E_1[m\tau_o(E_g) + \alpha_{n',nj}(E_g)] .$$

The above expression can then be integrated term by term to obtain Eq. 4-32 by using

$$\int_{u_1}^{u_2} E_1(z)dz = E_2(u_1) - E_2(u_1) \; ; \qquad \text{(A-11)}$$

Equation 4-33 can likewise be obtained from a term by term integration using

$$\int_{u_1}^{u_2} zE_1(z)dz = E_3(u_1) - E_3(u_2) + u_1E_2(u_1) - u_2E_2(u_2) \; . \qquad \text{(A-12)}$$

BIBLIOGRAPHY

1. G. I. Bell and S. Glasstone, Nuclear Reactor Theory, Van Nostrand Reinhold Co., New York, 1970.

2. L. Dresner, Resonance Absorption in Nuclear Reactors, Pergamon Press, Inc., New York, 1960.

3. J. B. Sampson and J. Chernick, "Resonance Escape Probability in Thermal Reactors," Progress in Nuclear Energy, Series I, Physics and Mathematics, Vol. II, Pergamon Press, Inc., London, 1958.

4. J. Chernick, "Calculation Methods for Heterogeneous Systems," BNL-622, Brookhaven National Laboratory, August 1960.

5. G. I. Bell, "Theory of Effective Cross Sections," LA-2322, Los Alamos Scientific Laboratory, October 6, 1959.

6. J. Chernick, Ed., "Proceedings of the Brookhaven Conference on Resonance Absorption of Neutrons in Nuclear Reactors," BNL-433, Brookhaven National Laboratory, 1957.

7. H. H. Hummel and D. Okrent, Reactivity Coefficients in Large Fast Power Reactors, American Nuclear Society, Hinsdale, Illinois, 1970.

8. L. W. Nordheim, "A New Calculation of Resonance Integrals," Nucl. Sci. Eng., 12, 457 (1962).

9. L. W. Nordheim, "A Program of Research and Calculations of Resonance Absorptions," GA-2527, General Atomic, August 28, 1961.

10. E. Creutz, H. Jupnik, T. Snyder, and E. P. Wigner, "Review of the Measurements of the Resonance Absorption of Neutrons by Uranium in Bulk," J. Appl. Phys., 26, 257 (1955).

11. E. P. Wigner, E. Creutz, H. Jupnik, and T. Snyder, "Resonance Absorption of Neutrons by Spheres," J. Appl. Phys., 26, 260 (1955).

12. E. Creutz, H. Jupnik, T. Snyder, and E. P. Wigner, "Effect of Geometry on Resonance Absorption of Neutrons by Uranium," J. Appl. Phys., 26, 271 (1955).

13. E. Creutz, H. Jupnik, and E. P. Wigner, "Effects of Temperature on Total Resonance Absorption of Neutrons by Spheres of Uranium Oxide," J. Appl. Phys., 26, 276 (1955).

BIBLIOGRAPHY (Continued)

14. J. Chernick and R. Vernon, "Some Refinements in the Calculation of Resonance Integrals," Nucl. Sci. Eng., 4, 649 (1958).

15. S. M. Dancoff and M. Ginsburg, "Surface Resonance Absorption in a Close-Packed Lattice," CP-2157, Argonne Metallurgical Laboratory, 1944.

16. I. I. Gurevich and I. Y. Pomeranchouk, "The Theory of Resonance Absorption in Heterogeneous Systems," Proceedings of the International Conference on the Peaceful Uses of Atomic Energy, 5, 466 (1956).

17. E. P. Wigner, "Review of Resonance Capture by Lumps," BNL-433, Brookhaven National Laboratory, 68 (1957).

18. L. Dresner, "The Effective Resonance Integrals of U-238 and Th-232," Nucl. Sci. Eng., 1, 68 (1956).

19. F. T. Adler, G. W. Hinman, and L. W. Nordheim, "The Qualitative Evaluation of Resonance Integrals," Second U. N. International Conference on the Peaceful Uses of Atomic Energy, 16, 142 (1958).

20. L. Dresner, "Resonance Absorption of Neutrons in Nuclear Reactors," ORNL-2659, Oak Ridge National Laboratory, March 10, 1959.

21. K. I. Spinney, "Resonance Absorption in Homogeneous Mixtures," J. Nucl. Energy, 6, 53 (1957).

22. N. Corngold, "The Effect of Finite Mass on Resonance Absorption in Slab Lattices," BNL-433, Brookhaven National Laboratory, 54 (1957).

23. R. Goldstein and E. R. Cohen, "Theory of Resonance Absorption of Neutrons," Nucl. Sci. Eng., 13, 132 (1962).

24. W. Rothenstein, "Collision Probabilities and Resonance Integrals for Lattices," Nucl. Sci. Eng., 4, 649 (1958).

25. D. C. Leslie, J. C. Hill, and A. Jensson, "Improvements to the Theory of Resonance Escape in Heterogeneous Fuel. 1. Regular Arrays of Fuel Rods," Nucl. Sci. Eng., 22, 78 (1965).

26. G. I. Bell, "A Simple Treatment for Effective Resonance Integrals in Dense Lattices," Nucl. Sci. Eng., 5, 138 (1959).

27. H. H. Hummel, "Equivalence Between Homogeneous and Heterogeneous Resonance Integrals in Cylindrical Geometry," Reactor Physics Div. Annual Report, July 1, 1964 to June 30, 1965, ANL-7110, Argonne National Laboratory, 319 (1966).

BIBLIOGRAPHY (Continued)

28. K. M. Case, F. de Hoffman, and G. Placzek, Introduction to the Theory of Neutron Diffusion, U. S. Gov't. Printing Office, Washington, D. C., 1953.

29. R. D. Richmyer, "Resonance Capture Calculations for Lattices by the Monte Carlo Method," BNL-433, Brookhaven National Laboratory, 82 (1957).

30. J. B. Sampson, "Attempted Monte Carlo Calculations of Resonance Escape Probability in a Graphite Lattice," BNL-433, Brookhaven National Laboratory, 92 (1957).

31. M. M. Levine, "Resonance Integral Calculations for U^{238} Lattices," Nucl. Sci. Eng., 16, 271 (1963).

32. Henry C. Honeck, "ENDF/B, Specifications for an Evaluated Nuclear Data File for Reactor Applications," BNL-50066, Brookhaven National Laboratory, May 1966 (Revised July 1967 by S. Pearlstein).

33. R. A. Karam, W. R. Robinson, and M. Salvatores," Comparison of ENDF/B Versions I, II, and III," Transactions of the American Nuclear Society, 15, 458 (1972).

34. R. B. Pond and C. E. Till, "A Comparison of ENDF/B and Schmidt U^{238} Data for Doppler Effect Calculations," Reactor Physics Division Annual Report, July 1, 1968 to June 30, 1969, ANL-7610, Argonne National Laboratory, 197 (1970).

35. A. L. Hess and R. G. Palmer, "Further Analyses of Plutonium-Fueled ZPR-3 Benchmark Criticals Using ENDF/B VERSION I, Applied Physics Division Annual Report, July 1, 1970 to June 30, 1971, ANL-7910, Argonne National Laboratory, 291 (1972).

36. A. L. Hess and R. G. Palmer, "Prescription of a Benchmark Model of ZPPR Assembly 2 for Data Testing of ENDF/B," ANL-7910, Argonne National Laboratory, 299 (1972).

37. Samuel Glasstone and Milton C. Edlund, The Elements of Nuclear Reactor Theory, D. Van Nostrand Company, Inc., New York, 1952.

38. H. C. Honeck, "The Distribution of Thermal Neutrons in Space and Energy in Reactor Lattices. Part I: Theory," Nucl. Sci. Eng., 8, 193 (1960).

BIBLIOGRAPHY (Continued)

39. H. C. Honeck and I. Kaplan, "The Distribution of Thermal Neutrons in Space and Energy in Reactor Lattices. Part II: Comparison of Theory and Experiment," Nucl. Sci. Eng., 8, 203 (1960).

40. H. C. Honeck, "A Thermalization Transport Theory Code for Reactor Lattice Calculations," BNL-5826, Brookhaven National Laboratory, September 1961.

41. B. Toppel and I. Baksys, "The Argonne Revised THERMOS Code," ANL-7023, Argonne National Laboratory, March 1965.

42. W. W. Engle, M. A. Boling, and B. W. Colston, "DTF-II, A One-Dimensional, Multigroup Neutron Transport Program," NAA-SL-10951, Atomics International, March 1966.

43. W. W. Engle, "A Users Manual for ANISN, A One-Dimensional Discrete Ordinates Transport Code with Anisotropic Scattering," K-1693, Oak Ridge National Laboratory, March 1967.

44. David Meneghetti, "Discrete Ordinate Quadratures for Thin Slab Cells," Nucl. Sci. Eng., 14, 295 (1962).

45. R. G. Palmer, J. P. Plummer, and R. B. Nicholson, "A Study of Several Methods for Analysis of Critical Assembly Heterogeneity," Nucl. Sci. Eng., 50, 229 (1973).

46. R. B. Nicholson, "Cross Section Averaging Schemes for Group Collapsing and Cell Homogenization in Neutron Transport Calculations for Critical Assemblies," ANL-7610, Argonne National Laboratory, 488 (1970).

47. F. Storrer, A. Khairallah, M. Cadilhac, and P. Benoist, "Heterogeneity Calculation for Fast Reactors by a Perturbation Method," Nucl. Sci. Eng., 24, 153 (1966).

48. Arne P. Olson and J. M. Stevenson, "Calculation of Heterogeneity Effects in ZPR-Type Reactors," Trans. Am. Nucl. Soc., 12 (2), 625 (1969).

49. R. N. Hwang, "Doppler Effect Calculations with Interference Corrections," Nucl. Sci. Eng., 21, 523 (1965).

50. Weston M. Stacey, Jr., "Advances in Neutron Continuous Slowing Down Theory," National Topical Meeting on New Developments in Reactor Physics and Shielding, TID-4500, Kiamesha Lake, N. Y., 143 (1972).

BIBLIOGRAPHY (Continued)

51. C. N. Kelber, "Improved Rational Escape Probability in Lumped Absorbers," Nucl. Sci. Eng., 22, 224 (1965).

52. Charles N. Kelber, "An Extended Equivalence Relation," Nucl. Sci. Eng., 42, 257 (1970).

53. A. Travelli, "A Modification of the Bell Approximation for Slab Geometries," Reactor Physics Division Annual Report, July 1, 1967 to June 30, 1968, ANL-7410, Argonne National Laboratory, 424 (1969).

54. J. P. Plummer and R. G. Palmer, "Extended Equivalence between Homogeneous and Heterogeneous Resonance Integrals in Slabs," Trans. Am. Nucl. Soc., 12 (2), 625 (1969).

55. D. M. O'Shea, B. J. Toppel, and A. L. Rago, "MC^2 -- A Code to Calculate Multigroup Cross Sections," ANL-7318, Argonne National Laboratory (1967).

56. Hellen M. Summer, "ERIC-2, A Fortran Program to Calculate Resonance Integrals and From These Effective Capture and Fission Cross Sections," AEEW-R 323, Atomic Energy Establishment, Winfrith, 1964.

57. L. C. Just, H. Henryson, II, A. S. Kennedy, S. D. Sparck, B. J. Toppel, and P. M. Walker, "The System Aspects and Interface Data Sets of the Argonne Reactor Computation (ARC) Series," ANL-7711, Argonne National Laboratory, 1971.

58. B. A. Zolotar, "Plans for an Argonne Reactor Computation (ARC) System ZPR Heterogeneity Package," ANL-7610, Argonne National Laboratory, 486 (1970).

59. R. G. Palmer and B. A. Zolotar, "Heterogeneity Algorithms for MC^2-2," Applied Physics Division Annual Report, July 1, 1969 to June 30, 1970, ANL-7710, Argonne National Laboratory, 393 (1971).

60. K. D. Dance, R. A. Karam, J. E. Marshall, and R. B. Pond, "Analysis of Central Reactivity Worths Incorporating Resonance Self-Shielding," ANL-7610, Argonne National Laboratory, 165 (1970).

61. D. C. Irving, "The Adjoint Boltzmann Equation and Its Simulation by Monte Carlo," ORNL-TM-2879, Oak Ridge National Laboratory, May 18, 1970.

62. W. M. Stacey, Jr., "Collision Probability Methods With Anisotropic Scattering," ANL-7910, Argonne National Laboratory, 495 (1972).

BIBLIOGRAPHY (Continued)

63. C. A. Stevens and C. V. Smith, "GAROL, A Computer Program for Evaluating Resonance Absorption Including Resonance Overlap," GA-6637, General Atomic, August 24, 1965.

64. P. H. Kier and A. A. Robba, "RABBLE, A Program for Computation of Resonance Absorption in Multiregion Reactor Cells," ANL-7326, Argonne National Laboratory, April 1967.

65. P. H. Kier, personal communication (April 1974).

66. P. H. Kier, "Modification of the Multigroup Resonance Absorption Code RABBLE," ANL-7610, Argonne National Laboratory, 486 (1970).

67. P. H. Kier, "Modification of the Multiregion Resonance Absorption Code RABBLE," ANL-7710, Argonne National Laboratory, 433 (1971).

68. E. E. Lewis, "A Boltzmann Integral Equation Treatment of Resonance Absorption in Reactor Lattices," Ph.D. Thesis, University of Illinois, 1965.

69. E. E. Lewis and F. T. Adler, "A Boltzmann Integral Equation Treatment of Neutron Resonance Absorption in Reactor Lattices," Nucl. Sci. Eng., 31, 117 (1968).

70. P. H. Kier, "RIFF RAFF, A Program for Computation of Resonance Integrals in a Two-Region Cell," ANL-7033, Argonne National Laboratory, August 1965.

71. A. P. Olson, "RABID: Integral Transport Theory Code for Neutron Slowing Down in Slab Cells," ANL-7645, Argonne National Laboratory, 1970.

72. Arne P. Olson, "Further Developments in Integral Transport Methods for Resonance Region Calculations in Plate-type Lattices Using the RABID Code," ANL-7710, Argonne National Laboratory, 434 (1971).

73. A. L. Hess, R. G. Palmer, J. M. Stevenson, "A Post-analytical Study of Eight ZPR-3 Benchmark Criticals Using ENDF/B Data," ANL-7710, Argonne National Laboratory, 224 (1971).

74. Arne P. Olson and Nam Chin Paik, "Heterogeneity and Criticality Studies on the Zero Power Plutonium Reactor (ZPPR) Assembly 2, A Demonstration Reactor Benchmark Critical," ANL-7710, Argonne National Laboratory, 146 (1971).

75. R. B. Pond and C. E. Till, "Analysis of Doppler Effect Measurements in CH_2-Softened Spectra, ZPR-9 Assemblies 13-17," ANL-7410, Argonne National Laboratory, 80 (1969).

BIBLIOGRAPHY (Continued)

76. L. G. LeSage and W. R. Robinson, "ZPR-9 Assemblies 19, 21, 22, and 24," ANL-7410, Argonne National Laboratory, 80 (1969).

77. R. A. Karam, L. R. Dates, W. Y. Kato, J. E. Marshall, T. Nakamura, and G. K. Rusch, "A 4000-Liter Uranium Oxide Fast Core, Assembly 6 of ZPR-6," ANL-7410, Argonne National Laboratory, 75 (1969).

78. R. A. Karam and J. E. Marshall, "Critical Mass Sensitivity to the Treatment of Heterogeneity Effects in a Large UC Fast Core, Assembly 5 of ZPR-6," Trans. Am. Nucl. Soc., 12 (2), 718 (1969).

79. R. A. Karam, J. E. Marshall, and K. D. Dance, "Analysis of Heterogeneity and Sodium-Void Effects in a 2700-Liter Uranium Carbide Fast Core, ZPR-6 Assembly 5," Nucl. Sci. Eng., 43, 5 (1971).

80. C. E. Till, J. M. Gasidlo, E. F. Groh, L. G. LeSage, W. R. Robinson, and G. S. Stanford, "Null Reactivity Measurements of Capture-to-Fission Ratios in U-235 and Pu-239," ANL-7610, Argonne National Laboratory, 176 (1970).

81. R. A. Karam, K. D. Dance, L. R. Dates, W. Y. Kato, J. E. Marshall, T. Nakamura, and G. K. Rusch, "Heterogeneity Effects in a Large UO_2 Core, Assembly 6 of ZPR-6," ANL-7410, Argonne National Laboratory, 133 (1969).

82. R. A. Lewis, L. G. LeSage, J. E. Marshall, E. M. Bohn, M. Salvatores, and G. S. Stanford, "Initial Plate-Rod Heterogeneity Measurements -- LMFBR Demonstration Reactor Critical Experimental Program," ANL-7910, Argonne National Laboratory, 169 (1972).

83. D. W. Madison and J. M. Gasidlo, "Foil Activation Analysis in Critical Facility Assemblies," Trans. Am. Nucl. Soc., 15 (2), 930 (1972).

84. W. Y. Kato, C. A. Preskitt, J. C. Young, J. M. Neill, C. D. Swenson, R. J. Armani, and J. H. Roberts, "Measurement of Reaction Ratios and Neutron Spectra in a Soft Spectrum Fast Reactor," ANL-7610, Argonne National Laboratory, 184 (1970).

85. J. C. Young, J. M. Neill, P. d'Oultremont, E. L. Slaggie, and C. A. Preskitt, "Measurement and Analysis of Neutron Spectra in a Fast Subcritical Assembly Containing U-235, U-238, and BeO," Nucl. Sci. Eng., 48, 45 (1972).

86. T. J. Yule and E. F. Bennett, "Measured Neutron Spectra in a Number of Uranium- and Plutonium-Fueled Reactor Assemblies," Nucl. Sci. Eng., 46, 236 (1971).

BIBLIOGRAPHY (Continued)

87. P. d'Oultremont, J. C. Young, J. M. Neill, and C. A. Preskitt, "Neutron Spectra and Kinetic Properties in Fast Sub-Critical Assemblies Containing Uranium-235, Uranium-238, and Carbon," Nucl. Sci. Eng., 45, 141 (1971).

88. H. Bluhm, "Spectrum Measurement in a Depleted Uranium Metal Block for Investigation of Discrepant U-238 Cross Sections," Trans. Am. Nucl. Soc., 15 (2), 898 (1972).

89. R. A. Karam, "Analysis of ZPR-6 Assembly 6A," ANL-7910, Argonne National Laboratory, 163 (1972).

90. M. P. Fricke and J. M. Neill, "The (n,n') Reaction in the Calculation of Fast Neutron Spectra," Nucl. Sci. Eng., 50, 392 (1973).

91. H. H. Hummel and W. M. Stacey, "Effects of the U-238 (n,n') Reaction in Fast-Neutron Spectrum Critical Assemblies," Nucl. Sci. Eng., 50, 397 (1973).

92. W. G. Davey, P. I. Amundson, P. J. Collins, and R. G. Palmer, "Heterogeneity Effects in ZPPR Assembly 2 -- A Plutonium-Fueled Demonstration Fast Reactor Study," Nucl. Sci. Eng., 51, 415 (1973).

93. T. J. Yule, E. F. Bennett, and I. K. Olson, "Measured Neutron Spectra in ZPR-6 Assembly 6A, ZPR-9 Assembly 25, and ZPR-9 Assembly 26, FTR-3," ANL-7710, Argonne National Laboratory, 183 (1971).

94. J. M. Otter, "Modified Rational Approximation to the Collision Probability in Lumped Resonance Absorbers," Trans. Am. Nucl. Soc., 7, 275 (1964).

95. I. I. Bondarenko, L. P. Abagyan, N. O. Bazazyants, and M. N. Nikolaev, Group Constants for Nuclear Reactor Calculations, Consultant Bureau Enterprises, Inc., New York, 1964.

96. Milton Abramowitz and Irene A. Stegun (Editors), Handbook of Mathematical Functions, Fifth Edition 55, 923, U.S.G.P.O., Washington, 1966.

97. Arne P. Olson, Gaussian Quadratures for $\int_1^\infty \exp(-x) f(x)\, dx/x^m$ and $\int_1^\infty g(x)\, dx/x^m$, Math. Comput., 23 (106), 447 (1969).

98. Anthony Ralston and Herbert S. Wilf, Ed., Mathematical Methods for Digital Computers, Volume II, John Wiley & Sons, Inc., New York, 1967, p. 133.

BIBLIOGRAPHY (Continued)

99. G. de Saussure, E. G. Silver, R. B. Perez, R. Ingle, and H. Weaver, "Measurement of the Uranium-238 Capture Cross Section for Incident Neutron Energies up to 100 keV," Nucl. Sci. Eng., 51, 385 (1973).

VITA

Kenneth David Kirby was born on May 29, 1945 in Morganton, North Carolina. He attended both grammar and high school in Drexel, North Carolina, where he graduated from high school in 1963 at the top of his class. In 1967 he received his Bachelor of Science Degree in Nuclear Engineering from North Carolina State University, where he had participated in the Engineering Honors Program. While a student at N.C. State, Mr. Kirby spent two summers in an intern program at Oak Ridge National Laboratory in Oak Ridge, Tennessee.

Mr. Kirby entered graduate school at the Georgia Institute of Technology in 1967 and completed his Master of Science Degree in Nuclear Engineering in 1968. He was then employed as a Nuclear Engineer by Lockheed-Georgia Company studying radiation environments associated with advanced nuclear rocket systems. He presented papers and is co-author of several technical reports in this area. During his employment, Mr. Kirby reentered graduate school as a part-time student to begin work on his Ph.D. in Nuclear Engineering.

In 1971 Mr. Kirby returned to graduate school on a full-time basis and took part in sponsored research concerning the feasibility of gaseous core nuclear power systems. At the June, 1973, American Nuclear Society Conference, he presented a paper entitled "Nuclear Analysis of Gas Core Reactor Configurations for MHD Power Generation," which is published in the ANS Transactions. Following this work, Mr. Kirby began his disserta-

tion research in the area of heterogeneous effects on effective cross sections and presented the paper "A General Method of Determining Effective Cross Sections for Heterogeneous Media" at the September, 1974, ANS Topical Meeting in Atlanta.

Mr. Kirby is married to the former Sharon Bradshaw of Drexel, North Carolina. He is a member of the American Nuclear Society, Tau Beta Pi, and Phi Kappa Phi.